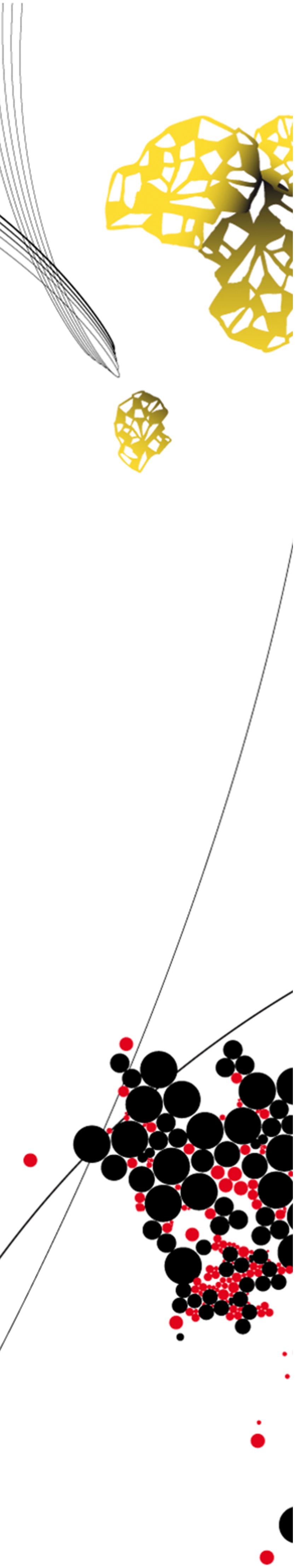

Faculty of Engineering Technology

Design and Mechanics of an electric superbike

Frank Eshuis s1977660
Álvaro de Gruijter Eguiluz s2028735
Henk Jekel s1802178
Michalis Savva s1927337
Henriko Schonewille s1746251
Romeo Veldhuis s1967843
Patrick Zieverink s1957252

B.Sc. Mechanical Engineering
June 2018

Supervisors:
dr. J. Hazrati Marangalou
ing. T.G.M. Krone

Mechanincal Engineering Group
Faculty of Engineering Technology
University of Twente
7500 AE Enschede
The Netherlands

Summary

The research started with a concept phase, in which using a morphological diagram with functions based on the requirements, three concepts were created. Eventually the winning concept was based on a trellis frame. It would be powered by a PMAC (Permanent Magnet Alternating Current) motor. The motor is placed with the axle perpendicular to the direction of movement of the bike and is connected to a two gear gearbox. The outgoing shaft of the gearbox is connected to the rear wheel by a chain. Disc brakes are chosen to decelerate.

In the materialisation phase the winning concept was elaborated on. Both drive train and frame had to be designed. Starting with the drive train, it was first determined what the maximum statical friction would be at the start. Using the power and torque graphs of the chosen motor, the gear ratios could be determined so that the motor would not slip during the race. Also a material selection was performed based on materials that were used for similar purposes. The chosen material for the shaft and gears is 25CrMo4 AISI 4130 steel. The bending stresses and contact stresses in the gears were determined to find the dimensions of the gears and the shafts. To connect the gears to the shafts it was determined that a key connection would not be sufficient, hence a spline connection was used. This all to ensure a safe and fast design. The Mohr's circle was used as a graphical representation to see if the shaft could handle the principle stresses, which it could.

Afterwards, the peak acceleration was analysed. To win the race it is very important to accelerate as quick as possible. When assuming a friction coefficient of 2.5, a little higher than the friction coefficient in Formula one, but a little lower than the friction coefficient in drag racing, the acceleration from 0 to 100 km/h will be within 1.2 seconds. When calculating this acceleration the rolling resistance, air resistance and moment of inertia are taken into account. If the friction coefficient would be lower, the acceleration would then also be slower and the time that the motor takes to accelerate from 0 to 100 km/h will be higher.

Consequently, the frame design will be summarized. The FEM (finite element method) was used to help out with the calculations for the frame design. Results obtained from hand calculations matched the results from the FEM program. Since the FEM package was validated, the results can be used to conclude that the overall stiffnesses are within the set requirements. The final weight of the frame will be an estimated 35,8 kg and the neck was reinforced to deal with the stresses while braking. The material used for the frame is Carbon steel, AISI 1015, annealed.

Concerning the connection of the front fork to the frame, a static bearing was used to support the neck of the frame. The chosen bearing was the DIN6210.

Next, the swing arm was analysed. The swing arm connection was designed to consist of an inverted U shape with two triangular frames on top on which the springs were attached. The connection between the frame and the swing arm allowed rotation only in the direction in which the rear wheel of the motorcycle rotates. Therefore bearings should be used. After calculating the radial and axial loads, a deep groove ball bearing was chosen, namely the DIN6308.

Finally, one of the welds of the frame was analysed. The type of weld selected is a corner weld, with no edge preparation. It was calculated that the minimum weld size, for the 40mm tube diameters, will be a 4.095mm fillet weld all around the tubes connected, meaning the minimum throat width will be 2.895mm all around the connection.

Contents

Summary iii

1 Introduction 1

2 Analysis 3
- 2.1 Problem definition 3
- 2.2 Design requirements 4

3 Concepts 7
- 3.1 Concept 1 - Blue 7
  - 3.1.1 Trellis frame 9
  - 3.1.2 PMAC 9
  - 3.1.3 Chain drive 9
  - 3.1.4 Two geared gearbox 10
  - 3.1.5 Two-sided Swingarm 10
  - 3.1.6 Disc brakes 10
- 3.2 Concept 2 - Green 10
  - 3.2.1 Beam frame 11
  - 3.2.2 BLDC motor 12
  - 3.2.3 One gear gearbox 12
  - 3.2.4 Belt drive 13
- 3.3 Concept 3 - Red 13
  - 3.3.1 Monocoque frame 14
  - 3.3.2 AC 3 phase induction motor 15
  - 3.3.3 Shaft system 15
  - 3.3.4 Three-geared gearbox 15
  - 3.3.5 One-sided swingarm 16
  - 3.3.6 Concept rating performance 16

4 Materialisation 19
- 4.1 Baseline Calculations 19

4.1.1 Slip conditions 19
4.1.2 Motor Power 20
4.2 Drive Train 21
4.2.1 Gear ratios 21
4.2.2 Material selection 23
4.2.3 Gear design 23
4.2.4 Bending stress 26
4.2.5 Contact stresses in the gears 29
4.2.6 Shaft design 31
4.2.7 Key design 35
4.2.8 Spline design 36
4.2.9 Shaft technical drawing 40
4.3 Mohr's Circle 41
4.3.1 Conclusion 43
4.4 Acceleration 43
4.4.1 Inertia 44
4.4.2 Rolling resistance 45
4.4.3 Air resistance 46
4.4.4 Total force 46
4.4.5 Requirement check 46
4.4.6 Maximum velocity 48
4.4.7 Conclusion 48
4.5 Frame design 49
4.5.1 Frame dimensions, connections and housing of electrical components 50
4.5.2 Material selection 52
4.5.3 Analysis of the frame: Finite Element Method 54
4.5.4 Hand calculations 61
4.5.5 Neck Bearings 63
4.5.6 Swing arm connection 64
4.5.7 Weld connections 69

5 Evaluation and redesign **73**
5.1 Drive train redesign 73
5.1.1 Air resistance 73
5.1.2 Gear ratios 74
5.1.3 Spline design 75
5.2 Frame redesign 76

5.2.1 Redesign frame dimensions, connections and housing of electrical components 76

6 Conclusions and recommendations 79

References 81

Appendices

A Concept drawings 85

B Dimensions of the superbike 89

C Product Sheet Yasa P400 91

D FBD Calculations 95

E Frequently used axle and gear materials 99

F Gearbox assembly drawing 103

G V, M and T diagrams 105

H Bearing selection 107

I Tables of principle stress and elongation 109

Chapter 1

Introduction

The purpose of this project is to design an electric superbike that fulfills specific requirements for racing. This project is inspired by the Electric Superbike Twente team (EST) which is a student team of the University of Twente participating in the MotoE competition for the first time in 2018-2019. In this competition only fully electric superbikes are allowed. They produced a high performance electric motor for competing. Therefore, they focused mainly on developing a self-engineered electric motor. In this report the focus is mainly on developing both an advanced drivetrain and an advanced frame.

This report begins by stating the requirements and will go on to concept creation and concept choice. Afterwards the frame and the drivetrain will be analysed further and finalized. Lastly an evaluation and redesign as well as a conclusion and discussion will determine if there are improvements that can be applied to improve the performance of the superbike.

Chapter 2

Analysis

Creating the best concepts begins with analysing the problem and stating the requirements. Afterwards, a morphological diagram is made to come up with three concepts from which the best one will be chosen as the final concept.

2.1 Problem definition

The goal of this project is to design a fully functional electric super bike. The bike will have to withstand certain forces. Electrical components will not be taken into account since they are fixed, as stated in the project description. It will have to have a high top speed and accelerate, brake and turn as fast as possible for at least 8 laps. During braking and accelerating, it is possible for one of the wheels to lose contact with the ground and during turning the bike can lean more than 60 degrees. The bike will be driven by a professional racer on tarmac, throughout the year, withstanding standard UK weather conditions. The safety of the rider must be taken into account, therefore in case of overheating or an accident, the bike must not explode or cause any harm to the rider.

Table 2.1: Required stiffness values of the super bike [1]

Direction	Stiffness	Unit
Lateral frame stiffness	1-3	kN/mm
Longitudinal frame stiffness	5-10	kN/mm
Torsional frame stiffness	3-7	kN/degree

As can be seen in Table 2.1, the frame should have various stiffnesses in different load cases. A good ratio between strength and flexibility is needed, so the bike is safe to operate. Also some dimensions are limited, which can be found in the Project Description [1] and are presented in Appendix B.

2.2 Design requirements

To be able to establish a good design, some design requirements have to be set. Afterwards the concepts that will be chosen can be rated according to these design requirements. Some requirements are taken from the Project Description [1] and some are introduced to ensure the desired outcome.

Table 2.2: Design Requirements

Frame	**Frame requirement**
1	The design must be a fully operational motorbike, this means all the components must be well defined and connected to the frame (e.g. no flying components).
2	The frame of the bike must meet the stiffness requirements to ensure a smooth ride during racing and specifically during cornering as can be seen in Table 2.1.
3	The bike frame must withstand the 5 kN load that is subjected to during braking.
4	The frame must be designed to fit the overall dimensions of the bike. These are given in the Project Description section 3.4. [1]
5	The bike frame must accommodate the electro motor and other standard parts such as wheels and front fork. The dimensions are given in the project description section 3.3 and 3.4. [1]
6	The rear wheel needs to have a spring-damper connection to the main frame and a swing arm connection to the main frame.
7	The frame can be only made from steel or aluminium, as slender elements.
8	The bike should be able to lean at least 60 degrees
Drive train	**Drive train requirements**
9	The drive train must connect the rear wheel to the motor
10	The electric motor must be compatible with the rest of electric components. Check section 3.3 of the Project Description [1] for the information about the electrical components.
11	No wheel hub motor and/or front wheel drive may be used
12	The drive train must include a transmission system between the motor and wheel

Performance	Performance requirements
13	The acceleration from 0 to 100 km/h of the super bike must be faster than 3 s.
14	The top speed of the super bike must be at least 200 km/h.
15	The superbike may only produce 110 dB
16	A geared transmission system must be integrated in the bike (addition to 11)
17	The motor may provide a maximum power of 160 kW
18	The motorbike must have a sufficient cooling system
19	The bike should weigh under 300 kg including the driver
20	The width of the bike must be less than 70 cm
21	The width of the seat of the rider must be under 40 cm
22	The super bike must be able to fulfill all the requirements independent of the weather conditions

More requirements can be derived in order to make the most efficient, fully functional superbike. For better results, the bike should have a low center of mass , as well as evenly distributed weight for improved balance. Also, the angle of the front fork plays an important role for the steering of the bike, but there will not be looked at in detail since the this angle is already given.

The frontal area will be taken into consideration when designing the frame, but it will not be a design requirement because it is difficult to decide the concepts upon this requirement.

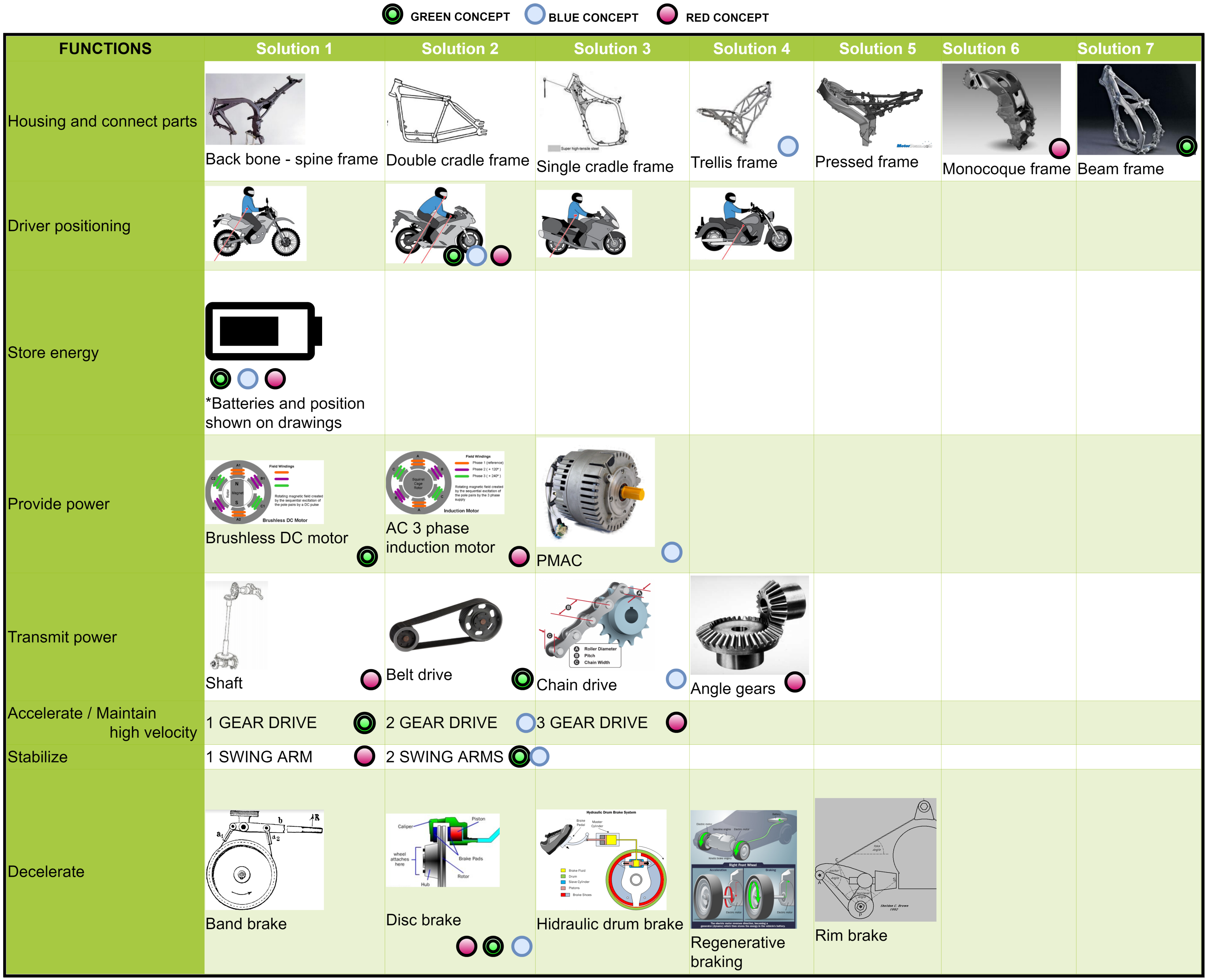

🟢 GREEN CONCEPT 🔵 BLUE CONCEPT 🔴 RED CONCEPT

FUNCTIONS	Solution 1	Solution 2	Solution 3	Solution 4	Solution 5	Solution 6	Solution 7
Housing and connect parts	Back bone - spine frame	Double cradle frame	Single cradle frame	Trellis frame 🔵	Pressed frame	Monocoque frame 🔴	Beam frame 🟢
Driver positioning		🟢 🔵 🔴					
Store energy	🟢 🔵 🔴 *Batteries and position shown on drawings						
Provide power	Brushless DC motor 🟢	AC 3 phase induction motor 🔴	PMAC 🔵				
Transmit power	Shaft 🔴	Belt drive 🟢	Chain drive 🔵	Angle gears 🔴			
Accelerate / Maintain high velocity	1 GEAR DRIVE 🟢	2 GEAR DRIVE 🔵	3 GEAR DRIVE 🔴				
Stabilize	1 SWING ARM 🔴	2 SWING ARMS 🟢 🔵					
Decelerate	Band brake	Disc brake 🔴 🟢 🔵	Hidraulic drum brake	Regenerative braking	Rim brake		

Super high-tensile steel
Field Windings
Rotating magnetic field created by the sequential excitation of the pole pairs by a DC pulse
Brushless DC Motor
Phase 1 (reference)
Phase 2 (+ 120°)
Phase 3 (+ 240°)
Squirrel Cage Rotor
Rotating magnetic field created by the sequential excitation of the pole pairs by the 3 phase supply
Induction Motor
Roller Diameter
Pitch
Chain Width
Caliper
Piston
wheel attaches here
Brake Pads
Rotor
Hub
Hydraulic Drum Brake System
Brake Pedal
Master Cylinder
Brake Fluid
Drum
Slave Cylinder
Pistons
Brake Shoes
Right Front Wheel
Acceleration
Braking

Figure 2.1: Sources of the pictures can be found at [2]–[11]

Chapter 3

Concepts

In the concept phase, various designs were made and worked out, in order to find the optimal design. The three concepts were labelled by a colour, Concept 1-blue, Concept 2-green and Concept 3-red. Which configurations were used and what design specifications where chosen, stood accordingly to the Morphological diagram, Figure 2.1. The morphological diagram focused on meeting the requirements through several functions. These functions were derived from the most important aspects when building an electric superbike and afterwards, these selected functions were expanded on each of the concepts obtained from the morphological diagram.

3.1 Concept 1 - Blue

The first concept, shown in Figure 3.1, is based on a trellis frame. This frame is made out of metal pipes which are welded together forming triangles resulting in a high strength frame. Also typical for this frame is that the motor is included as a stressed member, so it takes some form of loading. Usually steel is used for this type of frame. The motor that will be used is a PMAC (Permanent Magnet Alternating Current) motor, in which an AC current is the input, so a converter is required since a DC power source is supplied from the batteries. The motor is placed with the axle perpendicular to the centre line of the frame and is connected to a gearbox, as can be seen in Figure 3.1 . This gearbox has two gears, one for quick acceleration at low speeds and the other for higher speeds. The power from the outgoing shaft of the gearbox is transferred to the rear wheel using a chain, since this is a strong and relatively lightweight solution. Strength is very important here, because when the bike is accelerating, a lot of force will be loaded on this chain. Disc brakes are chosen to decelerate quickly, so a minimal amount of speed is lost in corners. A more elaborate explanation of the solutions can be found below and a drawing can be found in Figure 3.2 and an enlarged version can be found in A.1.

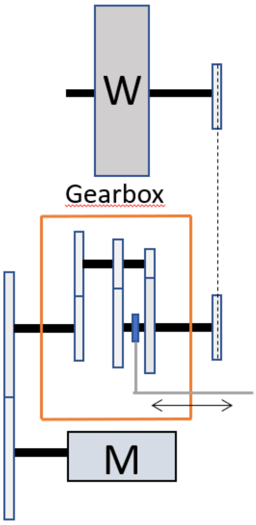

Figure 3.1: Transmission Concept 1

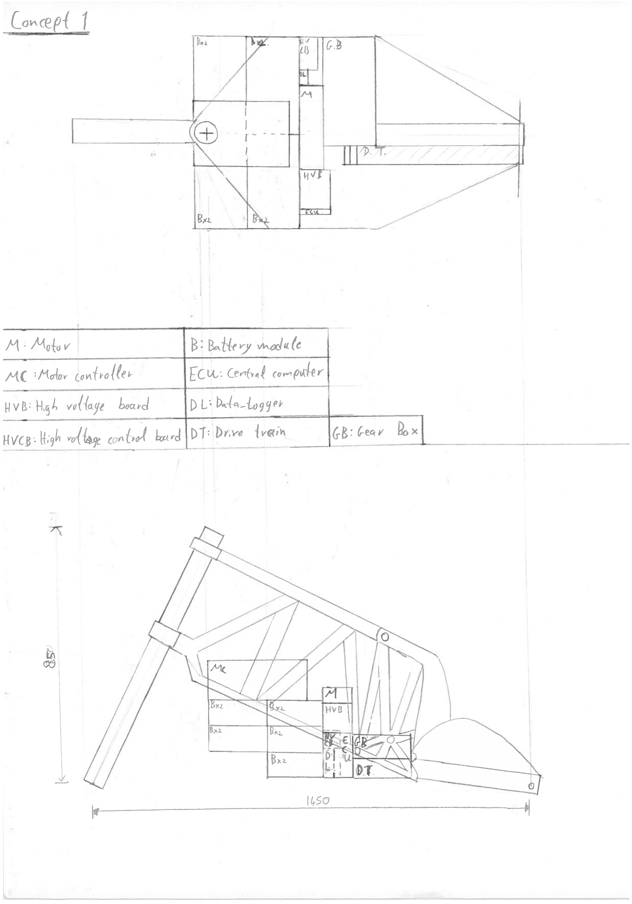
Concept 1
Bx2
G.B
M
D.T.
HVB
ECU
MC
DT
850
1650

M: Motor	B: Battery module	
MC: Motor controller	ECU: Central computer	
HVB: High voltage board	DL: Data-Logger	
HVCB: High voltage control board	DT: Drive train	GB: Gear Box

Figure 3.2: Drawing of Concept 1

3.1.1 Trellis frame

A trellis frame consists of multiple pipes welded together in triangular shapes. The shape gives the frame strength. Also typical for a trellis frame is the integrated engine in the bike. The engine is a stress member meaning that it takes some of the loads the bike undergoes during a race. Usually the frame is made out of steel or aluminum. This frame forms the body of the bike and everything is built around it. Most parts are directly mounted to the frame.

The advantages of this type of frame is that it is easy to adjust the design of the frame if it needs to withstand higher loadings and that it is light due to the integration of the engine. Because the engine takes load, it replaces a part of the frame resulting in a lighter bike. The downside of using this type of frame is that the engine needs reinforcement since it has to carry a load.

3.1.2 PMAC

For this concept a permanent magnet AC (PMAC) motor is chosen. This motor uses AC power to rotate its rotor, which has permanent magnets embedded into it. When the motor is powered on, an internal magnetic field is generated in the stator, which is filled with densely packed copper coils. This generated magnetic field causes the rotor to rotate. The benefit of a PMAC motor is that it has a high power density and the possibility of having a high speed output at high efficiency and a high torque output at low rpm. This will help the motorcycle to accelerate rapidly from the start and having a high efficiency at high speed ensures that the batteries will last throughout the race. A negative of this motor would be its price but since this is a unique superbike, cost is not a problem, as long as the performance is top notch.
Then it was necessary to search for a specific motor that is powerful and lightweight. Bosch, Parker and Yasa were investigated. Bosch had no specifications on its website except that they sell ”high quality motors”. Parker does sell a PMAC motor in their GVM line but only give ranges for the ability of their motors and no weight of the motor is given. Yasa does have a specific motor that fits the requirements. The Yasa P400, of which a torque, power and rpm diagram is included in Section 4.1.2. The complete specifications of this motor are given in Appendix C.

3.1.3 Chain drive

A chain drive can link two sprockets by making the sprockets teeth fit into the holes of the chain. The sprockets do not have to be the same size, so a more ideal ratio can be chosen for a good acceleration and top speed. The chain will be used to connect the outgoing shaft of the gearbox with the rear wheel. The disadvantage of using a chain is that it is heavier than for example a belt and requires lubrication.

3.1.4 Two geared gearbox

Since this gearbox has two gears, one will be used to achieve a high acceleration, while the other will be used to achieve a high top speed. The gear for acceleration has a high torque and lower rpm, because a higher force is required when increasing speed compared to maintaining a high speed. This is an advantage in comparison to a gearbox with just one gear. The disadvantages of using a two gear gearbox is that it takes up more space and it weighs more than a single-speed transmission. Also, a two gear gearbox has a lower efficiency, because some energy is lost in the gears and the extra shaft.

3.1.5 Two-sided Swingarm

The superbike will also have a swing arm, to connect the frame with the rear wheel. The swingarm is part of the rear suspension and needs to support the forces that are acting on the rear wheel, as well as the weight of the frame and the driver. The swingarm also needs to absorb bumps in the road, which it does by pivoting. For this concept and concept 2 it is chosen to have a two-sided swingarm. The advantage of using a two-sided swingarm in comparison with a one-sided swingarm is that the weight will be evenly divided and that the total weight per side will be lower.

3.1.6 Disc brakes

The disc brakes are used for the deceleration for this concept, as well as for the other two concepts. This type of brake uses hydraulics to press a piston against the discs, which make the wheel brake slow down. The advantage of using disc brakes is that it has a greater braking power than for example the drum and rim brakes whilst its weight is almost the same. The downside of using this kind of braking system is that the discs can become very hot, so a highly heat resistant material is required for the discs.

3.2 Concept 2 - Green

The design choices for concept 2 are noted by the green dots in Figure 2.1. A drawing of concept 2 can be found in Figure 3.3 and an enlarged version can be found in Appendix A.2.

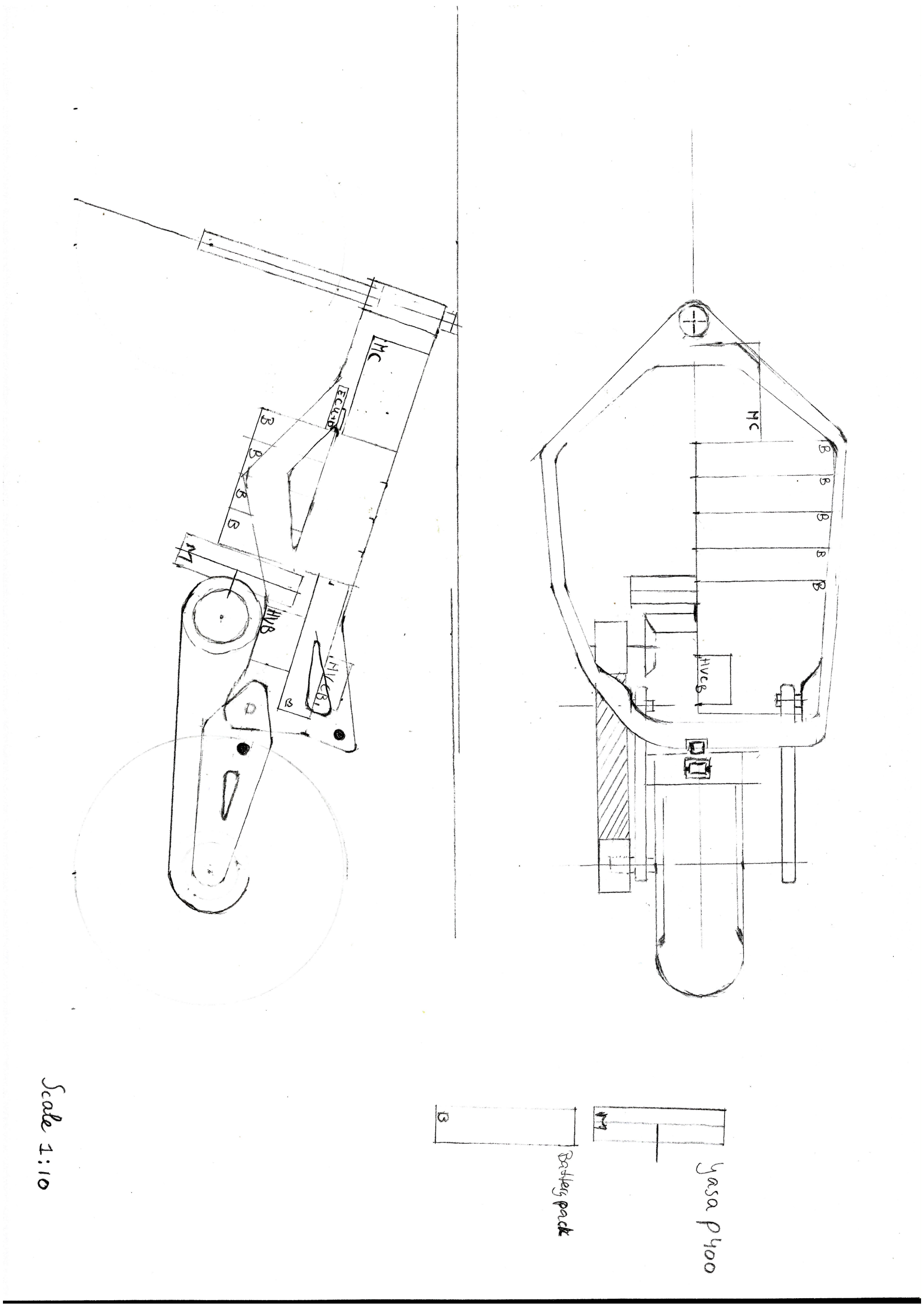

Figure 3.3: A drawing of Concept 2

3.2.1 Beam frame

The beam frame consists of thick and strong beams. Two beams wrap around the engine to join the steering head and swing arm in the shortest distance possible. This causes the rigidity of the frame to be quite high. The engine is a stressed member in the beam frame and as such it will support some of the loads. Typically beam frames are made of aluminium, making them very strong while they are not very heavy. The advantages of beam frames are its high rigidity and its low weight due to the use of primarily aluminium. Since the engine is also a stressed member, some of the loads that the frame would take will be taken by the engine. A disadvantage of the engine being a stressed member is that the motor may require some reinforcing, due to the loading it takes.

3.2.2 BLDC motor

It is decided to use a brushless DC motor for this concept. A BLDC (brushless direct current) motor is essentially the same as a permanent magnet AC motor. The BLDC motor is an improvement of the brushed DC motor. The biggest disadvantages of brushed DC motors is that the brushes wear down over time and they create a lot of resistance. The placement of these brushes in a brushed DC motor can be seen in Figure 3.4. The solution to this problem was to have the magnets turn instead of the coils. In order to allow it to turn at a lower resistance and therefore a higher efficiency it was necessary to use AC power. The name for the replacement of the brushed DC motor would still be called brushless DC motor even though the actual motor is a permanent magnet AC motor. Since the Yasa P400 is both a PMAC as well as a BLDC, this motor is chosen for the same reasons as stated in section 3.1.2.

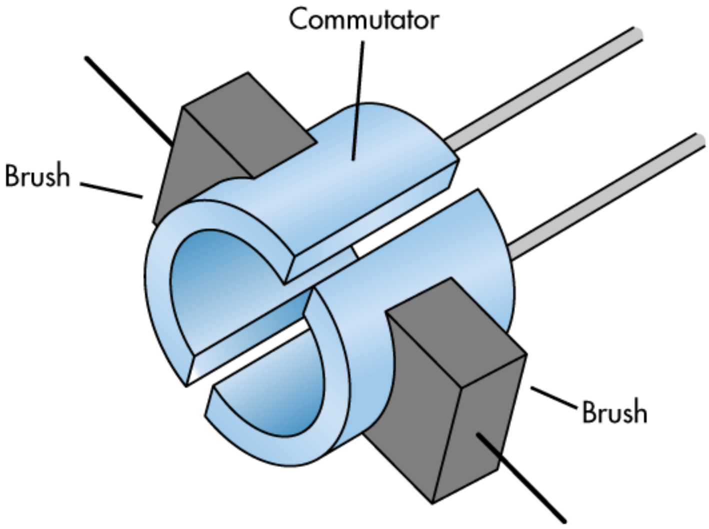

Figure 3.4: Brushed DC motor

3.2.3 One gear gearbox

Since only one gear is used in this concept, it is important that the one gear is sufficient for both acceleration and top speed. Using spiral bevel gears, which have an efficiency of 95-99% , a gear ratio of 1:4 is suitable [12]. Using this gear ratio of 1:4 the speed at maximum RPM can be calculated and also the torque at low RPM.

Considering the maximum RPM of the electric motor, 8000 RPM, and the established gear ratio of 1:4, the maximum speed of the super bike can be calculated:

$$v = \frac{rpm * 60 * i * \pi * D}{1000} \approx 234km/h \tag{3.1}$$

Also, the peak torque can be calculated. Referring to the data sheet in Appendix C, the peak torque the electric motor can provide is 370 Nm. The gear ratio 1:4 increases the torque to 370*4 = 1480 Nm.

3.2.4 Belt drive

A belt drive consists of a belt and two sheaves. One on the axle of the rear wheel and one on the out going shaft of the gearbox. A belt drive is smoother, quieter and cleaner than a chain drive. Additionally, belt drives have the potential to last for a very long time, often up to 150,000 kilometers, if properly maintained. However slip can occur in belt drives at high torque [13]. Additionally belts drives are less efficient than chain drives, so there is more powerloss in a belt drive than in a chain drive. Advancements in belt technology, like teethed belts, have alleviated some of these problems, but in general chains are more efficient.

3.3 Concept 3 - Red

The design choices of concept 3 are noted by the red dots in Figure 2.1. A drawing of concept 3 can be found in Figure 3.5 and an enlarged version of the concept drawing is presented in A.3.

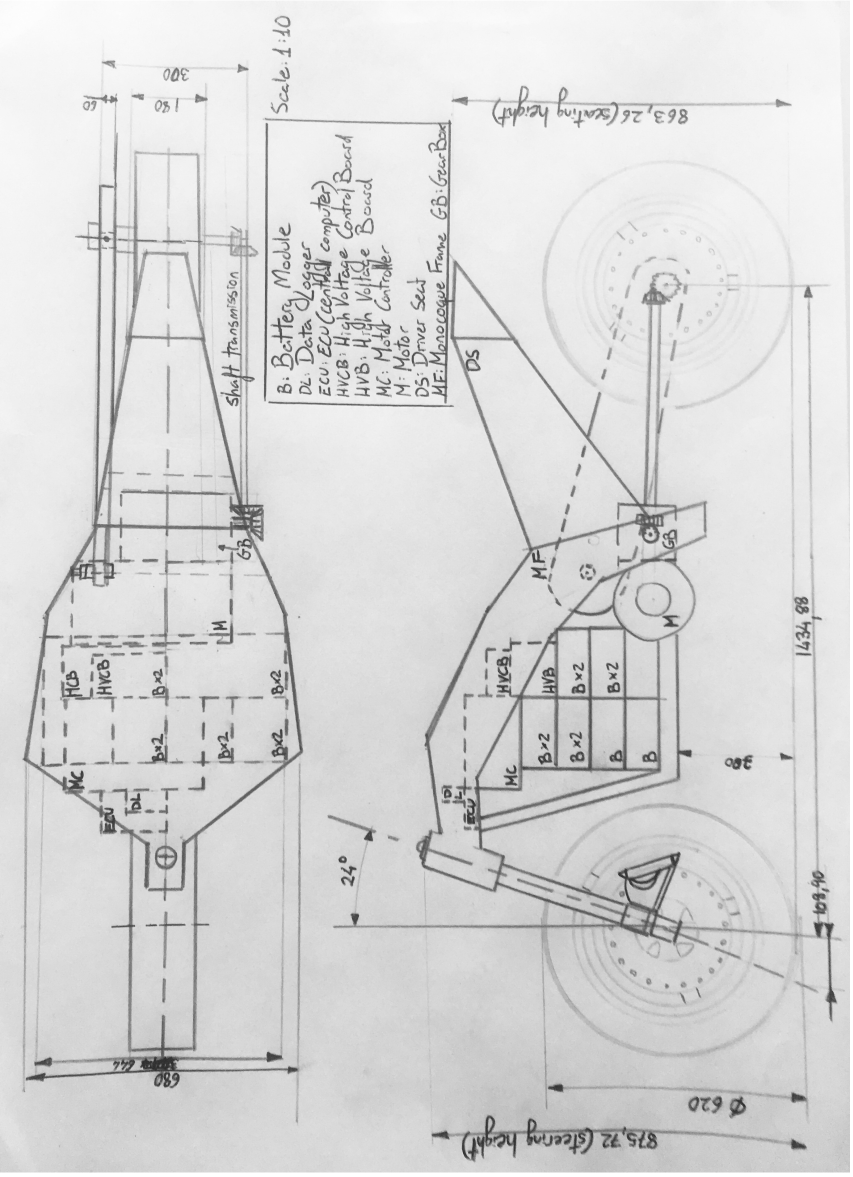
Scale 1:10
B: Battery Module
DL: Data Logger
ECU: ECU (central computer)
HVCB: High Voltage Control Board
HVB: High Voltage Board
MC: Motor Controller
M: Motor
DS: Driver Seat
MF: Monocoque Frame
GB: GearBox
shaft transmission
300
180
60
863,26 (seating height)
1434,88
380
24°
108,90
Ø 620
875,72 (steering height)
680
HCB
HVCB
HVB
B×2
B
MC
ECU
DL
M
GB
MF
DS

Figure 3.5: Drawing of Concept 3

3.3.1 Monocoque frame

The characteristics of a monocoque frame is that loadings are supported by its external skin. A monocoque frame consists of just one part. The materials that are often used for this type of frame are aluminum and carbon fiber. The advantages of this type of frame that is it is durable and that it is light. Other than the external skin, the monocoque frame takes almost no space, leaving a lot of free space for the engine, batteries and the gearbox. The downsides of this type of frame is that it is not rigid enough by itself, some other type of reinforcement is needed. It is also hard to analyse the loadings of the design because of the complex shape.

3.3.2 AC 3 phase induction motor

The AC 3 phase induction motor has a stator and a rotor. The stator is the non moving part located at the outside ring and the rotor is the moving part located on the inside cylinder. When connected to alternating current, the stator produces a rotating magnetic field.

A wire that carries current, produces a magnetic field around it. When you supply 3 phase alternating current to 3 coils laying next to each other, the magnitude of the formed magnetic field of all coils can be determined by the sum of the magnitude of the individual magnetic fields of the individual coils. Due to the arrangement of the coils and the fact that the alternating current is not supplied in phase with each other, the sum of the individual magnetic fields of the individual coils will have a constant magnitude but a different direction in time. This results in a rotating magnetic field. When you now put a closed cycle of conducting wire inside this stator with its rotating magnetic field something special happens. Faraday's law tells that when a closed cycle of conducting wire is exposed to a rotating magnetic field, an electromagnetic field will be induced. This electromagnetic field will produce a current inside the conductor. Lorentz' law tells us that when a conducting loop carrying a current is put inside a rotating magnetic field, it will start rotating along with the rotating magnetic field.

3.3.3 Shaft system

For this concept a shaft system is used to transmit the power from the gearbox to the rear wheel. This shaft is parallel to the drive direction and the rotation is transmitted to the rear wheel by spiral bevel gears. The advantages of using this kind of transmission is that it requires little maintenance. It also increases the stiffness from the rear wheel to the rest of the motorcycle and it acts as a stressed member, so it alleviates part of the loads off of the swingarm. The disadvantages of this transmission are a lower efficiency and that the shaft system heavier than for example a chain or a belt drive. Also there is the danger of a lock up if the down shift does not match the road speed. [14]

3.3.4 Three-geared gearbox

For this concept a three-geared gearbox is used. The advantage over a Two-geared gearbox is that there is also a gear for 'middle' speeds. This will become more beneficial in a circuit with for example a lot of corners, where the driver can now reach a higher power in a consistent manner. The downside of using more gears is that the gearbox will become heavier and that it will require more space.

3.3.5 One-sided swingarm

For this concept a one-sided swingarm is used instead of a two-sided swingarm. The only advantage of this type of swingarm is that maintenance on the rear wheel will be easier. The downsides of these kinds of swingarms are that it needs to be made more heavy than a two-sided one and that all the weight will be at one side.

3.3.6 Concept rating performance

In order to determine the most suitable concept design, a rating scheme was used to grade the concepts. Weighing factors were implemented to ensure that the most important requirements had the highest impact on the grade. In the scheme, 3 was chosen as a high and 1 is low, meaning 3 was in the best condition to meet the requirements. Also some requirements needed a pass to even be able to have a score at all, this was indicated with P (pass) or F (fail). The result of this can seen in Table 3.1 according to the requirements set in Table 2.2.

Table 3.1: Rating scheme of the 3 concepts

	Weighing factor	C1	C2	C3
All components need to be attached to the frame	P/F	P	P	P
The frame must meet the stiffness requirement	2	3	2	1
Bike must withstand the $5kN$ braking force	3	3	3	2
Bike must be able to fit the given dimensions	1	3	3	3
The bike needs to be able to accommodate parts such as the front fork and electro motor	2	3	3	3
A swing arm and spring damper need to be able to be connected to the frame	P/F	P	P	P
The frame can be made with aluminum or steel	P/F	P	P	P
The bike lean angle must be at least 60 degrees	3	1	1	1
Rear wheel must be connected to the motor	P/F	P	P	P
The electric motor needs to be compatible with the other electric components	1	3	3	2
No hub motor or front wheel drive may be used	P/F	P	P	P
There must be a transmission system between the motor and the rear wheel	P/F	P	P	P
The bike must accelerate from 0-100 km/h within 3 seconds	3	3	2	1
The top speed must be at least 200 km/h	2	3	3	2
The superbike must not produce more than 100 dB	1	3	3	3
A geared transmission system must be integrated in the bike	P/F	P	P	P
The motor may provide a maximum power of 160 kW	P/F	P	P	P
The motor must not overheat	P/F	P	P	P
The bike must weigh below 300 kg	2	2	3	1
The width of the bike must not exceed 70 cm	3	2	2	2
The width of the seat must not exceed 40 cm	2	2	2	2
The bike must withstand standard weather conditions	3	3	3	3
Total		71	68	53

As can be seen in Table 3.1 concept one had the highest score, meaning it was the most ideal concept design. Therefore this concept was selected to be optimized.

Chapter 4

Materialisation

To be able to elaborate on the chosen concept, some baseline calculations needed to be done to make sure that all requirements were met. After that calculations were done regarding the drive train and the acceleration of the bike. At last the frame is analysed by using the Matlab FEM-Package.

4.1 Baseline Calculations

4.1.1 Slip conditions

An important requirement of the bike is that it should not slip (especially at low velocity). The static friction is higher than the kinetic friction when it is about to slip. Which means that when the motorcycle starts slipping, the reaction force at the pavement will be lower than the friction force of the pavement when the wheel is about to slip. The motorcycle will have to accelerate as fast as possible. To do so, the force forward and thus the friction force with the pavement needs to be as high as possible. It can be concluded that the rear wheel should never deliver a higher force than the statical friction force of the pavement. Using this statical friction force, the maximum torque at the rear wheel can be calculated. If slip will or will not occur can be calculated by the equation for friction, it is assumed that the coefficient of friction, μ = 2.5 since it is expected that the statical friction coefficient will be lower than the drag coefficient at a drag race which is 4.0 [15] and that it is a bit higher than 1.7 which is the drag coefficient of the Formula 1. The normal force is calculated using the assumed weight of 300 kg.

$$F_F = \mu * F_N \approx 7357.5N \tag{4.1}$$

Using the calculated frictional force and multiplying it by the radius of the wheel, which is 0.31 m, the maximum torque of the shaft of the rear wheel is calculated:

$$T = F_F * R \approx 2280.8Nm \tag{4.2}$$

4.1.2 Motor Power

The battery system can deliver 700 V and 300 A, but the data sheet of the Yasa P400 is at 450 A. To be able to use the power and torque curves the in the specification sheet, the voltage is dropped to get to the needed 450 A. This resulted in a voltage of 467 as can be seen in Equation 4.3. This voltage line was drawn in red in the Power and Torque figure, Figure 4.1 as a red line. It can be seen that at 3000 rpm the motor has an almost constant power of about 110 kW and that the peak torque is maintained from 0 to 3000 rpm.

$$P = U * I = 700V * 300A = 467V * 450A \tag{4.3}$$

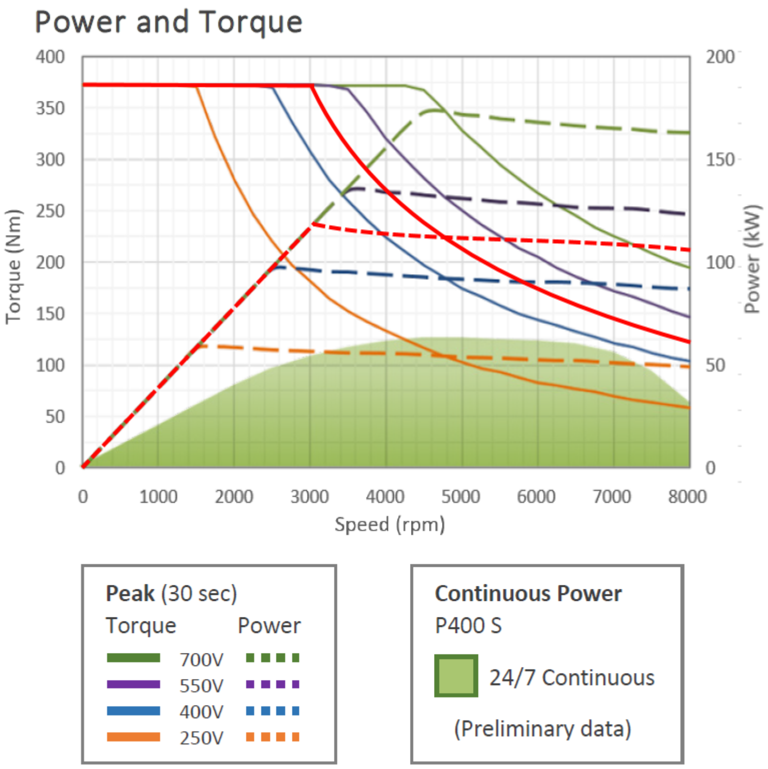

Figure 4.1: Power and Torque curve of the Yasa P400

4.2 Drive Train

Initially the optimal gear ratios are determined for the drive train. After that the maximum bending stresses and contact stresses are determined in the gears. If these would exceed the maximum allowable stresses of the chosen material, the gears would be made thicker. Next the forces on the outgoing shaft of the gearbox were computed and an optimal shaft was designed. Afterwards suitable bearings were found and a suitable way to mount the gears to this shaft was determined.

4.2.1 Gear ratios

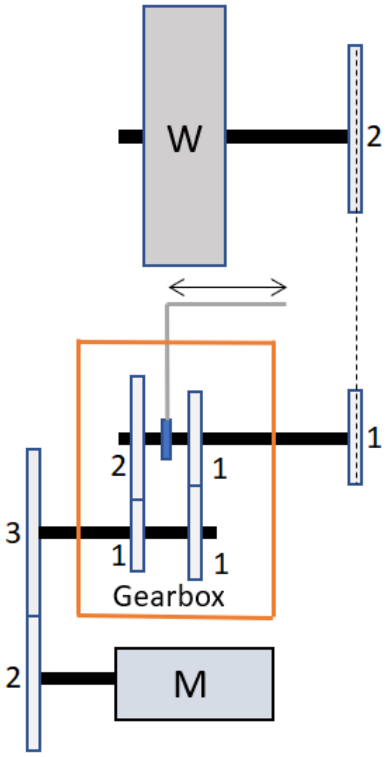

Figure 4.2: Transmission with determined gear ratios

A two geared gearbox was chosen, to provide both high acceleration and a high top speed. The maximum torque at the rear wheel before slipping has been calculated previously and the maximum torque of the motor can be found in the data sheet of the Yasa P400. In Figure 4.1, it can be seen that the motor has an almost stagnant power delivery from 3000 to 8000 rpm at 467 V, so the two gears should have an overlap at these rpms. Also the individual gear ratios can be seen in Figure 4.2 and it can be seen that the overall gear ratios are about 1:6 and 1:3. The reasoning behind the exact amount of teeth, that are shown in the figure, is done later on in this section. An overall gear ratio (VR) of 1:6 and 1:3 are chosen to ensure a measurable difference and an overlap in speed between gears, so no power drop would occur when shifting. It was assumed that the efficiency of a spur gear transition is 99$\%$ [16] and that the efficiency of the chain transmission is 95$\%$. However, an efficiency of 100$\%$ is chosen during stress calculations to generate a worst case scenario for the drive train due to a larger amount of energy going through them.

$$v = \frac{rpm * 60 * D_{wheel} * pi}{VR * 1000} \tag{4.4}$$

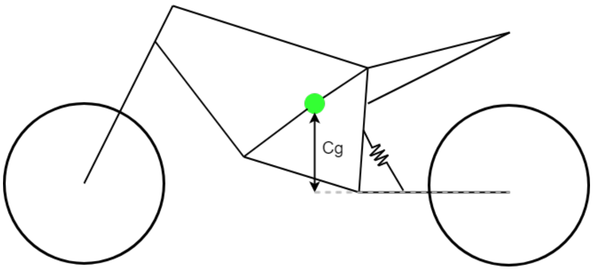

Figure 4.3: Centre of gravity in a motorcycle

Equation 4.4 shows how the speeds at a specific rotational speed and gear selection were calculated, the result can be seen in Table 4.1. Then the torques at the rear wheel at the specific rpm and these gear ratios were calculated according to Equation 4.5. Table 4.1 shows that the overlap between the two gear ratios is about 40 km/h and that there is enough torque to get to 311 km/h to overcome the air resistance, Equation 5.1.1. A drag coefficient, c_d, of 0.2 is assumed because the drag coefficient of a sports car is about 0.2 to 0.3 [17] and a motor is assumed to have a drag coefficient as good as the best sports car. Then a centre of gravity, c_g is assumed to be 0.5 m, a visualisation of this can be seen in Figure 4.3. The The needed torque at 311 km/h is 274.3 Nm, which is less than the 375 Nm that is delivered at that top speed. Also it can be concluded that the tire will not slip because the maximum torque of the rear wheel is 2220 Nm because it was calculated before (see Equation 4.1) that the tire will begin to slip when the torque is over 2280.8 Nm

$$T_{wheel} = T_{motor} * VR \tag{4.5}$$

$$F_D = \frac{1}{2} * \rho * v^2 * A * c_d \approx 548.5N \tag{4.6}$$

$$T = F_D * C_g \approx 274.3Nm \tag{4.7}$$

Table 4.1: The speeds of the different gears at different rpm

Gear ratio	**Rotational speed of the motor**(rpm)	**Speed** (km/h)	**Torque motor** (Nm)	**Torque wheel** (Nm)
1:6	3000	60	370	2220
	8000	155	125	750
1:3	3000	115	370	1110
	8000	311	125	375

4.2.2 Material selection

Material selection is done by looking into often used materials for gears and shafts. The chosen material for the shaft and gears is 25CrMo4 AISI 4130 steel (see Appendix E). It is also visible in this table that the material is suitable for flame or induction hardening. It is chosen to use grade 2 hardening, resulting in an allowable bending stress of 379.2 MPa and an allowable contact stress of 1310 MPa. The density of this material is 7850 kg/m^3. This is a material that is also already used in the Moto-E competition.

For the gearbox housing aluminium type 357 T6 was used because of the low density of 2700 kg/m^3. This material is commonly used in the automotive industry for similar purposes.

4.2.3 Gear design

To determine the right gears and the right gear combination, steps were followed and repeated with all of the gear ratios to determine the right design according to the predetermined estimated gear ratio, which can be seen in Figure 4.7. The steps for the first gear, the 2:3 spur gear, are shown to explain what is done. These steps were repeated afterwards for all other gear combinations. For the gear combinations inside the gearbox, so the 1:2 and 1:1 combinations, the total amount of teeth per combination must be the same and the module must be the same to ensure that the teeth ”bite” into each other. So the amount of teeth of the 1:1 combination should be the same as the amount of the 1:2 combination. The results of the following calculations will be used in the shaft and bearing calculations as well.

The gear that is calculated first is the gear that is on the shaft of the motor. The first step is to choose the lowest amount of teeth of the pinion that is allowed. This led to a choice of 14 teeth. The second step is to chose the number of teeth of the gear. This led to 23, because $N_g = 14 * \frac{3}{2} = 21$, which was not allowed due to a common divider, just like a gear with 22 teeth, therefore 23 teeth were chosen.

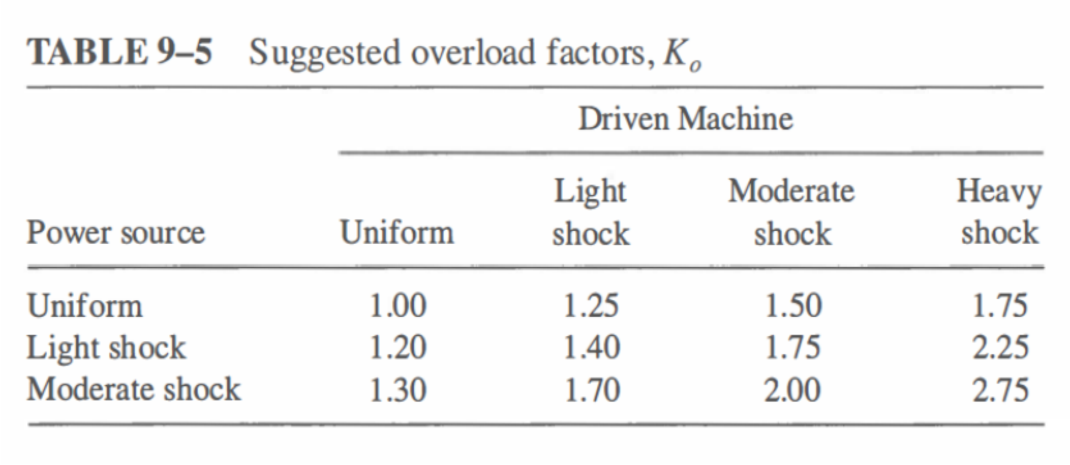

TABLE 9–5 Suggested overload factors, K_o

	Driven Machine			
Power source	Uniform	Light shock	Moderate shock	Heavy shock
Uniform	1.00	1.25	1.50	1.75
Light shock	1.20	1.40	1.75	2.25
Moderate shock	1.30	1.70	2.00	2.75

Figure 4.4: Suggested overload factors, K_0 [18]

After that an overload factor needed to be determined. The overload factor K_0 of 1.75 was chosen, because the power source has some light shock during acceleration and the superbike has moderate shock when going full throttle due to inertia. This overload factor will ensure that the gears and shafts will not break when peak loads occur that are greater than W_t, the tangential force, see Figure 4.5. A standard pressure angle of 20° was chosen, because this is one of the standard pressure angles and therefore a lot cheaper to produce than a custom one.

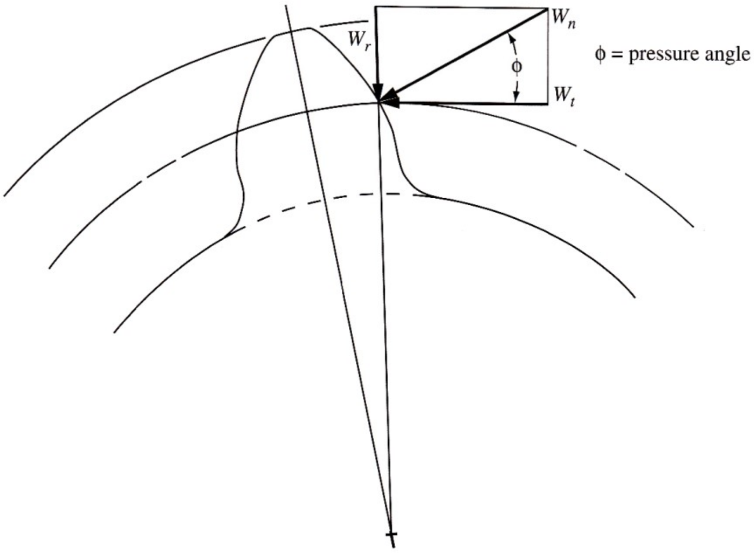

Figure 4.5: Tangential component, W_t [18]

The design power is computed by using Equation 4.8. The 110 kW power from the electric motor can be seen in Figure 4.1. After that a trail value for the module needed to be selected, this value was chosen to be 6. The diameter of the gear was also known because D = module*teeth = 6*14 = 84mm.

$$P_{des} = K_0 * P = 1.75 * 110 = 192.5kW \tag{4.8}$$

Now a specific width of the gear can be selected. To be able to determine the minimal width a ψ_d of 0.6 is chosen, because the gear is most likely carbonised and is in a cantilever position, as can be seen in Figure 4.6. For the gears inside the gearbox, a The maximum gear width is calculated in Equation 4.9. Then a gear width of 50mm is chosen to reduce the stress on the gears as much as possible.

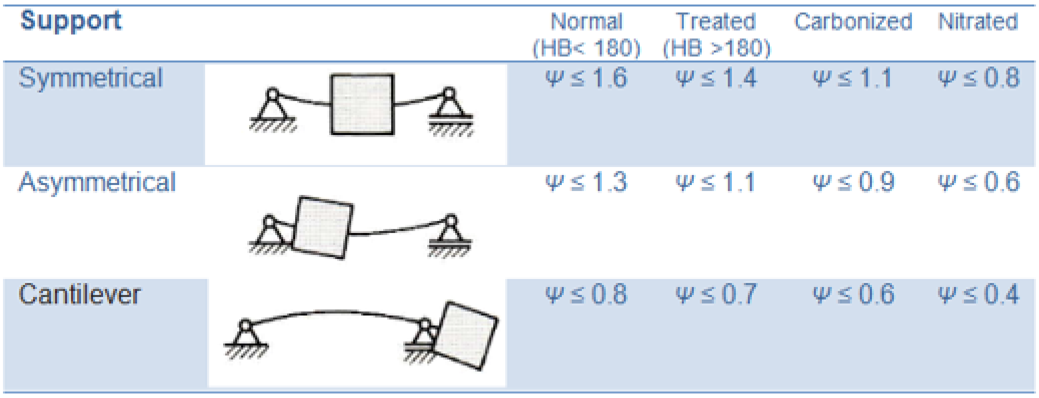

Support		Normal (HB< 180)	Treated (HB >180)	Carbonized	Nitrated
Symmetrical		$\Psi \leq 1.6$	$\Psi \leq 1.4$	$\Psi \leq 1.1$	$\Psi \leq 0.8$
Asymmetrical		$\Psi \leq 1.3$	$\Psi \leq 1.1$	$\Psi \leq 0.9$	$\Psi \leq 0.6$
Cantilever		$\Psi \leq 0.8$	$\Psi \leq 0.7$	$\Psi \leq 0.6$	$\Psi \leq 0.4$

Figure 4.6: Maximum ψ_d choices [**?**]

$$\psi_d = \frac{b_1}{D_1} \leq 0.6 \Rightarrow b_1 \leq D_1 * 0.6 = m * N_p * 0.6 = 6 * 14 * 0.6 = 50.4mm \tag{4.9}$$

Overall gear ratios

Until now a gear ratio of 1:6 and 1:3 was assumed, these cannot be established exactly due to common dividers. The final amount of teeth each gear has can be seen in Figure 4.7 . The final gear ratios are calculated in Equation 4.10 and 4.11

$$VR1 = \frac{14}{23} * \frac{14}{27} * \frac{19}{37} = \frac{1}{6.17} = 0.1621 \tag{4.10}$$

$$VR2 = \frac{14}{23} * \frac{21}{20} * \frac{19}{20} = \frac{1}{3.05} = 0.3282 \tag{4.11}$$

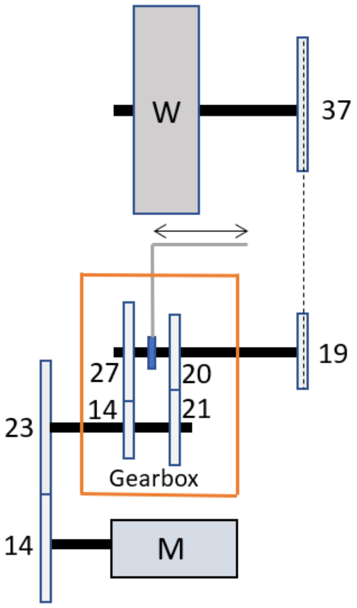

Figure 4.7: Transmission with the amount of teeth per gear

Conclusion

Table 4.2 shows the diameters, thickness and the torques on the different gears. Which gear is what can be seen in Figure 4.7 and the order of gears is from top to bottom in the table is from the motor to the wheel in Figure 4.7.

Table 4.2: Diameters and torques at the different gears

Gear teeth	**Module**	**Diameter** (mm)	**Thickness** (mm)	**Torque** (Nm)
14	6	84	50	612.7
23	6	138	50	1006.7
14	5	70	62	1006.7
27	5	135	62	1941
21	5	105	43	1006.7
20	5	100	43	959
19	10	190	20	1941
37	10	370	20	3781

4.2.4 Bending stress

Now all factors that are required to calculate the maximum bending stresses are known, as can be seen in Equation 4.12. The angular velocity of 3000rpm is chosen, because there the torque is at a maximum, as can be seen in Figure 4.1. Then the angular force on each tooth is calculated according to Equation 4.13. Finally the bending stress is calculated according to Equation 4.14. The value of 3.35 for the Y_{fa} is chosen from Figure 4.8.This will result in undercutting, but it was neglected, because this would otherwise result in difficult calculations.

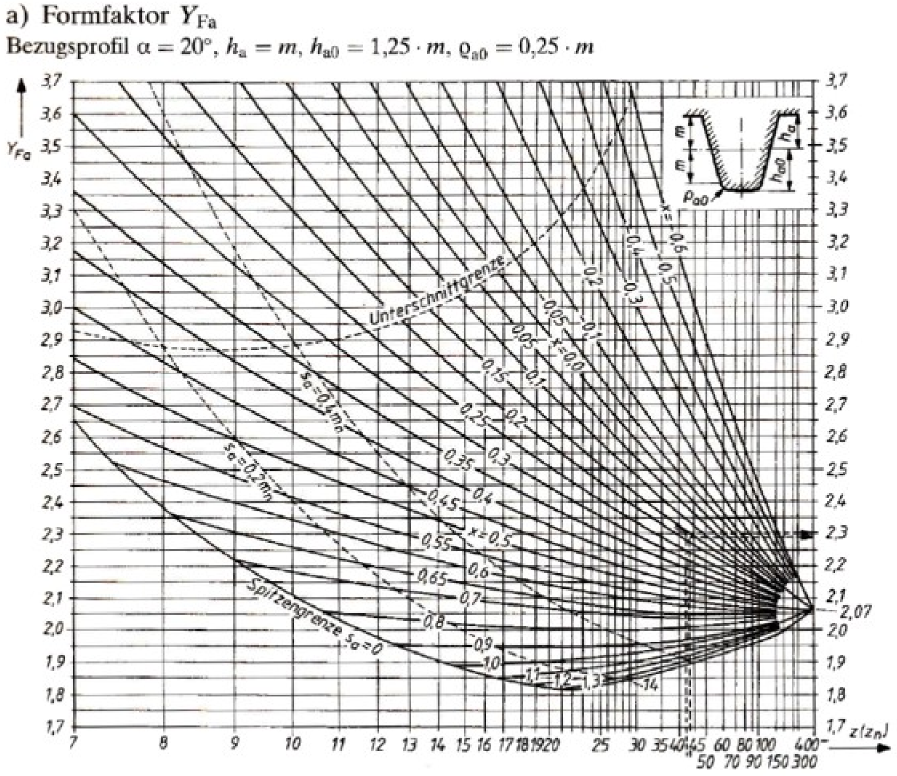

Figure 4.8: Form factor Y_{fa} for standard metric module based gears [18]

$$T_{max} = \frac{P_{des}}{\omega} = \frac{192,5 * 10^3}{3000/60 * 2 * \pi} = 612.7Nm \tag{4.12}$$

$$F_t = \frac{T}{1/2 * D_1} = \frac{612.7}{0.5 * 50 * 10^{-}3} = 24.5kN \tag{4.13}$$

$$\sigma_{bend} = \frac{F_t}{b * m} * Y_{fa} = \frac{24508}{50 * 6} * 3.35 = 273.7MPa \tag{4.14}$$

To be able to calculate the stresses inside the shafts and make detailed drawings, the torques, diameters and thickness of the gears need to be determined. For the calculations, the first gear ratio (1:6) is used because of higher torques that are produced at this gear ratio which is thus a more challenging situation than the second gear. For the gears inside the gearbox a module of 5 is chosen to be able to fit inside the available space (about 250x250x350mm) and reduce the bending stresses inside the gears as much as possible. An added benefit of this approach is that the required thickness will likely decrease.

For the 23 teeth gear that connects to the 14 teeth pinion the torque is the same as at the pinion. The diameter is given by the amount of teeth and the modulus. These knowns can together with the thickness of the gear be seen in Table 4.2.

$$T = T_{pinion} = 612.7Nm \tag{4.15}$$

$$D = 23 * m = 138mm \tag{4.16}$$

The value of ψ_d alternates between 0.6 and 0.9 according to if it is positioned as a cantilever or an asymmetrical gear inside the gearbox. The bending moments were computed to be able to make the best material choice possible according to the exact bending stresses. The value for the form factor were collected from Figure 4.8. Table 4.3 shows the bending stresses and other characteristics which were used to calculate them.

$$D = \frac{P}{\sin 180/N} \tag{4.17}$$

The last two gears are connected with each other by a chain and are therefore called sprockets. In order to find the right dimensions for these sprockets, first the design power must be computed. Lets assume that there is no power loss between the motor and the sprocket, then the power will be 110 kW. The design factor will become 1.3 when looking at Table 7-8 of the Machine Elements lecture notes [18]. Which will result in a design power of 143 kW. The nominal speed ratio that is needed is 2:1 so a small sprocket is chosen with 19 teeth and a big sprocket with 37 teeth. The small sprocket is chosen to have more than 17 teeth because when this sprocket has less than 17 teeth the difference in speed in the chain will become to big which would cause the polygon effect. The chain that is used is a chain number 100 single stranded. This results in a pitch of 15.875mm. Now that the amount of teeth of the sprocket and the pitch is known, the diameters of the sprockets can be calculated by using Equation 4.17. Where P is the pitch and N is the amount of teeth. The results of the diameter can be found in Table 4.3. In Table 4.3 a bending stress is calculated, this is done according to the bending stress for spur gears. It is assumed that the bending stress of a sprocket with chain is a significantly lower than the bending stress for spur gear, therefore the sprockets will not break.

Table 4.3: Diameters and torques at the different gears

Gear teeth	**Module**	**Diameter** (mm)	**Thickness** (mm)	**Torque** (Nm)	$\sigma_{bend}(MPa)$
14	6	84	50	612.7	162.9
23	6	138	50	1006.7	136.2
14	5	70	62	1006.7	311
27	5	135	62	1941	245.8
21	5	105	43	1006.7	254.2
20	5	100	43	959	258.7
19	10	96.4	20	1941	201.4
37	10	187.2	20	3781	202.0

4.2.5 Contact stresses in the gears

After calculating the bending stresses, it is known that the gears will not break due to contact stresses. In this section it is calculated if contact stresses could be the cause of failure.

The value of these stresses can be calculated by using Equation 4.18 where F_t is the normal force on the gear teeth in N, b the width of the gear in mm, D the pitch diameter in mm, u the teeth ratio, Z_h the curvature ratio which is 2.5 for spur gears, Z_e the elasticity factor and E' the reduced E modulus. The E modulus of the material is 210 GPa The values for all gears can be found in Table 4.4 including the maximum contact stress. Looking at the found values, the highest contact stress is 1123 MPa. Since the maximum allowable contact stress of the material is 1310 MPa the gears will not fail.

$$\sigma_h = \sqrt{\frac{F_t}{bD}\frac{u+1}{u}} Z_h Z_e \tag{4.18}$$

$$Z_e = \sqrt{0.175E'}$$

$$\frac{1}{E'} = \frac{1-\nu^2}{E}$$

Table 4.4: Contact stresses in the gear teeth

Gear teeth	**Gear ratio u**	**Diameter** (mm)	**Thickness** (mm)	**Ft** (N)	$\sigma_{contact}(MPa)$
14	23/14	84	50	7294	837
23	23/14	138	50	7294	653
14	27/14	70	62	14381	1123
27	27/14	135	62	14381	809
21	21/20	105	43	9588	1019.7
20	21/20	100	43	9588	1045
19	37/19	190	20	10216	1010
37	37/19	370	20	10216	724

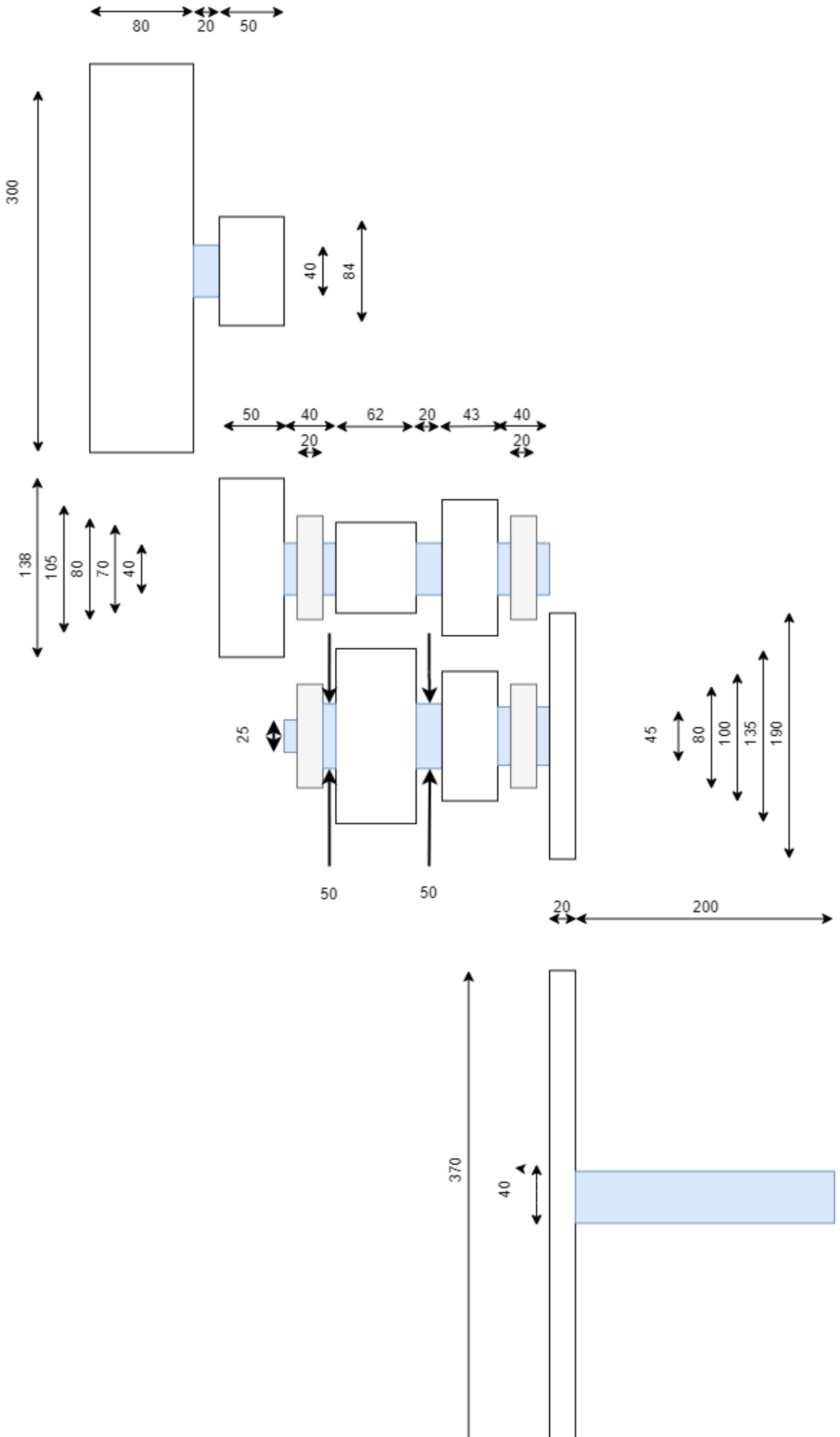
80
20
50
300
40
84
50
40
62
20
43
40
20
20
138
105
80
70
40
25
45
80
100
135
190
50
50
20
200
370
40

4.2.6 Shaft design

For one of the shafts of the drive train a shaft calculation is done. The shaft chosen for this is the outgoing shaft of the gearbox. It is chosen to look at this shaft when the gearbox is in the first gear since the torque on the shaft will be the highest. This shaft can be seen schematically in Figure 4.10. Since the gearbox is in the first gear, the gear with 20 teeth does not have any forces acting on it. The orange rectangles are where the bearings are located.

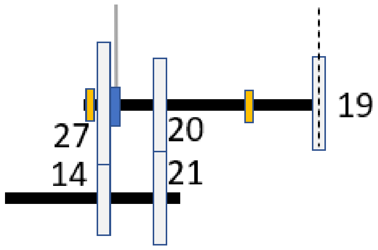

Figure 4.10: Shaft used for the shaft calculations

In order to do a proper shaft calculation, first all of the forces and moments that are acting on the shaft need to be known. These forces are all coming from the 27 toothed gear and the 19 toothed gear on this shaft (see Figure 4.10). The first gear has forces acting on it from another gear. Knowing that the spur gears used have a pressure angle of 20°, the force can be translated to a x and y force. The other gear has forces on it from a chain. A free body diagram of these two gears is show in Figure 4.11.

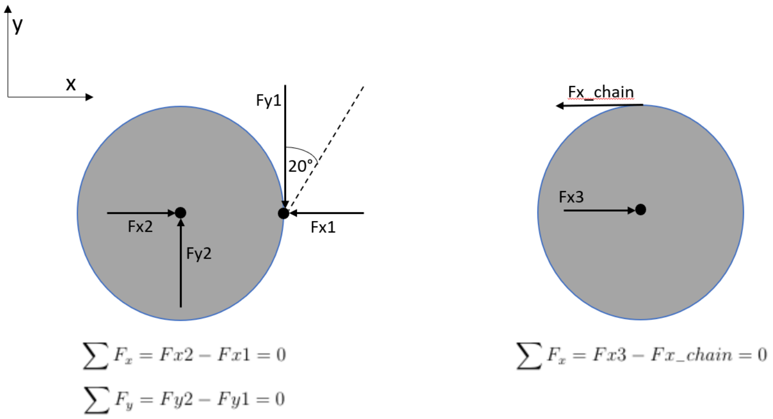
y
x
Fy1
20°
Fx2
Fx1
Fy2
$\sum F_x = Fx2 - Fx1 = 0$
$\sum F_y = Fy2 - Fy1 = 0$
Fx_chain
Fx3
$\sum F_x = Fx3 - Fx\_chain = 0$

Figure 4.11: FBD of the 27 toothed gear (left) and the 19 toothed gear (right)

The force that is acting on the first gear, by an angle of 20°, can be calculated by using Equation 4.19, where T is the torque, F is the force and r is the radius of the pitch circle of the gear. The values of T and r can be found in the third row of Table 4.3. This results in a force of 28.7kN. This can be translated to a x and y force as can be seen in Equation 4.20. The force that is acting on the second gear can also be calculated by Equation 4.19, by using the seventh gear of Table 4.3, which results in a Fx_chain of 10.2kN and thus Fx3 is also 10.2kN.

$$T = F * r \implies F = \frac{T}{r} \tag{4.19}$$

$$Fy1 = Fy2 = F{*}cos(20) = 27kN \quad and \quad Fx1 = Fx2 = F{*}sin(20) = 9.8kN \tag{4.20}$$

Next to the gears there are also two bearings located on the shaft. These bearings are required to apply reaction forces to the shaft. These bearings will restrain all translations of the shaft, leaving only a rotation around the z axis. The free body diagrams of the shaft, from 2 angles, can be seen in Figure 4.12 and the equilibrium equations can be found in Equations 4.21 4.22 4.23 4.24. Now there are four equilibrium equations so the four bearing forces can now be calculated. The values of all forces in the shaft can be found in Table 4.5.

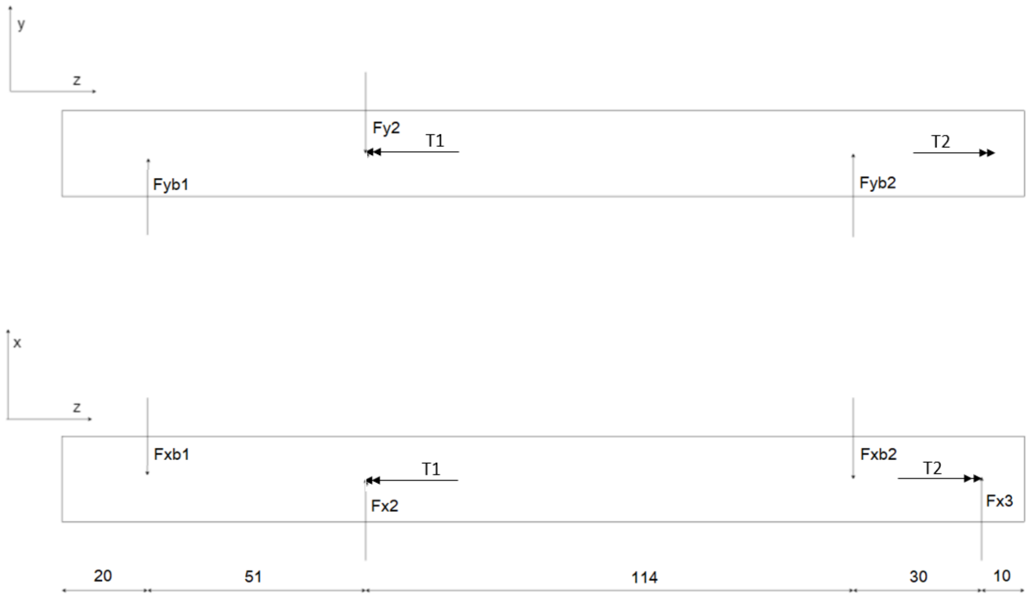

Figure 4.12: FBDs of the outgoing shaft

$$\sum F_x = -Fxb1 + Fx2 - Fxb2 + Fx3 = 0 \tag{4.21}$$

$$\sum F_y = Fyb1 - Fy2 + Fyb2 = 0 \tag{4.22}$$

$$\sum My_{bearing1} = -0.051 * Fy2 + 0.165 * Fyb2 = 0 \tag{4.23}$$

$$\sum Mx_{bearing1} = 0.051 * Fx2 - 0.165 * Fxb2 + 0.195 * Fx3 = 0 \tag{4.24}$$

Table 4.5: Forces on the shaft

Name	Force
Fy2	27 kN
Fx2	9.8 kN
Fx3	10.2 kN
Fyb1	18.7 kN
Fyb2	8.3 kN
Fxb1	4.9 kN
Fxb2	15.1 kN

Now that all forces are known the diameters of the shaft can be calculated. In order to do that, shear, moment and torque diagrams of the shaft should be made. These diagrams can be found in Figure 4.13 and an enlarged version can be seen in Appendix G. To calculate the minimum required diameter of the shaft when it experiences both a moment and torsion, the following equation is used:

$$D = \sqrt[3]{\frac{32N}{\pi}\sqrt{(\frac{K_t M}{s_n})^2 + \frac{3}{4}(\frac{T}{s_y})^2}} \tag{4.25}$$

Another equation exists with which the minimal diameter can be calculated, using only the shear force, when there is no moment and no torsion applied.

$$D = \sqrt{\frac{2.94K_t(V)N}{s_n}} \tag{4.26}$$

Where M is the applied moment, T is the applied torsion, s_n is the fatigue limit of the material and s_y is the yield limit of the material which are s_n = 460 MPa and s_y = 560 MPa. K_t and N are constants, dependent on the geometry and the material respectively. Considering that this calculation is executed on a gearbox, which experiences dynamic loading, a N-safety factor is used of 2.0, since the loadings are known. The value for K_t is dependent on the geometry and it is in this case dependent on the radius of the fillets of the changes in diameter. Considering that the bearings will be pressed against the shaft upon a change in diameter, a sharp fillet is required. Thus a value of 2.5 is used for K_t.

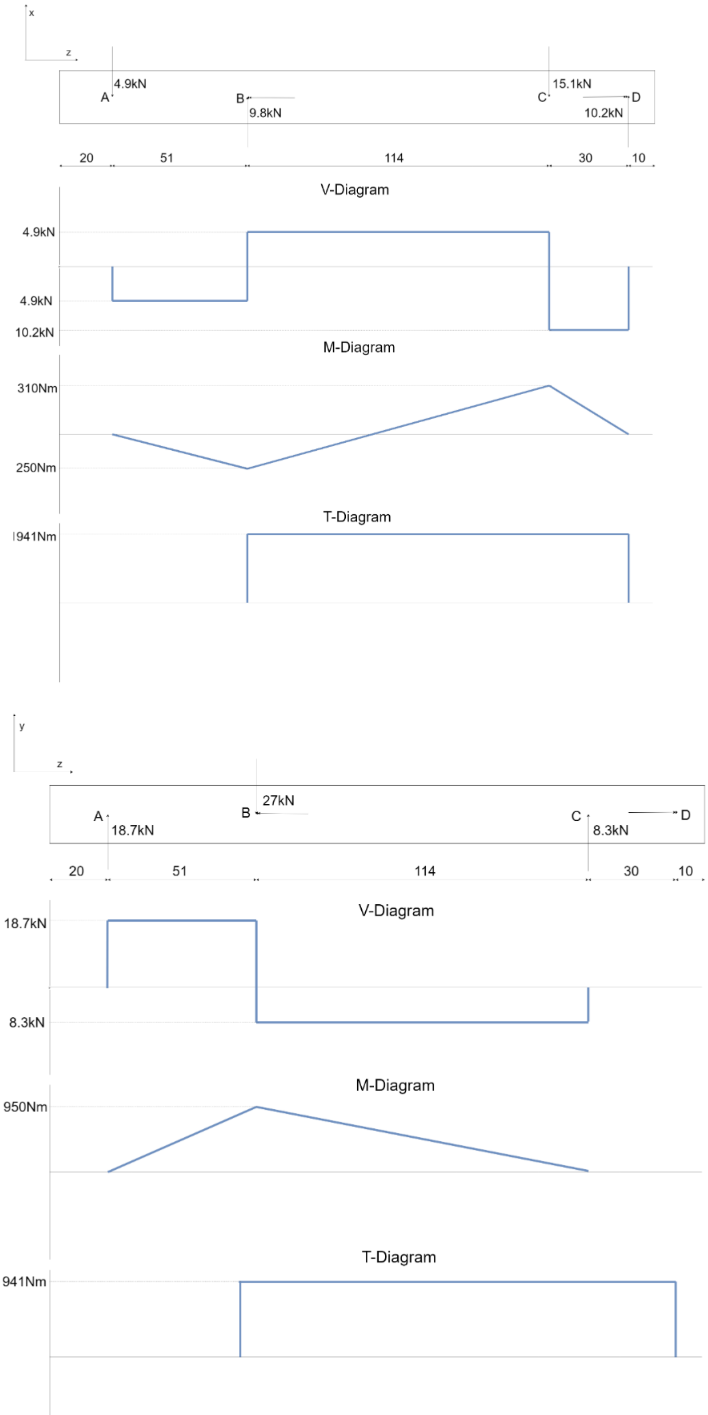
x
z
4.9kN
A
B
9.8kN
15.1kN
C
D
10.2kN
20
51
114
30
10
V-Diagram
4.9kN
4.9kN
10.2kN
M-Diagram
310Nm
250Nm
T-Diagram
941Nm
y
z
27kN
A
18.7kN
B
C
8.3kN
D
20
51
114
30
10
V-Diagram
18.7kN
8.3kN
M-Diagram
950Nm
T-Diagram
941Nm

Figure 4.13: The FBDs of the outgoing shafts with its shear, moment and torsion diagrams. Enlarged versions can be found in Appendix G

Considering the first part of the shaft from the left side until point A, before which any moment or torsion is applied, Equation 4.26 can be used. The shear force in this part can be calculated by the following Equation:

$$V = \sqrt{(4900)^2 + (18700)^2} = 19331.3N \tag{4.27}$$

Entering this value in Equation 4.26 gives the following diameter.

$$D = \sqrt{\frac{2.94 * 2.5 * 19331.3 * 2}{460 * 10^6}} = 24.85mm \tag{4.28}$$

This value is rounded up to 25mm so that it is possible to find a suitable bearing.

The second part of the shaft, from point A until point C, can be calculated by using Equation 4.25. The value for the torsion is taken as 1941Nm, since this does not change. The applied moment in this part of the shaft reaches its maximum at point B, where it can be calculated by the following equation:

$$M = \sqrt{(950)^2 + (250)^2} = 982Nm \tag{4.29}$$

Entering this values in Equation 4.25 yields the following result.

$$D = \sqrt[3]{\frac{32 * 2}{\pi}\sqrt{(\frac{2.5 * 982 * 10^3}{460 * 10^6})^2 + \frac{3}{4}(\frac{1941 * 10^3}{560 * 10^6})^2}} = 49.97mm \tag{4.30}$$

This value is rounded up to 50mm, so that a suitable bearing can be found.
The last part of the shaft, from point C until the right end, can be calculated once again by using Equation 4.25. Since the moment in the x-z plane is the only moment that is present, this moment of 310 Nm will be used to calculate the required diameter. The applied torsion is the same as for part AC, 1941 Nm.

$$D = \sqrt[3]{\frac{32 * 2}{\pi}\sqrt{(\frac{2.5 * 310 * 10^3}{460 * 10^6})^2 + \frac{3}{4}(\frac{1941 * 10^3}{560 * 10^6})^2}} = 41.24mm \tag{4.31}$$

This value of 41.24 mm is rounded up to 45 mm so that a suitable bearing may be found.

Now that the diameter of the shaft and the loads that are applied on the bearings are known a suitable bearing can be found [19]. The chosen bearings can be seen in Figure 4.15. The bearings are chosen after evaluating the applied forces which can be seen in Table 4.5, and taking the calculated diameter(s) of the shaft portions in consideration. These bearings will be clamped into wall of the gearbox so that the outer diameter will not rotate or move.

4.2.7 Key design

Now that the shaft diameter is known, the calculation for the connection of the gear to the shaft can be done. Since a key is a cheaper option than a spline, this option is chosen. To find the dimensions of the key, various steps have to be performed. First of all the width and height of the key should be determined. According to DIN

6885, [20], a shaft with a diameter of 50mm, requires a key with a width of 16mm and a height of 10mm.
Now a material should be chosen for the key, typically C45 steel is used.

Table 4.6: Yield Strength of the involved parts

Part	Yield Strength
Key	340 N/mmˆ2
Shaft	460 N/mmˆ2
Gear	460 N/mmˆ2

Now a safety factor should be incorporated, since the super bike will be in operation for relatively short periods, a safety factor N, of 2 is assumed. This leads to new allowable shear and compressive forces:

$$\tau = 0.5 * \frac{\sigma_y}{N} = 85 N/mm^2 \tag{4.32}$$

$$\sigma = \frac{\sigma_y}{N} = 230 N/mm^2 \tag{4.33}$$

Then the length of the key can be calculated by Equations 4.34 and 4.35. In these equations, the gear with the maximum amount of torque is used, with a value of 1941 Nm of torque. d is the diameter of the shaft and b and h are the width and height of the key. τ and σ are the previously calculated values.

$$\tau = \frac{F}{A_s} = \frac{2 * T}{d * b * l} \rightarrow l = 57mm \tag{4.34}$$

$$\sigma = \frac{F_t}{Ac} = \frac{4 * T}{d * h * l} \rightarrow l = 67.5mm \tag{4.35}$$

Both of these values are the minimum length that is required of the key. Since the thickness of the gear is 62mm, it can be seen that the key would have to be longer than the gear itself, and thus it is not possible to use a key in this situation, so a spline will have to be used.

4.2.8 Spline design

As was established before, it is impossible to use a key to secure the gears and a thus a spline will be used. First, an equation should be established to be able to calculate the dimensions of the spline. This can be calculated by the following equation, where N is the amount of splines, D is the major diameter, and d is the minor diameter:

$$T = 1000 * N * \frac{(D^2 - d^2)}{8} \tag{4.36}$$

The gears should be connected to the shaft by a permanent fit spline, since they should not move under loading.

Table 4.7: Spline Dimensions

Splines	Width	Height	Minor Diameter
Six	0.250D	0.050D	0.900D

$$T = 1000 * 6\frac{D^2 - 0.7396D^2}{8} = 142.5D^2(U.S.) \rightarrow T = 3619.5D^2(S.I.) \tag{4.37}$$

Thus the diameter can be calculated by:

$$D = \sqrt{\frac{T}{3619.5}} = 23.2mm \tag{4.38}$$

Thus, the required diameter is less than the diameter of the shaft. This means that the spline is able to withstand the forces regardless of the diameter of the spline, since the shaft diameter is larger than the minimum spline diameter. Since the shaft diameter is 50mm, the minor diameter d should be equal to the shaft diameter. From this the width, major diameter and height of the splines can be calculated according to Table 4.7.

Table 4.8: Spline Dimensions

Minor diameter (d)	Major diameter (D)	Height (h)	Width (W)
50 mm	55.6 mm	2.8 mm	13.9 mm

In Figure 4.14 the dimensions of the spline can be seen.

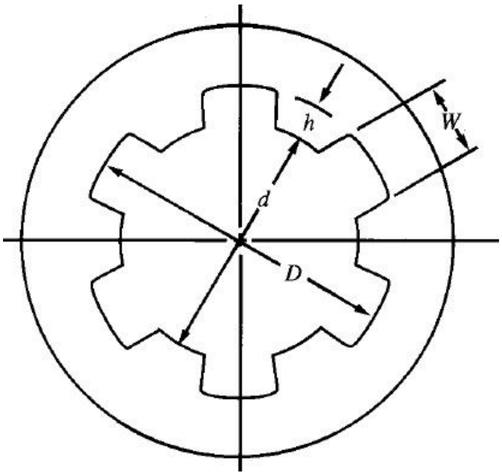

Figure 4.14: Spline Dimensions

Now that the dimensions of the spline, and the keys on the spline are known, the shear stress and the compression stress in any individual key can be calculated. This can be done by using Equation 4.34 and 4.35. There is assumed that the length of the spline is equal to the thickness of the gear, in this case 63mm:

$$\tau = \frac{F}{A_s} = \frac{2 * T}{d * b * l} \rightarrow \tau = 88.03MPa \tag{4.39}$$

$$\sigma = \frac{F_t}{Ac} = \frac{4 * T}{d * h * l} \rightarrow \sigma = 880.27MPa \tag{4.40}$$

These shear and compressive stresses are the total stresses. Considering that the spline has 6 keys, the final shear stress and compressive stress for each individual key can be calculated as follows:

$$\frac{88.03}{6} = 14.67MPa \tag{4.41}$$

$$\frac{880.27}{6} = 146.71MPa \tag{4.42}$$

Since the spline is made of the same material as the shaft, the maximal shear stress and compressive stress need to be recalculated, using the actual yield strength of the material.

$$\tau = 0.5 * \frac{\sigma_y}{N} = 115MPa \tag{4.43}$$

$$\sigma = \frac{\sigma_y}{N} = 230MPa \tag{4.44}$$

Since the calculated shear and compressive stresses are lower than the allowed shear and compressive stresses, the calculated spline is sufficient. This spline is also sufficient for the other gear, which experiences $\frac{959}{1941} = 0.495$ times the the forces, but is $\frac{62}{43} = 1.5$ times as thick, resulting in a shear stress and compressive stress that is $0.495 * 1.5 = 0.7425$ times the previously found shear stress in Equations 4.41 and 4.42.

The final gear on the shaft has not yet been calculated, this gear has a thickness of 20mm, and experiences the same torque, 1941 Nm. Using the same spline in this situation will result in forces that are $\frac{62}{20} = 3.1$ times as high, which results in 454.8 MPa which exceeds the value established in Equation 4.44. Thus, a spline with more than 6 keys needs to be used. In this case, it is assumed that 16 separate keys will be sufficient. First, the dimensions relative to the diameter are given, assuming that the spline is a permanent fit:

Table 4.9: Spline Dimensions

Splines	Width	Height	Minor Diameter
Sixteen	0.098D	0.045D	0.910D

Since the shaft diameter is 45mm, the minor diameter of the spline is 45mm. This gives the following dimensions.

Table 4.10: Spline Dimensions

Minor diameter (d)	Major diameter (D)	Height (h)	Width (W)
45 mm	49.45 mm	2.23 mm	4.85 mm

$$\tau = \frac{F}{A_s} = \frac{2 * T}{d * b * l} \rightarrow \tau = 889.35 MPa \tag{4.45}$$

$$\sigma = \frac{F_t}{Ac} = \frac{4 * T}{d * h * l} \rightarrow \sigma = 3868.46 MPa \tag{4.46}$$

This shear stress and compressive stress are the total stresses. Considering that the spline has 16 different keys, the final shear stress and compressive stress can be calculated as follows:

$$\frac{889.35}{16} = 55.6 MPa \tag{4.47}$$

$$\frac{3868.46}{16} = 241.8 MPa \tag{4.48}$$

While the shear stress is acceptable, the compressive stress exceeds the 'safe' compressive stress of 230 MPa. This is deemed acceptable, since a safety factor of 2 is used, and the superbike is only in operation for a short time during the race.

4.2.9 Shaft technical drawing

Now that all of the dimensions of the shaft, its splines, and the appropriate bearings have been found, a technical drawing is made with all the dimensions and the bearings in it.

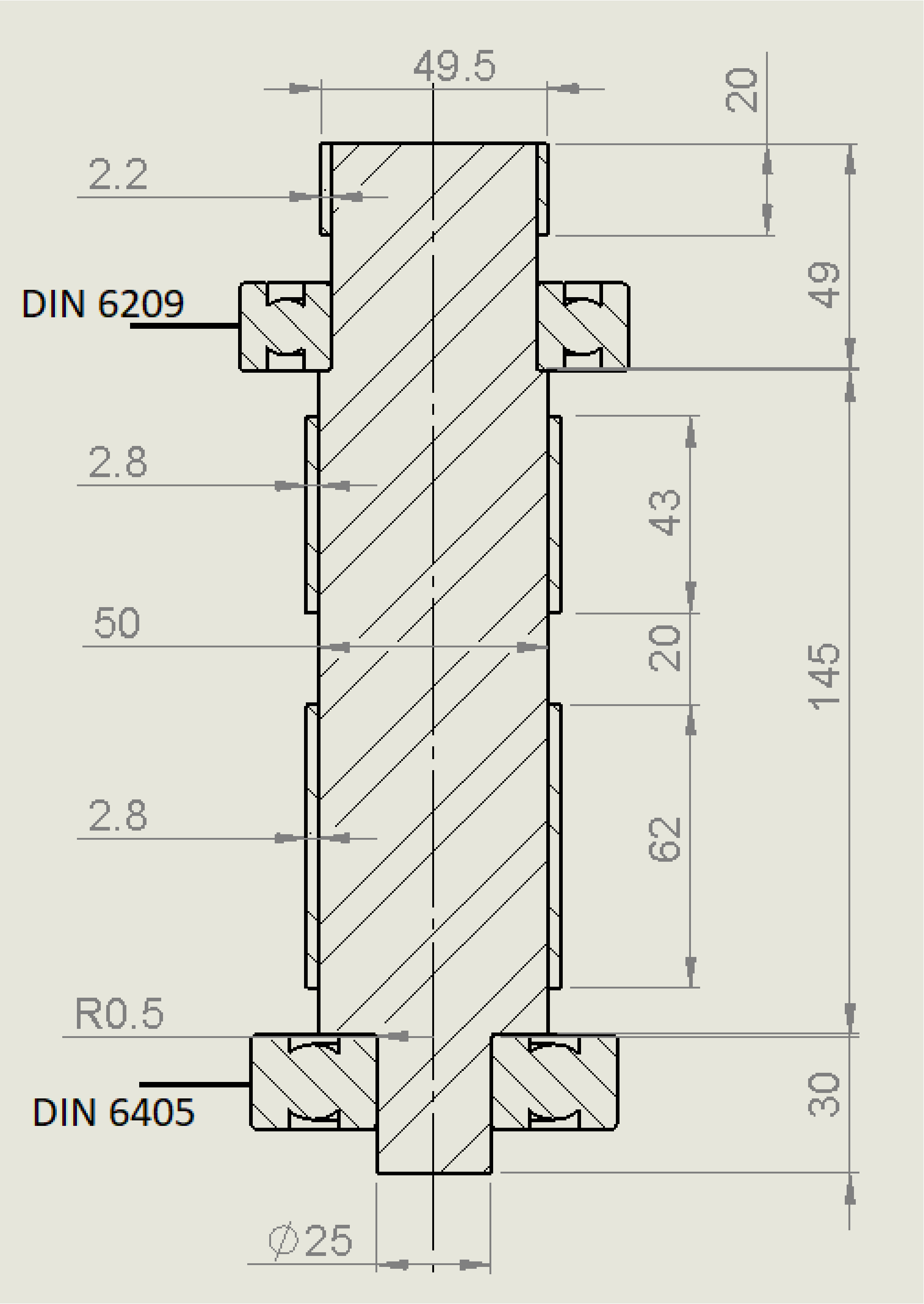
49.5
2.2
DIN 6209
2.8
50
2.8
R0.5
DIN 6405
∅25
20
49
43
20
145
62
30

Figure 4.15: Technical drawing of the shaft and its bearings

4.3 Mohr's Circle

A Mohr's circle is used to illustrate the normal and shear stresses on the subject. The outgoing shaft of the gearbox is chosen as the subject. The shear, moment and torsion diagrams of the outgoing shaft are displayed in Figure 4.13. Because the moments are vectors the total vector can be calculated using Pythagoras, as can be seen in Equation 4.49 where it is calculated at point B. The total moment is at a maximum at point B, therefore this point is used for the Mohr's circle. In Figure 4.16 the situation is visualised. This figure displays the situation of the shaft perfectly, except that the y and z are switched around.

$$M_{tot}(B) = \sqrt{950^2 + 250^2} = 982Nm \tag{4.49}$$

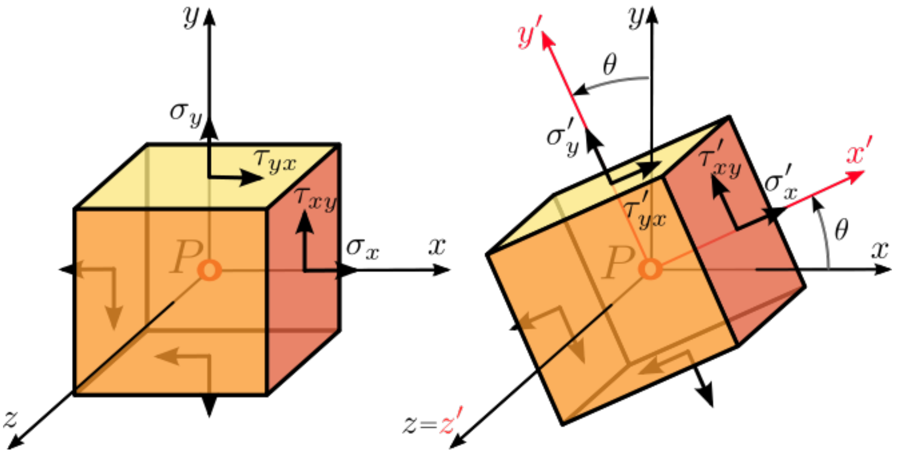

Figure 4.16: Stress situation at point B, [21]

Now it is known that the highest moment is at point B, the normal stress is calculated for both of the FBD's and added up afterwards. These calculations can be seen in Equation 4.50. The shear stress is calculated in Equation 4.51.

$$\sigma_z = \frac{M}{\frac{\pi}{32}D^3} => \sigma_{z,Mx} = \frac{250}{\frac{\pi}{32}0.05^3} = 20.4MPa \wedge \sigma_{z,My} = \frac{950}{\frac{\pi}{32}0.05^3} = 77.4MPa \tag{4.50}$$

$$\tau_{xy} = \frac{T}{\frac{\pi}{16}D^3} = \frac{1941}{\frac{\pi}{16}0.05^3} = 79.1MPa \tag{4.51}$$

$$\sigma_{tot} = \sigma_{z,Mx} + \sigma_{z,My} = 90.8MPa \tag{4.52}$$

Now that the total normal stress and the shear stress are known, the centroid and the radius of the outgoing shaft of the gearbox can be calculated as can be seen in Equation 4.53 and 4.54. At this point the fact that stress in the y direction is zero will be used.

$$\sigma_{avg} = \frac{\sigma_{ztot} + \sigma_y}{2} = \frac{90.8 + 0}{2} = 45.4MPa \tag{4.53}$$

$$\tau_{max} = R = \sqrt{(\frac{\sigma_z + \sigma_y}{2})^2 + \tau_{xy}^2} = \sqrt{(\frac{90.8 + 0}{2})^2 + 79.1^2} = 91.2MPa \tag{4.54}$$

Now all data from the stress analysis is used to make the Mohr's circle to graphically determine the stress components acting on a differently oriented plane passing through point B. The Mohr's circle is drawn in Figure 4.17. To check if the Mohr's circle is correct the orientation of the principle stresses can be determined and checked with the figure. The required calculation can be seen in Equation 4.55 and this angle is the same as in Figure 4.17, the outcome is therefore correct.

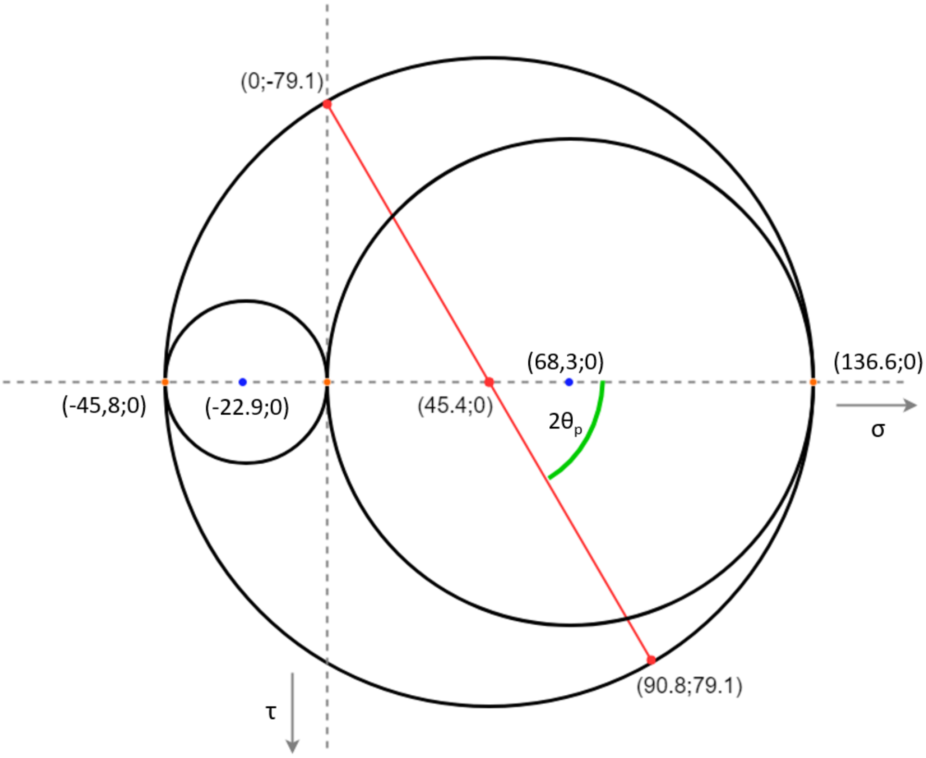

Figure 4.17: Mohr's circle of the outgoing shaft of the gearbox

$$\tan(2\theta_p) = \frac{\tau_{xy}}{(\sigma_y - \sigma_z)/2} => 2\theta_p = \arctan(\frac{\tau_{xy}}{(\sigma_y - \sigma_z)/2}) = \arctan(\frac{79.1}{(0 - 90.8)/2}) = -60.15^\circ \tag{4.55}$$

In the Mohr's circle the absolute shear stress, and the maximum and minimum normal stresses are displayed graphically. These are calculated in Equation 4.57

and 4.56. This means that the maximum and minimum normal stresses are 136.6 MPa and -45.8 MPa respectively. The orientation of the block, as displayed in Figure 4.16, 2 principle stresses are found. Therefore the second principle stress is 0 since the minimum and maximum principle stress are σ_1 and σ_3 respectively. These are calculated in Equation 4.56 and 4.57. Then the middle points and the radii can be calculated. The middle points are done in a similar way to Equation 4.53, the radii of the circles are calculated according to Equation 4.58

$$\sigma_1 = \frac{\sigma_z - \sigma_y}{2} - \sqrt{(\frac{\sigma_z + \sigma_y}{2})^2 + \tau_{xy}^2} = \frac{90.8 + 0}{2} - \sqrt{(\frac{90.8 + 0}{2})^2 + 79.1^2} = -45.8MPa \tag{4.56}$$

$$\sigma_3 = \frac{\sigma_z - \sigma_y}{2} + \sqrt{(\frac{\sigma_z + \sigma_y}{2})^2 + \tau_{xy}^2} = \frac{90.8 + 0}{2} + \sqrt{(\frac{90.8 + 0}{2})^2 + 79.1^2} = 136.6MPa \tag{4.57}$$

$$R = \frac{\sigma_{min} + \sigma_{max}}{2} \tag{4.58}$$

After finding the principle stresses, the Von Mises yield criterion should be used to determine if the material can handle these principle stresses. This is checked in Equation 4.59 and the result is that it passes this test, because the yield strength of AISI 41030 is between 320 and 400 MPa, and this is higher than the 232.4 MPa from the Von Mises yield criterion.

$$\sigma_{yield} > \sqrt{\frac{(\sigma_1 - \sigma_2)^2 + (\sigma_2 - \sigma_3)^2 + (\sigma_3 - \sigma_1)^2}{2}}$$
$$= \sqrt{\frac{(136.6 - 0)^2 + (0 - -45.8)^2 + (-45.8 - 136.6)^2}{2}} = 232.4MPa \tag{4.59}$$

4.3.1 Conclusion

In conclusion, the Mohr's circle was used to find that the shaft can handle the principle stresses, that the maximum shear stress is 91.2MPa and that minimum and maximum principle stresses are -45.8 and 136.6MPa respectively.

4.4 Acceleration

There are three major kinds of resistances that the superbike needs to overcome: the total moment of inertia of the drive train, the rolling resistance and the air resistance. When all those resistances are known the effective acceleration of the superbike can be calculated.

4.4.1 Inertia

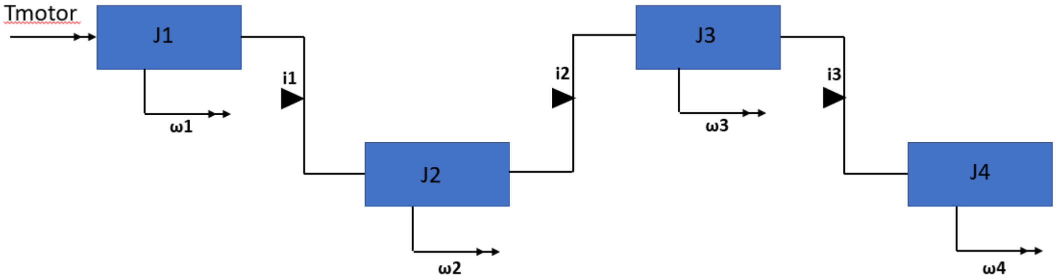

Figure 4.18: Schematic sketch of the transmission

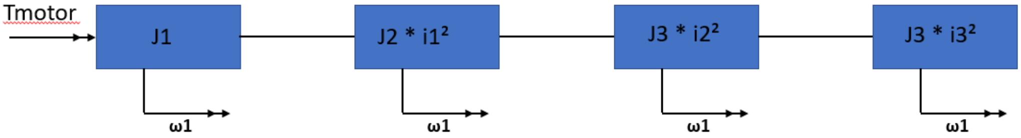

Figure 4.19: Reduced schematic sketch of the transmission

To be able to calculate the moment of inertia, I, Equation 4.60 was used. The results of these calculations can be seen in Equation 4.62, 4.61 and 4.63 and a visual representation can be seen in Figure 4.18 and 4.19. The thickness of the wheel and rim are assumed to be $31cm$ and $10cm$. The weight of the wheel is assumed to be 10kg. Then the inertia of the chain is neglected, due to the negligible weight. The gear ratios, i_1,i_2 and i_3 are $\frac{14}{23}$,$\frac{21}{20}$ and $\frac{19}{37}$ respectively. The moment of inertia is calculated twice because a two gear gearbox is used. The moment of inertia differs for the two sets of gears.

$$J = \frac{1}{2} * m * r^2 = \frac{1}{8} * \rho * v * D^2 = \frac{\pi}{32} * \rho * b * D^4 \tag{4.60}$$

$$J_{wheel} = \frac{1}{2} * m * r^2 = \frac{1}{8} * m * (D_1^2 + D_2^2) = 0.5305 kg * m^2 \tag{4.61}$$

$$J_{total} = J_1 + J_2 * i_1 + J_3 * i_1 * i_2 + J_4 * i_1 * i_2 * i_3 = 0.1894 \rightarrow if : i_2 = \frac{14}{27} \tag{4.62}$$

$$J_{total} = J_1 + J_2 * i_1 + J_3 * i_1 * i_2 + J_4 * i_1 * i_2 * i_3 = 0.3383 \rightarrow if : i_2 = \frac{21}{20} \tag{4.63}$$

To be able to calculate the acceleration, the weight is calculated of all the parts. In Table 4.11 the weight of the gears and the housing can be seen. The weight of

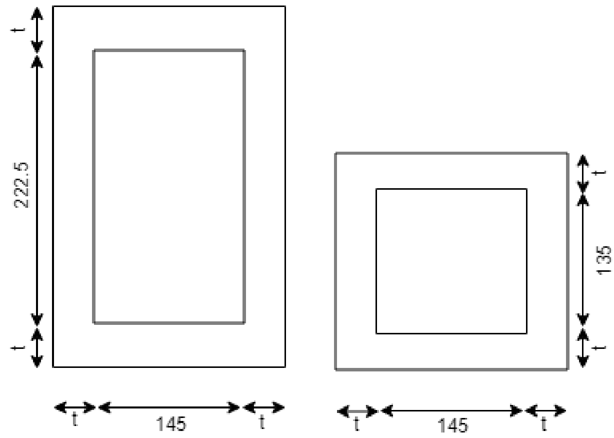

Figure 4.20: Schematic drawing of the gearbox housing

the gears and shafts is calculated according to Equation 4.64 and the weight of the housing is calculated according to Equation 4.65 and 4.66. The dimensions can be seen in Figure 4.20. The density of the gears and axles is 7850kg/m^3, due to the chosen material, AISI 4130 steel. For the housing a density of 2700kg/m^3, this saves about 2/3 of the weight compared to AISI 4130, around 9.5kg, of the gearbox by using aluminium instead of steel.

$$mass_{gear} = \frac{\pi}{4} * D^2 * b * \rho \tag{4.64}$$

$$V_{housing} = V_{out} - V_{in} = (0.145+2t)*(0.2225+2t)*(0.135+2t) - 0.145*0.2225*0.135 = 0.0018m^3 \tag{4.65}$$

$$Mass_{housing} = V_{housing} * \rho = 0.0018 * 2700 = 5.0kg \tag{4.66}$$

Table 4.11: Diameters and torques at the different gears

Part	**Weight** (kg)
Gears and shafts	47.9
Housing	5.0
Total	52.9

4.4.2 Rolling resistance

The rolling resistance can be calculated by the following equation, where C_{rr} is the rolling resistance coefficient, and N is the normal force. N is taken to be 9.81*300 =

2943 N, and C_{rr} is 0.025, according to [22].

$$F_r = C_{rr}N = 73.58N \tag{4.67}$$

4.4.3 Air resistance

The air resistance can be calculated by using Equation 4.4.6. The speed is taken at a value of 27.78 m/s, an estimated drag coefficient of 0.2 (c$_d$), a density of 1.225 kg/m^3 and an estimated frontal area of 0.6 m^2, assuming the bike is 0.6 m wide and 1 m high.

$$F_D = \frac{1}{2} * \rho * v^2 * A * c_d \approx 56.7N \tag{4.68}$$

4.4.4 Total force

To be able to accelerate the bike itself, a force is needed. The acceleration force is calculated in Equation 4.69. Then this force is added up to the air and rolling resistance to get the total force needed. Then the total torque can be calculated according to Equation 4.71

$$F_{acc} = m * a = 300 * \frac{100/3.6}{3} = 2777.8N \tag{4.69}$$

$$F_{total} = F_r + F_D + F_{acc} = 2908.1N \tag{4.70}$$

$$T_{total} = T_{wheel} = F_{total} * 0.5 * D = 2908.1 * 0.5 * 0.62 = 901.5Nm \tag{4.71}$$

4.4.5 Requirement check

$$T_m - T_{wheel} * i = J_{tot} * \frac{d\psi}{dt} => T_m = J_{tot} * \frac{d\psi}{dt} + T_{wheel} * i \tag{4.72}$$

To check if the motor can accelerate to 100km/h within 3 seconds, Equation 4.72 should used. With $\frac{d\psi}{dt}$ should be the angular acceleration, and the torque at the wheel, T_{wheel}, is the torque needed to drive at 100km/h, which can be calculated with the acceleration force. The calculation of air resistance should be calculated at a lower speed, because of the exponential nature of the air resistance, which can be seen in Figure 4.21. The blue line represents the $100km/h$ line. However, by assuming a too high air resistance on average, it is ensured that it can cope with the additional resistances, which were neglected. Since most of the acceleration is expected to be in the first gear, the gear ratio of the first gear is used to calculate the inertia. Therefore the inertia is 0.1894. Then Equation 4.72 is filled is, as can be seen in Equation 4.74, which resulted in a needed torque of 147Nm of the motor. The motor can deliver 370Nm peak therefore it can still accelerate even faster than the required 3 seconds. The total force needed to get to the 100km/h is 2908.1N which is a lot lower than the force that the tires can handle just before slip, which was calculated in Section 4.1.1 to be 7357.5N.

$$\frac{d\psi}{dt} = \frac{a}{\pi D} = \frac{\frac{100/3.6}{3}}{\pi 0.62} = 4.75 rad/s \tag{4.73}$$

$$T_m = 0.1894 * 4.75 + 901.5 * \frac{1}{6.17} = 147.0Nm \tag{4.74}$$

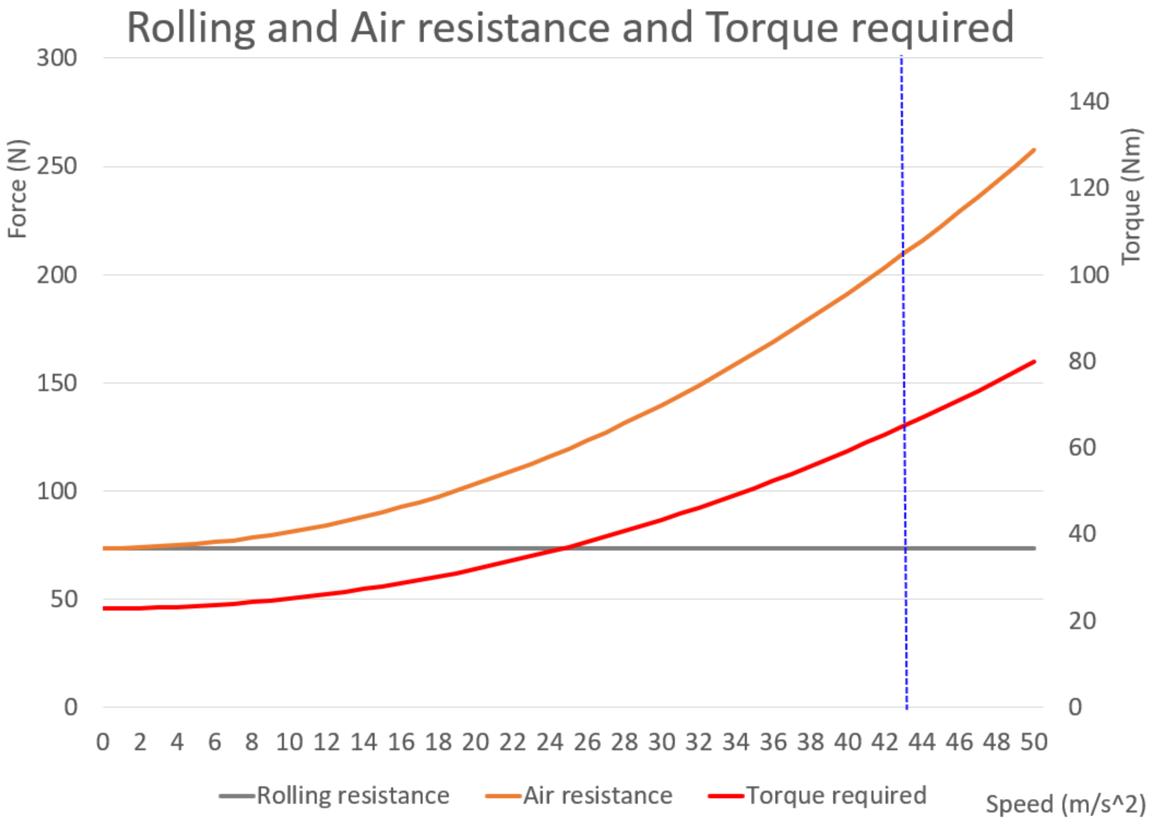

Figure 4.21: Rolling and Air resistance and the Torque required

Now that it was known that an acceleration to 100km/h in 3 seconds can be achieved, it will be checked if an acceleration of 1.5 seconds is achievable as well. This is done similar to Equations 4.69, 4.73 and 4.74. This resulted in a total force of $5686N$ and a torque what the motor should deliver of 287.5Nm. This force is still a smaller than the maximum force that the tires can handle just before slip, therefore the same procedure is used to calculate the torque needed at an acceleration to

100km/h within 1 second. This resulted in a total force needed of 8463.6N and a torque of the motor of 427Nm. This means that both the tires and the motor would not be able to accelerate within 1 second. Then the same procedure was used to check if an acceleration to 100km/h within 1.2 seconds was possible. This time the total force was 7075N and the torque required from the motor was 358Nm which is just below the slip condition and the maximum deliverable torque.

4.4.6 Maximum velocity

A maximum velocity of 311 km/h is calculated before in Section 4.2.1, but with this calculation there is not looked if the motor can deliver enough torque to overcome the resistances. When the motorbike is going top speed, the acceleration is 0 and the acceleration force is the same as the resistance forces. Due to this the inertia does not impact the velocity any more so the torque at the rear wheel is the torque of the motor times gear ratio 3:1. The torque of the motor at 8000 rpm is 125 Nm as can be seen in Figure 4.1. This results in a torque of 375 Nm at the wheel, which results in a force usable for acceleration of 375/0.31 = 1209.7N. The rolling resistance and the air resistance still need to be taken into account. The rolling resistance is 73.58N as mentioned before and the air resistance force can be calculated by using Equation again, but now for a velocity of 311 km/h. Combining the rolling resistance and the air resistance gives the total resistance as seen in Equation 5.1. Since the acceleration force of 1209.7N is higher than the total resistance force of 622N the velocity of 311 km/h is achievable.

$$F_{resistance} = F_r + F_D = F_r + \frac{1}{2} * \rho * v^2 * A * c_d \tag{4.75}$$

$$F_{resistance} = 73.58 + \frac{1}{2} * 1.225 * (311/3.6)^2 * 0.6 * 0.2 = 622N$$

4.4.7 Conclusion

In conclusion, it can be said that the acceleration from 0 to 100km/h is exceptional, but only due to a high assumption of the friction coefficient of the tires and a really high gear ratio of 1:6.

4.5 Frame design

For a competitive electric superbike, it is important to have a strong and stiff frame to house all the parts. Therefore the frame was checked on several important aspects. First a look was taken at the fitting of all the electric components in the bike. After this, an analysis was made to calculate the stiffnesses and strength of the frame. Based on the results form this analysis, the frame was adjusted to meet all requirements. Furthermore, a material was chosen to help meet the requirements. Next, a choice for the bearings in the neck was made. These connect the frame to the front fork. After that, a look was taken at the swing arm connection. Finally, since a welded frame was chosen, a weld calculation was made to check the stresses in the frame.

4.5.1 Frame dimensions, connections and housing of electrical components

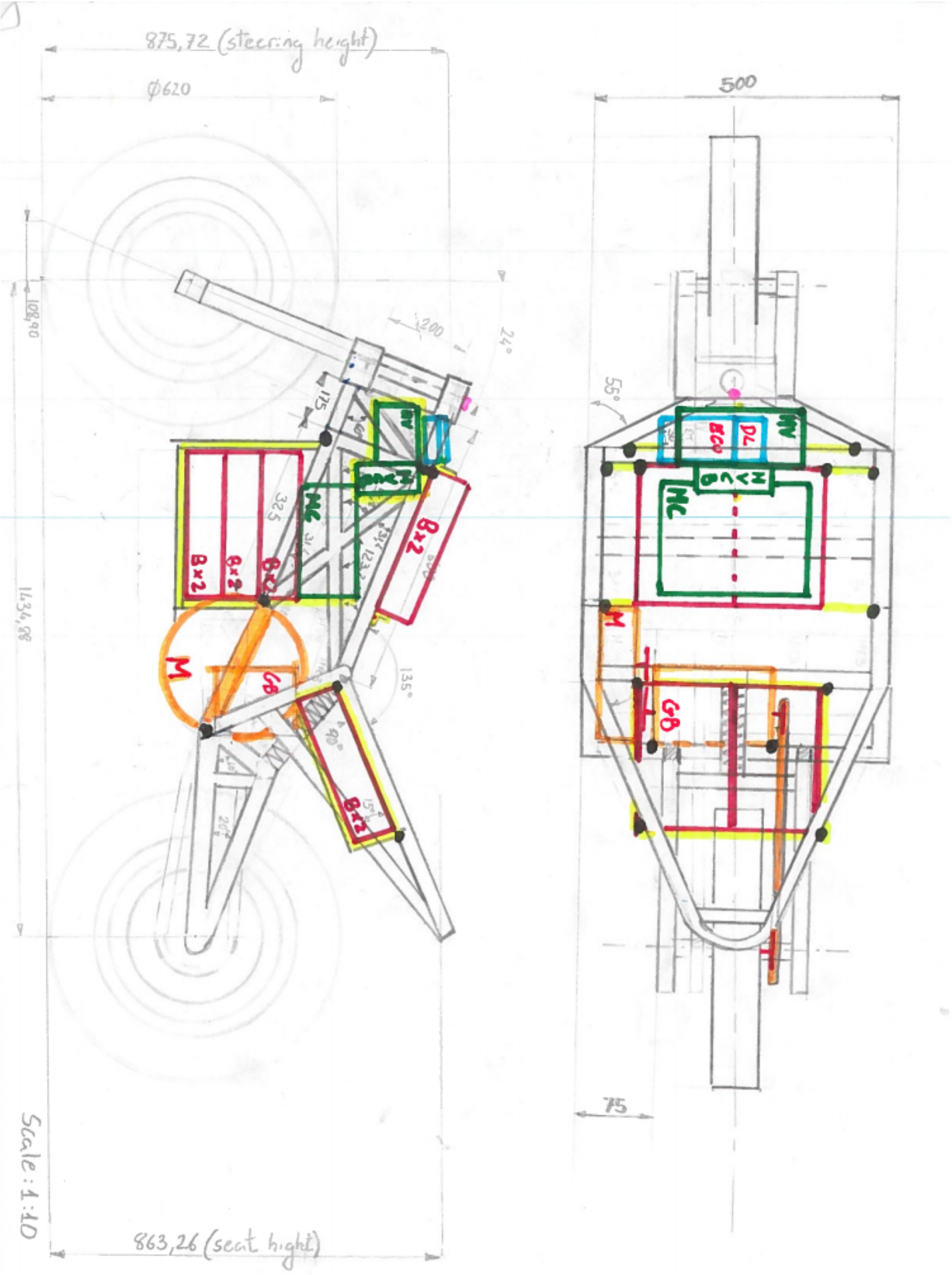
875,72 (steering height)
∅620
500
108,90
200
24°
175
55°
325
B×2
B×2
B×2
B×2
B×2
MC
M
GB
135°
90°
15°
20°
1134,88
DL
BCU
75
Scale : 1 : 10
863,26 (seat hight)

Figure 4.22: Dimensions and location of electrical components

Frame dimensions and electrical components and connections can be seen in Figure 4.22.

These dimensions were set in order to meet the requirements, where the maximum width of the motorcycle is 0.7m. Since it is based on a trellis-frame, tubes are

Table 4.12: Components of the motorcycle

Abbreviation	**Component**	**Weight (kg)**
DL	Data-logger	2
ECU	ECU-central computer	2
DL	Data-logger	2
B	Battery module	8
HVCB	High voltage control board	2
HV	High voltage board	2
MC	Motor controller	12
M	Motor	24
GB	Gearbox	52.9

welded together throughout the frame and the swing arm is connected to the frame in two points with bearings as well as with a spring. Moreover, in Figure 4.22, the placement of the electrical components on the motorcycle can be seen. The motor is connected in the frame in such a way that it becomes an element of the frame, and therefore being modelled in FEM (finite element method) as a connection between nodes.

Batteries were placed evenly on the bike focusing on giving stability to the driver with a low centre of gravity as well as placing them towards the front to prevent wheelies. The motor weighs 24kg and the gearbox weighs 52.9kg. Thus a low position was necessary and one third of the gearbox will have to be on the same side as the motor whereas the other two third should be on the other side with respect to the symmetry line of the motorcycle. In this way a perfect balance is obtained, without taking the chain into account. The batteries are placed at a height of 300mm, Figure 4.22 and the maximum width at the bottom of the motorcycle is 360mm. Because of this, a turning angle of 60 degrees is possible.

The electrical components are attached in several nodes, that can be seen in Figure 4.22, these components are held through a sub frame which can be made of the same material chosen for the frame and therefore can be connected through welds. There are 4 sub frames for all the components installed in the motorcycle.

Additionally, to check whether the displacements of components made the cornering angle of 60 degrees still possible the following calculation where made according to figure 4.23.

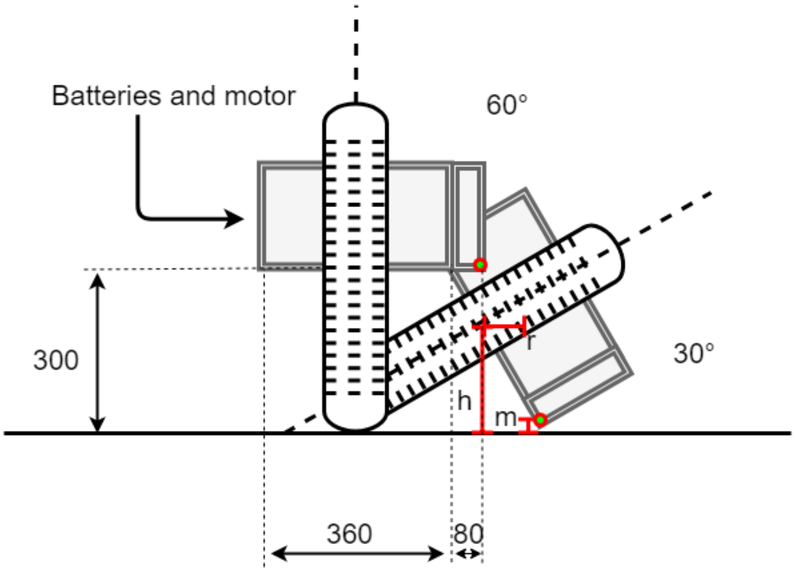

Figure 4.23: Motorcycle cornering - Front view

Firstly, it was checked whether the lower batteries placed on the bottom of the motorcycle would still enable a cornering angle of 60° . Since we knew they were at a height of 300 mm from the ground and 180 mm away from the symmetry line in which an extra 80mm where taken into account from the motor, the following calculations where derived to see at what height was distance m from the lowest point when cornering from the ground, this can be seen in figure 4.23.

$$h = cos(30) * 300mm = 259.8mm \tag{4.76}$$

$$r = sin(30) * (180mm + 80mm) = 130mm \tag{4.77}$$

$$m = tan(30) * 130mm = 75.05mm \tag{4.78}$$

Therefore, it can be seen that this displacement of motor and batteries, being both at the lowest position of the frame, was optimum for a 60° cornering with a 75.05 mm separation from the ground. This mean the leaning requirement of the motorcycle was met when including the components.

4.5.2 Material selection

In order to obtain a suitable frame which meets the requirements several variables are taken into account: Processing of a trellis frame (mechanical elements), safety factors (based on FEM calculations and thermal properties), connections between frame parts (weldability), lightness (density), strength (yield strength). Therefore an equilibrium between strength, stiffness and weight will determine the optimal selection.

Since the frame is built as a Trellis-frame consisting of 35 tubes of different lengths with a wall thickness of 3mm, and an outer diameter of 0.03m, connected through welding in 35 spots (nodes), weldability was determined to be a main factor when choosing the material for the frame. Also avoiding different shapes and sizes along each beam was taken into account to avoid high stress concentrations, FEM calculations determined the beams subjected to more stress, therefore the material should withstand at least those stresses and an extra parameter (frame should withstand bigger stresses than the ones which appear on FEM) could be used for safety. A starting performance index was derived, Equation 4.79 was used and combined with a selection of metals which perform ideally under various processes: extrusion (hot forming), weldability, in which shrinkage must be considered when welding, strength, stiffness and density. Price was not considered since the racing motorbike is designed to have a maximum performance, hence the price should not be a drawback in this case.

$$PI_{frame} = \frac{\sigma_y}{\rho} \tag{4.79}$$

From the following performance index, which looks at the maximum yield limit with a minimum density, combined with CES EduPack, FEM (how the frame reacts when loads are applied into the frame) and considering both options(aluminium and steel),a carbon steel was selected as the material for all the beams composing the trellis frame. The most suitable material chosen for this purpose, which is already used in the automotive industry, is: Carbon steel, AISI 1015, annealed. [23]

Physical and mechanical properties of this material can be seen in Table 4.13.

Table 4.13: Properties of Carbon steel, AISI 1015, annealed

Properties	**Minimum**	**Maximum**
Density (kg/m^3)	$7.8 * 10^3$	$7.9 * 10^3$
Young's Modulus (GPa)	205	215
Yield Strength (MPa)	255	315
Tensile strength (MPa)	345	430
Poisson's ratio	0.285	0.295

4.5.3 Analysis of the frame: Finite Element Method

An important part of the superbike is a sturdy frame that can deal with the forces it is submitted to during a race. It needs the right stiffness to absorb some of the loads, it needs to be strong enough and it needs to be as light as possible. In order to achieve this, the frame was modelled in Matlab. Based on the results, the frame was adjusted to fulfil the stiffness requirements as well as to prevent failure.

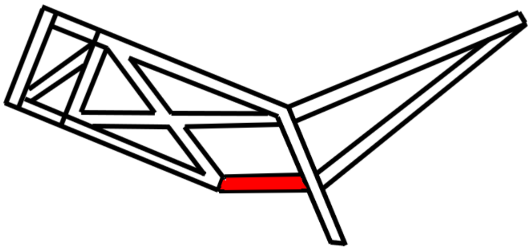

Figure 4.24: Frame elements - Side view

Next, the frame of the bike was modelled in Matlab using FEM, in order to calculate the internal forces acting on the beams and the deformation the frame goes through when those forces are acting on it. The initial model uses tubes with a diameter of 50mm, with a wall thickness of 4mm, which results the frame weighting 81 kg. This will result in a total weight of the bike of 201 kg. Important to note is that the red element in Figure 4.24 is the motor, but it is modelled in FEM as a tube.

Another important assumption is that not all components (e.g. motor controller) are directly connected to a node, so their weight is not hanging on one node, but hanging on two or three nodes. It was assumed that these components are connected to their closest nodes, instead of hanging from the nearest elements. This gives different results, which are more accurate than when a new node was introduced to support the components. This is partly because the weight of the components has a relatively small influence on the frame compared to the braking and acceleration forces.

In the first model, aluminium was used as the frame material, which resulted in high deformations at the front of the bike. The stresses acting on some of those elements exceeded the yield limit of the material so adjustments needed to be made to prevent failure. Also, for weldability purposes it was better to use a steel frame.

The stiffnesses of the initial aluminium frame are within the boundaries set in the requirements, as can be seen in Table 4.14.

Table 4.14: Stiffness of the initial frame

	Required stiffness (kN/mm)	Calculated stiffness (kN/mm)
Lateral	1-3	1.8479
Longitudinal	5-10	5,0454
Torsional	3-7	4.5576

Right stiffnesses are important, because elastic deformation will absorb some of loads during a race, resulting in a smoother ride. The three stiffnesses are calculated by looking into three different load cases, applying a dummy force of 1 kN, or a torque of 1000Nm, and using the deformation from FEM.

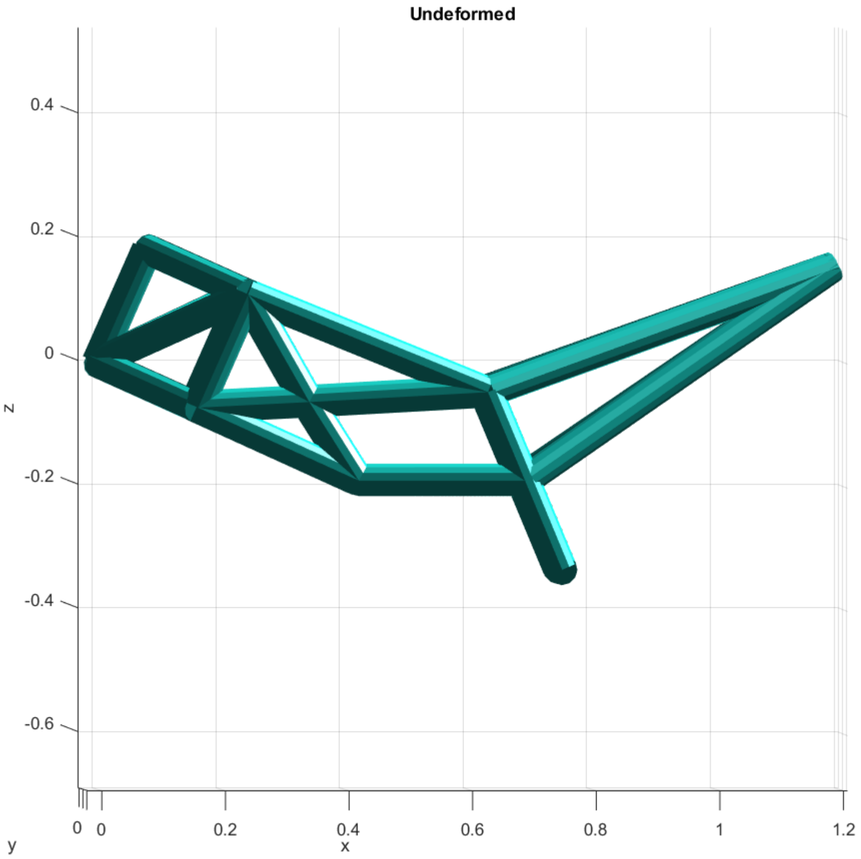

Figure 4.25: Undeformed Frame - Side view

The deformation plots (Figure 4.26 and 4.27) show a high deformation of the front of the bike compared to the undeformed frame in Figure 4.25, so the front must be reinforced for the final concept. This also follows from the FBD of the front fork, shown in Figure 4.34, where forces of 22,2 kN apply to the front of the bike, which are then distributed over the frame. The force in the top node of the fork is distributed

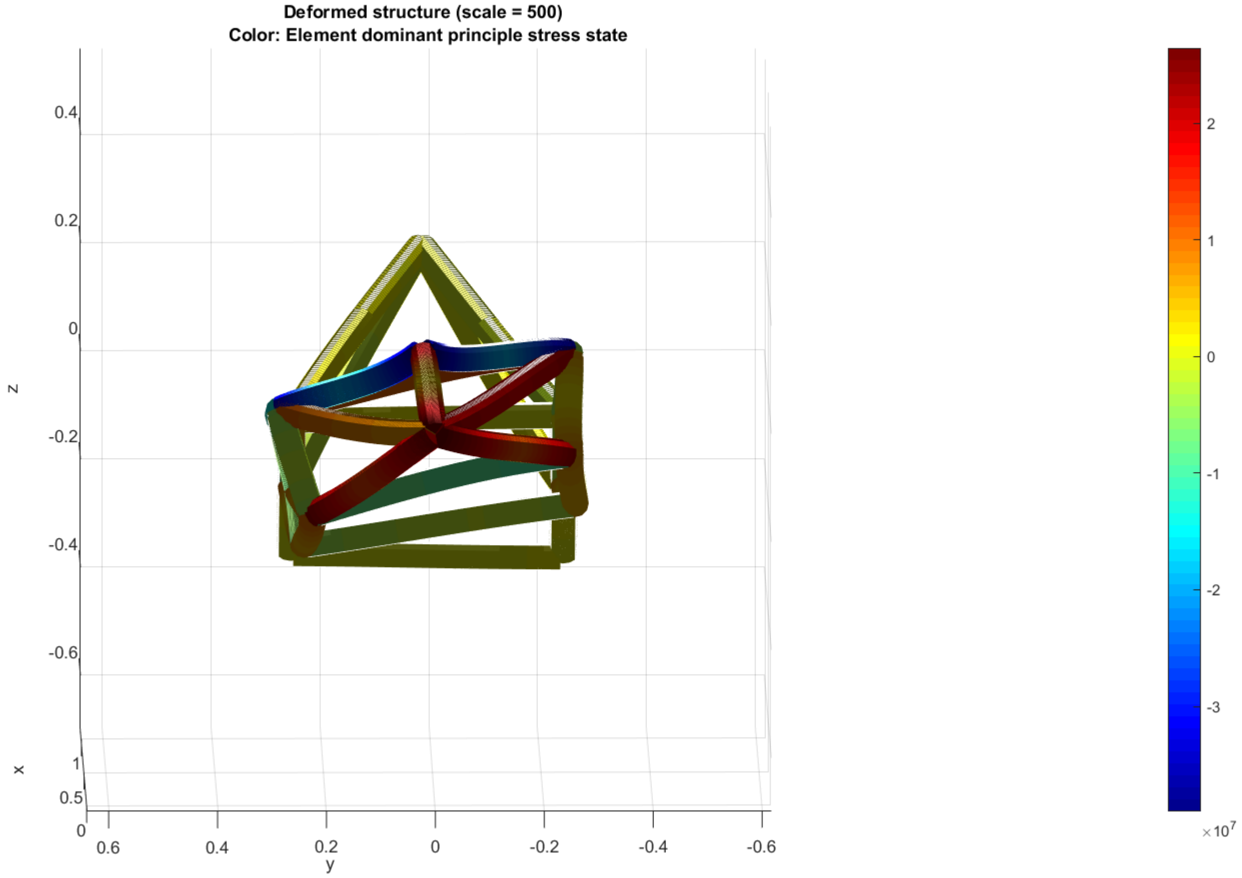
Deformed structure (scale = 500)
Color: Element dominant principle stress state
z
0.4
0.2
0
-0.2
-0.4
-0.6
x
1
0.5
0
0.6
0.4
0.2
0
-0.2
-0.4
-0.6
y
2
1
0
-1
-2
-3
×10^7

Figure 4.26: Deformation plot while braking - Front view (internal stresses are given in $Pa * 10^7$)

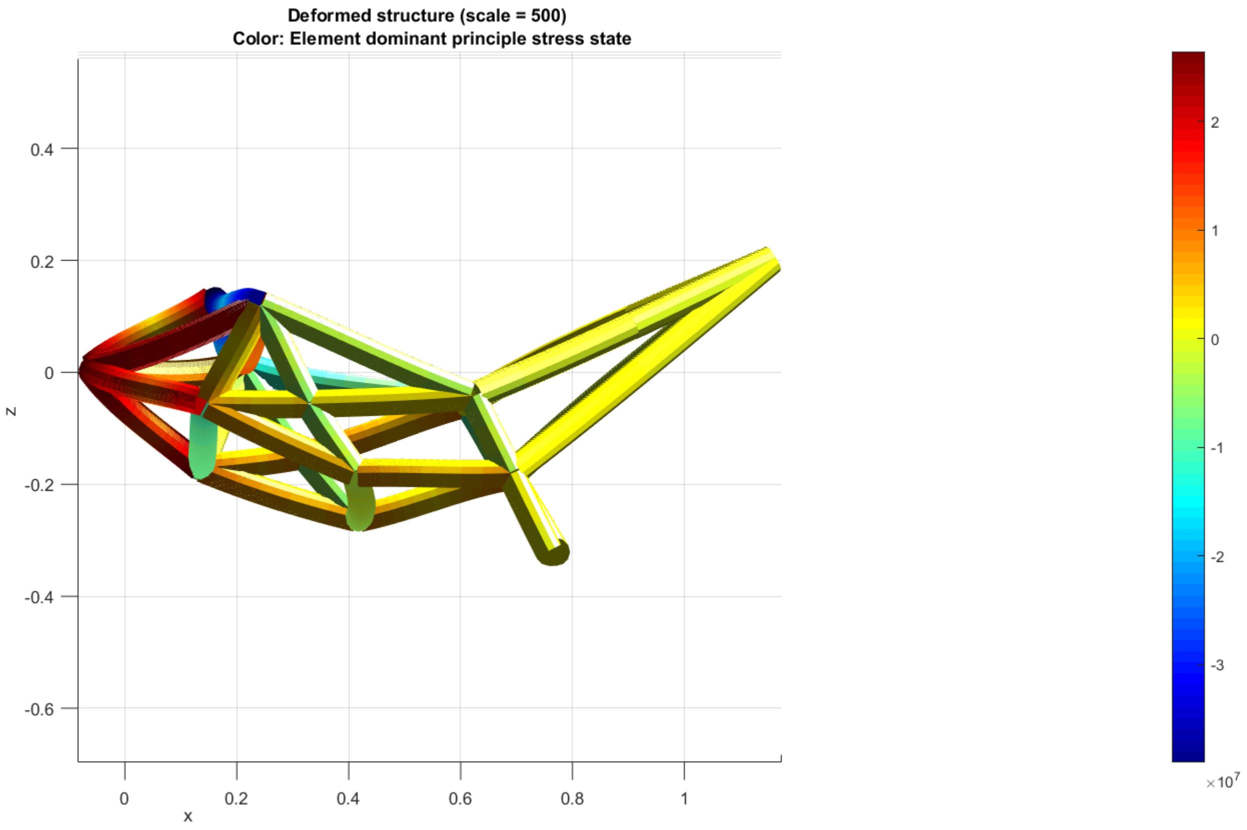

Figure 4.27: Deformation plot while breaking - Side view (internal stresses are given in $Pa * 10^7$)

over two beams, so stress into those beams are high (up to 30 MPa). In section 4.5.5 a deeper look will be taken into the neck.

Because changes were made to the frame, the stiffness had to be recalculated. After some iterations, stiffness values of Table 4.15 were found.

For a competitive electric superbike, it is important to have a strong and stiff frame to house all the parts. Therefore the frame was checked on several important aspects. First a look was taken at the fitting of all the electric components in the bike. After this, an analysis was made to calculate the stiffnesses and strength of the frame. Based on the results form this analysis, the frame was adjusted to meet all requirements. Furthermore, a material was chosen to help meet the requirements. Next, a choice for the bearings in the neck was made. These connect the frame to the front fork. After that, a look was taken at the swing arm connection. Finally, since a welded frame was chosen, a weld calculation was made to check the stresses in the frame.

The longitudinal stiffness relatively low, but due to the weight savings this was to be expected. If there is less material, stiffness will go down. Lateral and torsional

Table 4.15: Stiffness of the final frame

	Required stiffness (kN/mm)	Calculated stiffness (kN/mm)
Lateral	1-3	2,4001
Longitudinal	5-10	5,0322
Torsional	3-7	6,3388

stiffness are relatively high, but this is due to the strong front. Because the front was reinforced, the stiffnesses also went up.

Dimension considerations

After getting the correct stiffnesses and looking into internal stresses, it was found that some elements have to handle high amounts of stresses, while others barely take any load. The dimensions of the tubes can be found in Figure 4.28. The highest principle stress in the final design is over 70 MPa. For all principle stresses, see Appendix I.4. With these new dimensions, an estimation could be made of the weight of the frame. By assuming an average length of 50 cm for each element, the found weight was around 35,8 kg.

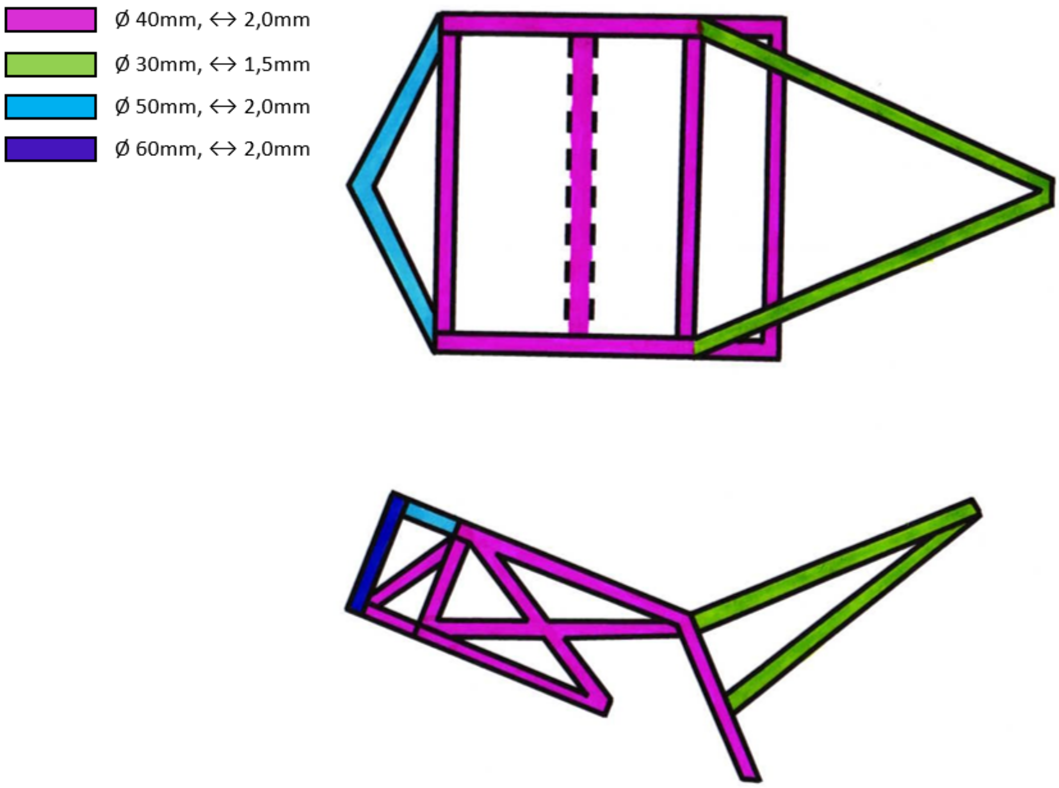

Figure 4.28: Tube dimensions of the frame - Top and side view respectively

Also, the motor was not modelled correctly, so another beam was added to the frame to represent the motor. The two red elements in Figure 4.29 now represent the motor. On the opposite site of the frame there is no motor to take forces. However, the two red beams are present on that side of the frame.

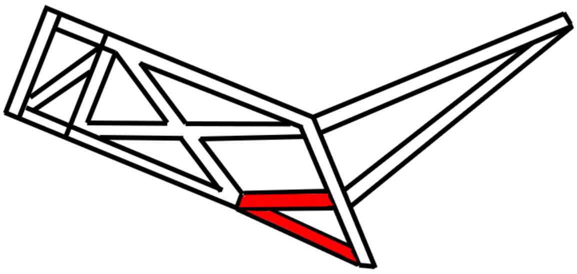

Figure 4.29: Correct modelling of the frame with the motor - Side view

After these adjustments, the deformation plots in Figures 4.30 and 4.31 were found. To see all the deformations per node, see Appendix I.2

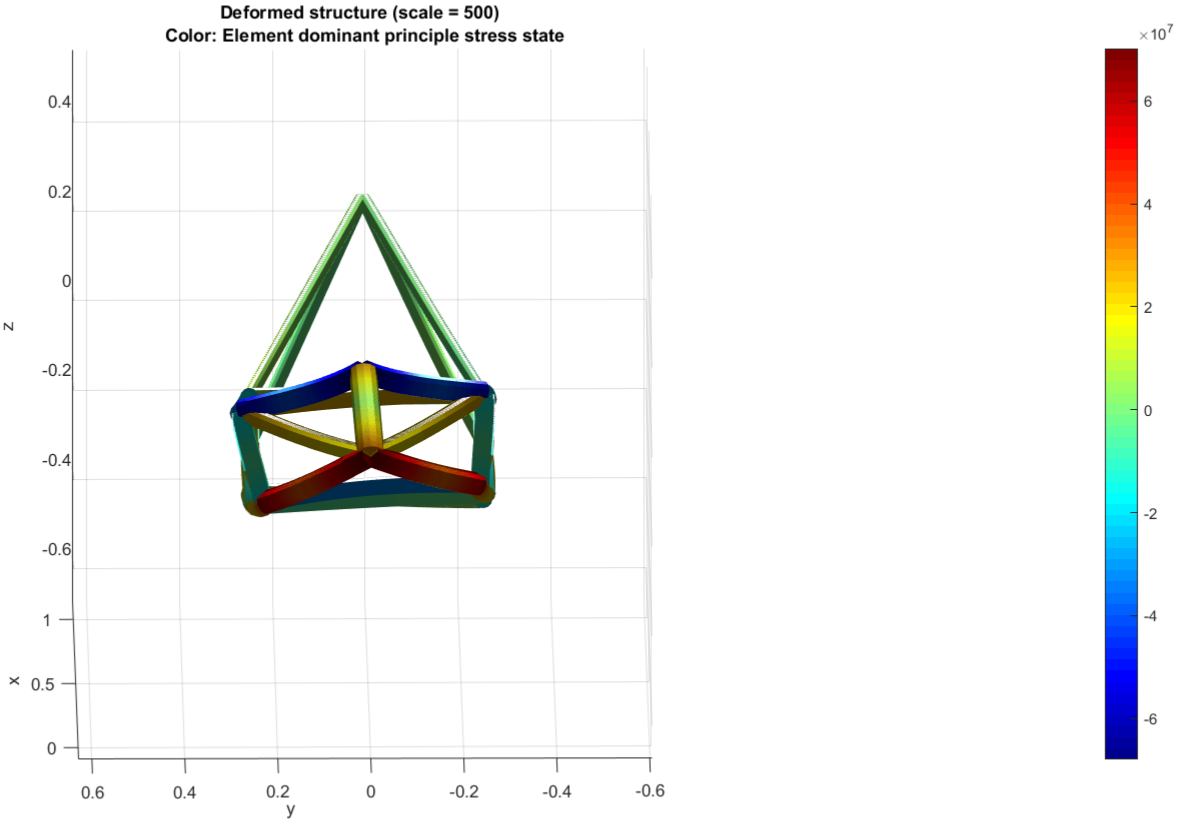

Figure 4.30: Deformation plot while breaking after adjustments - Front view (The stresses are given in $Pa * 10^7$)

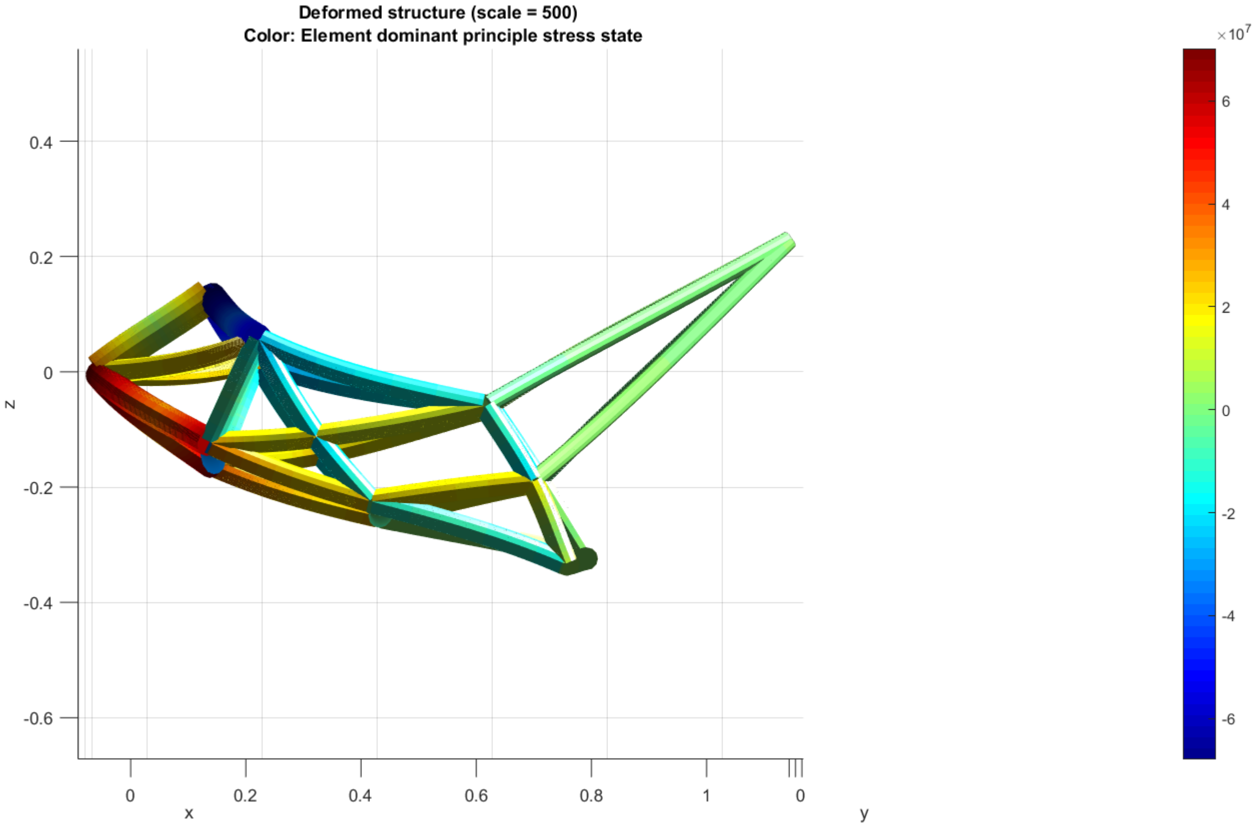

Figure 4.31: Deformation plot while breaking after adjustments - Side view (The stresses are given in $Pa * 10^7$)

Figure 4.31 clearly shows that the deformation of the front has been reduced. This makes sense because of the bigger tubes, as well as a stronger material. The frame now has the right stiffnesses to absorb some of the forces during racing and is also strong enough to handle the braking forces. The top of the neck gets deflected about $1mm$, which is within 1% of the length of the neck, so it can be seen as an acceptable value.

4.5.4 Hand calculations

In order to see if the results displayed were correct. Hand calculations of stresses were made on one of the elements to check if the Finite Element Method program is a reliable source to calculate the stresses of the elements in the frame, As can be seen in Figure 4.32:

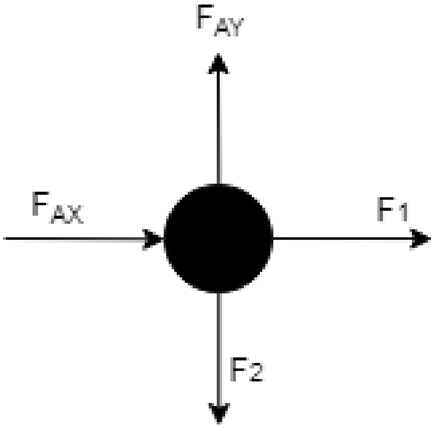

Figure 4.32: Stresses on the node on the front of the frame

$$\Sigma Fx = 0, F_1 = -F_{Ax} \tag{4.80}$$

$$\Sigma Fy = 0, F_3 = F_{Ay} \tag{4.81}$$

$$F_3 = 5573.6N \tag{4.82}$$

$$A_{beam} = \pi * (R^2 - r^2) = \pi * (0.025^2 - 0.021^2) = 0.578mm \tag{4.83}$$

$$\sigma = F/A = 5573.6/0.578 * 10^-4 = 9642021.64Pa = 9.6MPa \tag{4.84}$$

And then the torsional stresses using Figure 4.33:

$$N(x) = -F_{BY} \tag{4.85}$$

$$V(x) = F_{BX} \tag{4.86}$$

$$M(x) = x * F_{BX} \tag{4.87}$$

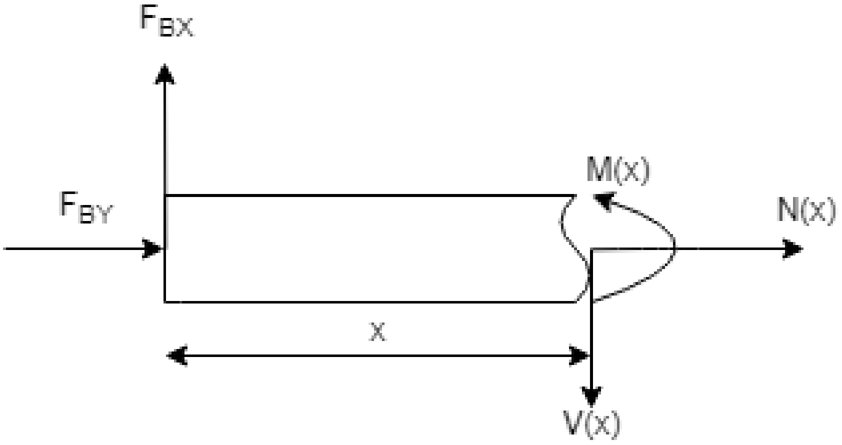

Figure 4.33: Torsional stresses on the element

Here L is 0.2 m, and y is 0.025 m.

$$I = \pi/4 * (r_o^2 - r_i^2) = 6.16 * 10^-7m^4 \tag{4.88}$$

$$\sigma(x) = -y * M(x)/I \tag{4.89}$$

$$\sigma(L) = -135481331.2Pa = -135.5MPa \tag{4.90}$$

Since the node on the bottom is connected to 4 other beams, the value found for $\sigma(L)$ must be divided by 4. Thus: $\frac{\sigma(L)}{4} = \frac{-135.5}{4} = -33.88MPa$
Finally, the two stresses are added to calculate the total stresses acting on the element: $-33.88 + 9.6 = 24.28MPa$.
The result obtained from FEM is 21.2 MPa. The small deviation was expected due to the fact that the formulas that were used to obtain the values during the hand calculations were simplified and because some assumptions were made.

Conclusions on the frame design

Results obtained from hand calculations match the program used for the Finite Element Method. Since the FEM package was validated, the results can be used to conclude that the overall stiffnesses are within the set requirements. The final weight of the frame will be an estimated $35,8kg$ and the front is reinforced to deal with the stresses while braking. In order to check if the whole bike is sturdy enough, different load cases should be analysed, for instance when cornering at an angle of $60°$. Therefore the limit situations the frame can withstand can be analysed for further improvements of the frame design.

4.5.5 Neck Bearings

Looking at the calculations above, the forces acting from the frame towards the neck of the bike are the largest during braking, so a choice of bearing which can withstand these forces needed to be made. Firstly, a new FBD had to be made to calculate the forces acting on the bearing at the neck. As can be seen in Figure 4.34, there is only axial load acting on the bottom bearing. That is due to the fact that the design was made such that the upper bearing is fixed and can only take radial load while the bottom bearing can take radial and axial load. Resulting from this, the weight of the bike will be completely handled by the bottom bearing.

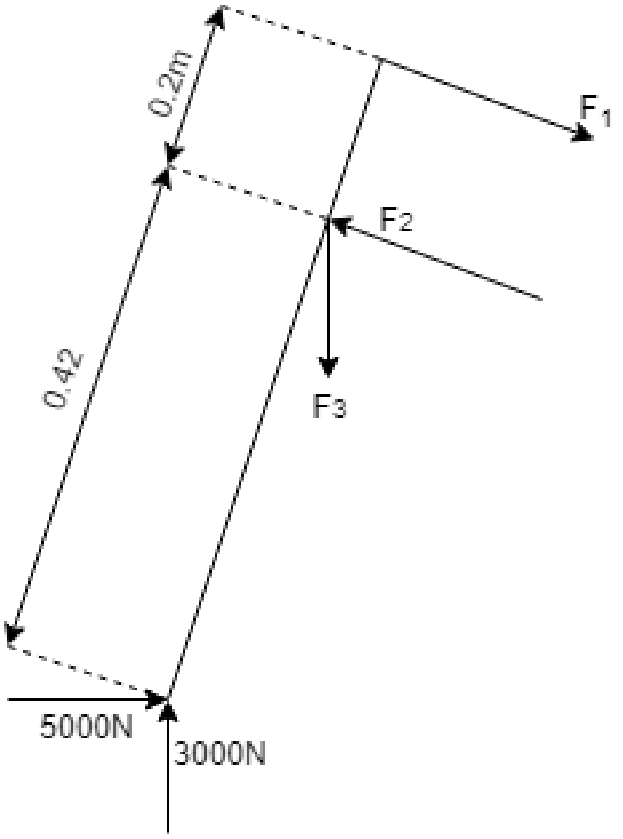

Figure 4.34: FBD of the neck with the weight of the bike

Using the 3 equations of equilibrium, the 3 unknown forces can be calculated:

$$\Sigma F_x = 0 => 5000 + F_1 * cos(24) - F_2 * cos(24) = 0 \tag{4.91}$$

$$\Sigma F_y = 0 => 3000 - F_3 + F_2 * sin(24) - F_1 * sin(24) = 0 \tag{4.92}$$

$$\Sigma M_B = 0 => -F_1 + 5000 * cos(24) * 0.42 - 3000 * sin(24) * 0.42 = 0 \tag{4.93}$$

Table 4.16: Forces on the neck bearings

Force type	Force (kN)
F_1	7.01
F_2	12.5
F_3	5.2

Since the rotations of the bearing are less than $10 rev/min$ it can be considered a static bearing. Afterwards, the radial, F_r, and axial loads, F_a, were calculated, with which the equivalent static load (P_0) was calculated and, in turn, with a safety factor (s) of 2, gave the static rating load C_0.

$$F_r = F_2 + F_3x = 14.61kN \tag{4.94}$$

$$F_a = F_3y = 4.75 \tag{4.95}$$

$$P_0 = 0.6 * F_r + 0.5 * F_a = 11.14kN \tag{4.96}$$

$$C_0 = s * P_0 = 22.28kN \tag{4.97}$$

Therefore the chosen bearing should withstand at least a static rating load of $22.28kN$. Having said this the chosen bearings were deep groove ball bearings. The pair selected were $DIN6210$.

4.5.6 Swing arm connection

When looking at the swing arm, one key factor is taken into account. This is the bearing type and size. In the following sections the forces when accelerating and the forces when turning at 60° will be determined. These will then be added up to the chain tension and the normal force of the bike. This will then result in a bearing choice according to a DIN standard. Afterwards the set up of the complete swing arm connection is explained. This is done to ensure a swing arm connection that performs correctly under racing conditions.

Radial and axial load calculations

The swing arm connection for the motorcycle consisted of an inverted U shape, with two triangular frames on top on which the spring is attached and whose purpose consists on damping the shocks during the race. It was designed to withstand the forces coming from the rear wheel, spring, motorcycle weight, chain tension and the frame, as well as the weight of the motorcycle when cornering at 60°.

The connection between the frame and the swing arm, allows rotation only in the direction in which the rear wheel of the motorcycle rotates. Therefore, static bearings will be used. These bearings were set inside the swing arm and mounted with a shaft onto the frame allowing only movement of the swing arm, which will be subjected to the spring connected to the frame and the incoming forces stated above. Firstly, Figure 4.35 shows a schematic view as well as a FBD of the connection of the swing arm and the rear wheel as well as the chain. Forces coming from the rear wheel were already calculated for the drive train and the forces of the chain are retrieved from Table 4.5. The forces acting on the axle of the rear wheel are calculated below.

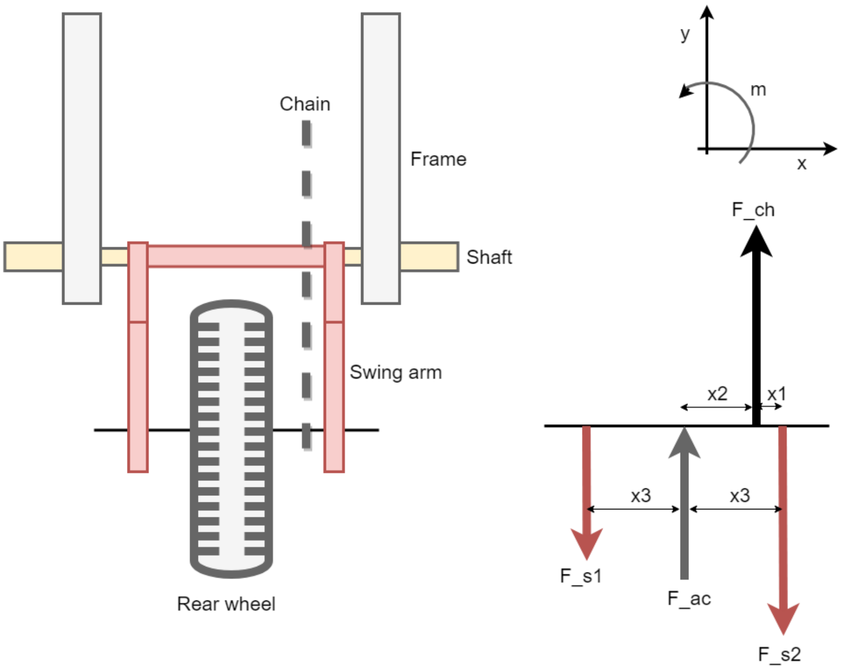

Figure 4.35: Swingarm connection - Top view

Table 4.17: Distances in Figure 4.35

$x_1(m)$	$x_2(m)$	$x_3(m)$
0.02	0.10	0.12

$$\Sigma F_y = 0 => -F_{ch} + F_{s1} + F_{s2} - F_{ac} = 0 \tag{4.98}$$

$$\Sigma M_{@Fs1} = 0 => x_1 * F_{ch} + x_3 * F_a - 2 * x_3 * F_{s2} = 0 \tag{4.99}$$

Table 4.18: Forces on the swing arm bearings

Force type	**Force (N)**
F_{ch}	10200
F_{ac}	2778
F_{s1}	2239
F_{s2}	10739

Secondly the total forces coming from the rear wheel, F_{ac}, and acting separately on the chain side, F_{s2} and the non-chain side, F_{s1}, were used in Figure 4.37 in order to obtain the radial forces acting on the bearings of the swing arm. The method of sections on the bearing point was used. An assumption was made that the spring was at a stationary position in order to be able to calculate the forces, in reality this angle can change slightly when racing. The incoming forces to each respective bearing are derived.

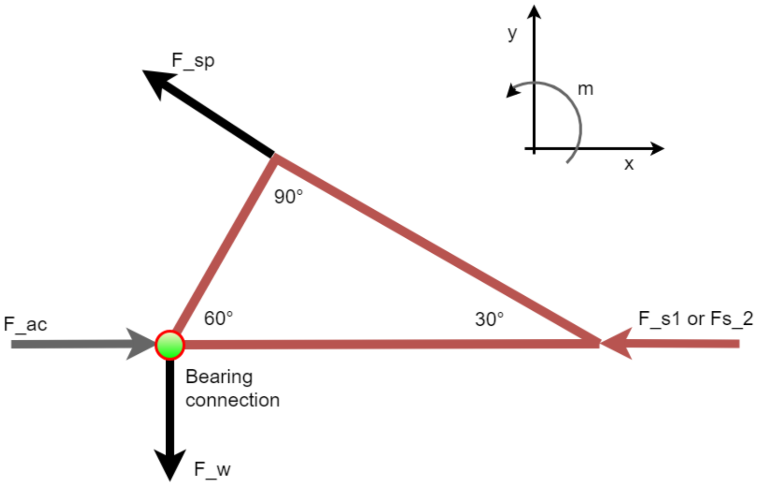

Figure 4.36: Swing arm - Side view

$F_w(weight) = 3000kN$

$$\Sigma F_y = 0 => sin(30) * F_{sp} - F_w = 0 \rightarrow F_{sp} = 6000N \tag{4.100}$$

Using the method of sections the following can be found.

$$F_{total1} = -F_{ac}/2 + cos(30) * F_{sp} + F_s1 = 14546N \tag{4.101}$$

$$F_{total2} = -F_{ac}/2 + cos(30) * F_{sp} + F_s2 = 6046N \tag{4.102}$$

The axial load when cornering can then be calculated:

$$Axial - load = cos(60) * F_w = 1500N \tag{4.103}$$

The maximum axial load the lower bearing will experience when turning, was found to be 1500N. Moreover, it was seen that the incoming forces to the bearing had different radial loads, being the bearing on the side of the chain the one conditioned to the biggest radial load (14546N), influenced by the chain tension.

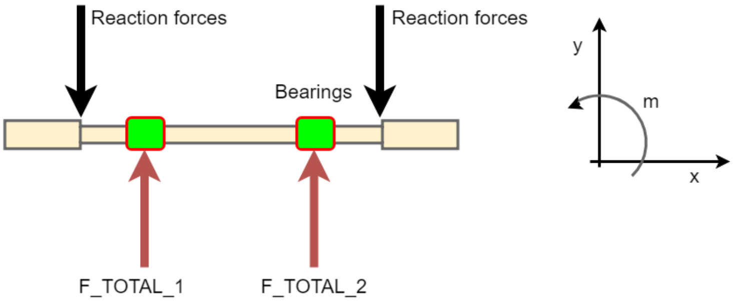

Figure 4.37: Bearing displacement - Top view

Bearing selection

From the calculations above, the resultant actual radial loads (F_r) were 6046N and 14546N, for the bearing located on the opposite side of the chain side and for the bearing located on the chain side, respectively. Moreover, when cornering at 60° the bearing closest to the ground was subjected to 1500N of actual axial load which at the moment of cornering will be the maximum axial force of the two bearings. All these loads where derived from the FBD's.

The bearings selected for the swing arm could be different from each other, but in order to keep the design of the swingarm connection in symmetry and size, the biggest radial and axial loads where used in this case for both bearing selection. From Table 14.3 on Appendix H.1, a deep groove ball bearing was selected while being subjected to the following conditions:

$$F_r = 14546kN \tag{4.104}$$

$$F_a = 1,5kN \tag{4.105}$$

$$e = \frac{F_a}{F_r} = \frac{1500kN}{10,739kN} = 0.1031 \tag{4.106}$$

Since Table 14.3 on Appendix H.1 shows that for deep ball groove bearings are $e_o = 0.025$ then if:

$$\frac{F_a}{F_r} <= e_o \tag{4.107}$$

The radial and axial load factors were found to be X=1,Y=0 due to $e{<}{=}e_o$. This can be checked in Appendix H.1. By using Equation 4.109 the static equivalent load can be determined:

$$P_o = X * F_r + Y * F_a \rightarrow X = 1, Y = 0$$

$$X = 1, Y = 0 \tag{4.108}$$

Therefore, the static equivalent load will be equal to the actual radial load.

$$P_o = 1 * 14,546kN \tag{4.109}$$

Additionally, a safety factor of 1.5 will be applied to obtain the minimum static radial load.

$$C_o = P_o * S_o = 10,739kN * 1.5 = 21,819kN \tag{4.110}$$

In conclusion, the selected bearing should withstand at least a static radial load of 21819 N. Having said this the chosen bearings where deep groove ball bearings. The pair selected were $DIN6308$ [19], with 90mm outer diameter and 40mm bore diameter and a weight of 0.63kg each.

Connection set up

The connection points can be seen in Figure 4.35. The aim is that all components have the correct diameter and fit together accordingly. Firstly, the tubes coming from the frame will be placed 500mm away from each other, with a diameter of 40mm each. Therefore, to avoid side movement of the swing arm, the swing arm will have a separation from the frame tubes of 5mm in total and the remaining space was filled with to collars of 50mm to reduce side movement. The width of the swing arm was set to be 355mm. The aim was to get the force coming from the chain tension closest to the symmetry line, therefore the tighter the components in this case to the symmetry line, the smaller the loads would be on the swing arm connection.

Both end tubes of the frame were made as solid tubes of the same steel material as the frame, to prevent malfunction due to corrosion such as the case of galvanic corrosion. These solid tubes have a diameter of 40 mm due to the importance that they should withstand the incoming forces coming from the swing arm. These solid tubes were machined with a whole in which the shaft going through the swing arm will be inserted. These wholes placed 50mm from the end of the tubes a had a diameter of 30 mm in which the shaft was inserted and mounted. Since a DIN 6308 deep groove ball bearings were used, the inner diameter of the bearings was 40 mm. The outer ring of the bearing was fixed while the inner ring could rotate. A collar consisting of an outer diameter of 40mm and a wall thickness of 5 mm means a shaft of 30mm of diameter was inserted throughout the swingarm and connected to the solid bars of the frame. The bearing displacement, the rods and the swing arm, all together, made the complete connection.

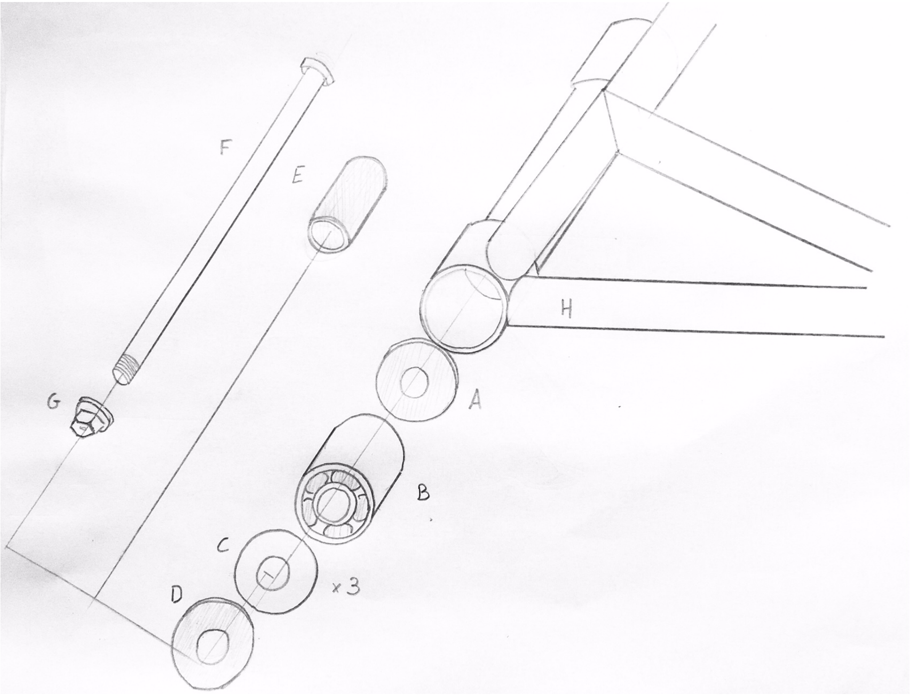

Figure 4.38: Connection components

Firstly, an inner shield (A) is inserted into the swingarm cavities (consisting of an inner diameter of 40mm and an outer diameter of 90mm). Secondly, by using an interference fit between the swing arm and the DIN 6308, the bearing (B) will be set in position and centered. Afterwards a set of washers (C) were introduced while using grease as well. Moreover, an outer shield (D) was placed. Finally, the collar (E) was inserted and then the shaft (F) was mounted so that the swingarm (H) was fully connected to the frame.Moreover, two 500mm collar are placed in the shaft to tighten the connection between the frame and the swing arm and therefore side motion is decreased to 2.5mm on each side This set up was performed in both connections of the swing arm. Therefore, a connection between the swingarm (starting at the rear wheel) and the frame is finally obtained. This can be seen in Figure 4.38.

4.5.7 Weld connections

When designing the connections of the frame, it was decided to weld the tubes of the frame. Thus a welding calculation is performed in order to obtain information on the design of the welded joints. Following the results derived in FEM, the resultant forces and moments acting on the frame when braking were taken into account, as can be seen in Figure 4.27.

The weld connection on the frame which was analysed consisted of the neck tube of the frame and the bottom left tube, this can be seen in the side view of the motorcycle design. It corresponds to elements 1 and 3 on node 1 on Appendix I.1. Knowing the forces on this tube are under tension and the material selected for the frame is a type of steel, the following calculations were derived in order to obtain a precise idea of the welds subjected to the biggest loadings, therefore this can be already seen as a safety factor since other connections of the frame will possibly have smaller resultant forces and moments acting on them. Moreover, a safety factor of 2 is taken into account in the resultant force calculation.

The geometry of the joint can be seen in Figure 4.39 consists of two circular tubes both consisting of a wall thickness of 2.5mm and an outer diameter of 4mm. They are joined at an angle of 90°.

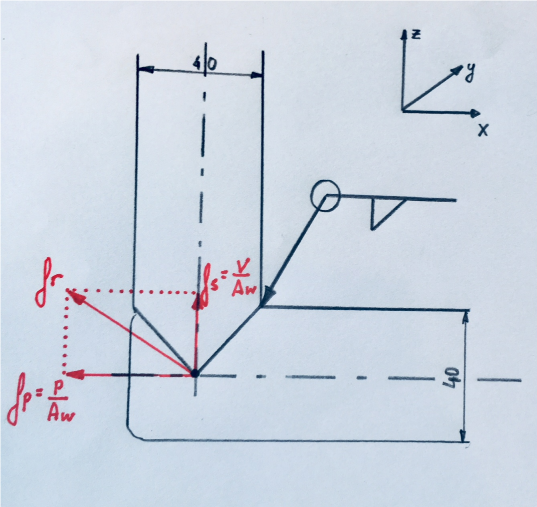

Figure 4.39: Welded tubes

The type of weld selected in this case for calculations is a corner weld, with no edge preparation (fillet weld). The method used to determine the size of the weld was the Method of treating the weld as a line. This method analyses the weld for each type of loading to determine the force per 25.4mm of weld size due to each load. In this method this loadings were considered: Direct tension or compression, direct vertical shear, bending and twisting. The type of stresses the joint is subjected to in the frame of the motorcycles were direct tension, vertical shear and bending. The bending moment was neglected in the calculations since the moment values obtained from FEM in this node were 0. Figure 4.40 shows the geometry of the weld used for calculations.

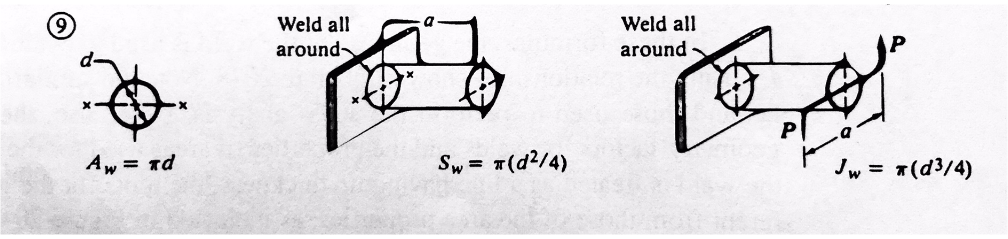

Figure 4.40: Weld geometry

The geometry of the tubes determined the following formulas to be used:

$$A_w = \pi * D \tag{4.111}$$

$$S_w = \pi * \frac{D^2}{4} \tag{4.112}$$

$$S_w = \pi * \frac{D^3}{4} \tag{4.113}$$

The forces were calculated in the following calculations, afterwards these forces were combined vectorially and finally, when choosing a suitable electrode for the welding, the maximum force on the weld was divided by the allowable force from the electrode used to determine the required leg size of the weld.

To compute the forces of the weld, in this case only direct tension and vertical shear, the geometry factor A_w was calculated with Equation 4.111.

$$A_w = \pi * 40mm \tag{4.114}$$

To determine the loading of direct tension, Equation 4.115 is used:

$$f_p = \frac{P}{A_w} \tag{4.115}$$

$$f_p = \frac{P}{A_w} = \frac{-1.6691 * 10^4 N}{\pi * 40mm} = -132.83N/mm \tag{4.116}$$

To determine the loading of direct vertical shear, Equation 4.120 is used:

$$f_s = \frac{V}{A_w} \tag{4.117}$$

$$f_s = \frac{V}{A_w} = \frac{3.3756 * 10^3 N}{\pi * 40mm} = 26.86N/mm \tag{4.118}$$

These forces will be combined using parallelogram method because they are both vectors and a safety factor N of 2 was taken into account in this step.

$$f_r = \sqrt{f_p^2 + f_s^2} = 135.508N/mm \tag{4.119}$$

$$f_r = 135.50871N/mm * N = 271.016N/mm \tag{4.120}$$

If an E60 electrode is selected for the welding (appropriate in this case for the steel being used), the allowed force per 25.4mm of weld leg size will be 1681N/mm. Then the required leg size will be 4.121 :

$$w = \frac{271.016N/mm}{1681N/mm} * 25.4mm = 4.095mm \tag{4.121}$$

Finally, the throat (t) width of the fillet weld will be:

$$t = 0.07 * w = 2.895mm \tag{4.122}$$

Therefore the minimum weld size, for the 40mm tube diameters, will be a 4.095mm fillet weld all around the tubes connected, meaning the minimum throat width will be 2.895mm all around the connection.

Chapter 5

Evaluation and redesign

5.1 Drive train redesign

In the drive train there are some areas of improvement, such as the air resistance, gear ratios and spline design.

5.1.1 Air resistance

In the previous calculations of the air resistance an estimate was made of the frontal area. This estimate was made with the ideal bike in mind, where the total height of the bike was 1 meter and the width $60cm$, however this will not be the case.
The frontal area is calculated according to the dimensions in Figure 5.1. The area within the red lines is the frontal area of the bike, and the remaining area is present due to the rider. To calculate the frontal area, simple arithmetic can be used, yielding a final frontal area of .67 m^2. This value is higher than the originally used frontal area, and as such will result in a slightly higher air resistance.
Another point of improvement is the coefficient of drag. Initially it was assumed that the drag coefficient was equal to 0.2, because the value lay in line with estimations. After some more digging it was deemed the opposite, the drag coefficient is actually worse for motorcycles then some minivans. It turned out that motorcycles are in fact not aerodynamic at all, and produce a significant amount of turbulent flow, mostly caused by the unrounded edges of the rider and certain parts (mirrors etc.). The drag coefficient that was found to be more realistic is 0.6, according to [24]. This will have a large influence on the air resistance, since the drag coefficient is 3 times larger than before, the air resistance will also become three times larger.

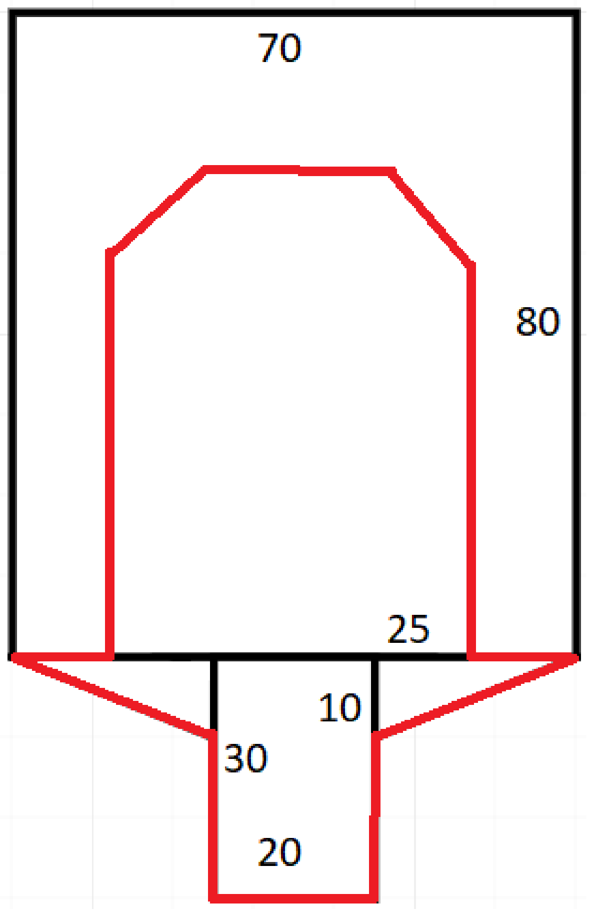

Figure 5.1: Frontal area of the superbike

Since there are new values for the frontal area and the coefficient of drag, the top speed can be calculated according to these values.

$$F_{acc} = F_r + F_D \implies 1209.7 = 73.58 + \frac{1}{2} * \rho * v^2 * A * c_d \tag{5.1}$$

$$2272.24 = \rho * v^2 * A * c_d \implies v = \sqrt{\frac{2272.24}{\rho * A * c_d}} = 245km/h$$

5.1.2 Gear ratios

When designing the overall gear ratios, there was not enough knowledge about how to do it. The 1:3 and 1:6 were chosen just to have an overlap in speed and an measurable difference between the gears. And the individual gear ratios were chosen such like they all were spur gears and without any thought about the best chain what could be chosen.

A module of 10 for the chain was chosen, but most MotoGP bikes use a module of 5 for the chain and these chains have a lot less losses and run more smoothly due to more investment into these types of chains. Then a gear ratio form the output shaft of the gearbox to the rear wheel of about 1:4 would have been chosen, because these are the most common for motorbikes. The result would have been that the gearbox had significantly less torque on the gears and shafts. This would have reduced the stresses in the gears and therefore the thickness could reduce. The benefit of that is that there is less mass to accelerate and that there is less inertia, which would increase acceleration as well.

If a redesign of the gear ratios itself would be unfeasible, still weight could be reduced. For example the 14/23 gear from the electric motor to the gearbox, the stresses are quite low. Therefore the thickness of the gear could be decreased to decrease the rotating weight and total weight. Also weight could be saved by hollowing out some parts of the gears, just like it is done at the bikes of road cyclists. This would also decrease the rotating and total weight.

5.1.3 Spline design

As was established in Section 4.2.8, the forces that the spline experiences in the final gear on the outgoing shaft exceed the allowed forces. This was caused by the 'low' thickness of the gear, and as such the short length of spline. One way to improve the compressive strength of the spline (which was insufficient) is by increasing the inner diameter, which also means that the shaft diameter is increased. Taking a trial value of 50 mm for the inner diameter, yields the following results.

Table 5.1: Spline Dimensions

Splines	Width	Height	Minor Diameter
Sixteen	0.098D	0.045D	0.910D

Since it is assumed that the inner diameter is 50mm, the following values can be calculated according to table 5.1.

Table 5.2: Spline Dimensions

Minor diameter (d)	Major diameter (D)	Height (h)	Width (W)
50 mm	54.95 mm	2.47 mm	5.39 mm

Now the same calculations can be performed.

$$\tau = \frac{F}{A_s} = \frac{2*T}{d*b*l} \rightarrow \tau = 720.22MPa \tag{5.2}$$

$$\sigma = \frac{F_t}{Ac} = \frac{4*T}{d*h*l} \rightarrow \sigma = 3143.32MPa \tag{5.3}$$

This shear stress and compressive stress are the total stresses. Considering that the spline has 16 different keys, the final shear stress and compressive stress can be calculated as follows:

$$\frac{720.22}{16} = 45MPa \tag{5.4}$$

$$\frac{3143.32}{16} = 196.5MPa \tag{5.5}$$

The values for the shear and compressive stress are both lower than the 'safe' values, and thus increasing the inner diameter of the spline to 50mm yields a spline design that stays within safe ranges.

5.2 Frame redesign

5.2.1 Redesign frame dimensions, connections and housing of electrical components

Starting with the positioning of the electrical components, a modification concerning the weight and balance of the bike had to be made since the weight of the gearbox appeared to be heavier. This meant that in order to have a correct balance on the motorcycle, on both the right side and left side of the motorcycle of Figure 4.22, components were rearranged. The ideal situation is to divide the total weight(104.9 kg) of the components(including gearbox and motor) evenly between the left and right side. The final arrangement of the motorcycle implies that the motor and 2/3 of the gearbox to be placed on the left side of the motorcycle (34.86kg of the 52.9kg of the gearbox), meaning that 41.63kg had to balanced on the other side. This was made possible by moving the high Voltage Control Board(2kg), the Data Logger(2kg), the ECU-central computer(2kg) to the right side and place them on top of the Motor Controller(12kg), which would be moved also fully to the right side. This made the weight on the right side still 3.99kg less, therefore if the weight of the chain is considered, an optimal balance may be achieved.

When looking at the frame design consisting of the trellis frame, angles on the side tubes of the bike where connected in many different and complex angles. Thus, to make production more feasible, these angles were changed into standard angles of 30, 60 and 120 for the side beams conforming the X shape in the frame.

Moreover, when the connections of the frame were subjected to welding procedures, in the case of using circular tubes, it was ideal to have all tubes of the frame shaped to match the initial frame design. This was achieved by the method of tube profiling, which will enable quality connections between the tubes. The advantage of this method was that it can be done with a milling cutter or even with tube notching saws. Two straight cuts on a tube will have a perfect fitting onto the connected rounded tube, making a precise fitting joint. Additionally, this method can easily adjust connections when in the real frame differs from the design dimensions since tube profiling is an easy method to apply to tubes in little time.

With the redesigned steel frame, the motorbike can withstand the maximum force of 5kN with reasonable deformation as well as the lateral, longitudinal and torsional stiffnesses within the acceptable limits. An advantage of using steel tubes is that, since steel is stronger than aluminum, the thickness and diameter of the tubes can be smaller, and thus, lighter. On the other hand, steel has a higher density, but since strenght has a higher priotrity than weight, steel was chosen. Another benefit of the use of steel in the frame is that there will not be any problems with the welding of the frame, since welding aluminum would require further treatment to restore the properties of the frame.

Chapter 6

Conclusions and recommendations

In conclusion, when designing a racing bike, it is crucial to take multiple aspects into account. Requirements must be set and the design should be optimized from there. Not only should grip, speed and acceleration be examined, but also strength and stiffness play a major role during a race.

Considering the drive train various improvements are possible. The thickness of the walls of the gearbox is rather high, it is possible to reduce the wall thickness to reduce the weight of the gearbox. If a different gear ratio is chosen, the stresses developed in the different parts of the gearbox can change, possibly removing weight. Changes in the dimensions of the parts as a result of changing stresses can then also result in a lower weight.

To improve the frame any further, more load cases can be examined such as cornering and accelerating. These cases will show different internal stress, which can result in a need for adjustments of dimensions. Furthermore, the deformation plots show unexplainable asymmetries, while being modelled completely symmetrical. To explain this, a deeper look should be taken into the Matlab code.

Overall, the design of a motorbike must be focused on the specific requirements and therefore be developed in a direction in which both the frame and the drive system are in coherence with each other. Thus results should be analysed in order to obtain specific information, that when combined, can give a good insight of how an electric superbike should be designed.

Bibliography

[1] dr. J. Hazrati, “Project Description: Design and Mechanics 2017-2018,” 2018.

[2] W. Harris, “How Motorcycles Work,” 2003. [Online]. Available: https://auto.howstuffworks.com/motorcycle2.htm

[3] “Iconfinder,” 2017. [Online]. Available: https://www.iconfinder.com/

[4] J. A. Sheldon Eucldean Brown, “The Geometry of Cantilever brakes,” 2008. [Online]. Available: https://www.sheldonbrown.com/cantilever-geometry.html

[5] C. Parashar, “What are differences between Disc brake and Drum brake?” 2017. [Online]. Available: https://www.quora.com/What-are-differences-between-Disc-Brake-and-Drum-Brake?redirected_qid=7901223

[6] K. Nice, “How Disc Brakes Work,” 2000. [Online]. Available: https://auto.howstuffworks.com/auto-parts/brakes/brake-types/disc-brake1.htm

[7] N. familjebok, “Uggleupplagan. 4. brant - cesti,” 1905. [Online]. Available: http://runeberg.org/nfbd/0139.html

[8] H. Singh, “What is regenerative braking system? how does it work?” 2017. [Online]. Available: https://www.quora.com/What-is-Regenerative-braking-system-How-does-it-work

[9] F. A. Khan, “17. pulsar 200ns - pressed steel perimeter frame - thrice the lateral stiffness of p220,” 2012. [Online]. Available: https://www.flickr.com/photos/motorbeam/7656783520/in/photostream/

[10] R. Jubilee, “Belt drive,” 2013. [Online]. Available: https://www.slideshare.net/rajat_jubilee/belt-drive

[11] unknown, “Cam drives,” 1999-2006. [Online]. Available: http://www.dansmc.com/camchain.htm

[12] ——, “Gear efficiency,” 2012. [Online]. Available: http://www.meadinfo.org/2008/11/gear-efficiency-spur-helical-bevel-worm.html

[13] M. staff, “Motorcycle final-drive systems compared,” 2016. [Online]. Available: https://www.motorcyclistonline.com/mc-garage-video-motorcycle-final-drive-systems-compared

[14] J. Glimmerveen, “Shaft system,” 2017. [Online]. Available: https://www.thoughtco.com/shaft-drive-motorcycle-or-chain-drive-743302

[15] unknown, “Tire friction and rolling resistance coefficients,” 2016. [Online]. Available: http://hpwizard.com/tire-friction-coefficient.html

[16] Roymech, “Gears - gear efficiency,” 2013. [Online]. Available: http://www.roymech.co.uk/Useful_Tables/Drive/Gear_Efficiency.html

[17] unknown, “The drag coefficient of an object in a moving fluid influence drag force,” 2004. [Online]. Available: https://www.engineeringtoolbox.com/drag-coefficient-d_627.html

[18] M. Z. T. Krone, W. Wits, “Machine Elements,” 2017.

[19] unknown, “Din bearings,” 2018. [Online]. Available: http://www.dinbearings.us/product.asp.htm

[20] tandwielen.com, “Spiebaan volgens din 6885,” unknown. [Online]. Available: https://www.tandwielen.com/spiebaan

[21] M. unknown, “Mohrs circle,” 2018. [Online]. Available: https://en.wikipedia.org/wiki/Mohr%27s_circle

[22] K. Nice, “How tires work,” unknown. [Online]. Available: https://auto.howstuffworks.com/tire4.htm

[23] unknown, “Steel Grades - SAE AISI,” unknown. [Online]. Available: https://tubingchina.com/steel.htm

[24] M. uharlik, “Motorcycle aerodynamics,” 2016. [Online]. Available: http://canadamotoguide.com/2016/05/04/motorcycle-aerodynamics/

[25] H. Wittel, D. Muhs, D. Jannasch, and J. Vossiek, “Roloff / matek machineonderdelen,” 2011. [Online]. Available: https://www.boomhogeronderwijs.nl/media/8/9789039526958_20070903_9789039526958.pdf

[26] unknown, “Formelsammlung und berechningsprogramme anlagenbau,” 2017. [Online]. Available: https://www.schweizer-fn.de/festigkeit/festigkeitswerte/stahl/stahl_start.php

Appendix A

Concept drawings

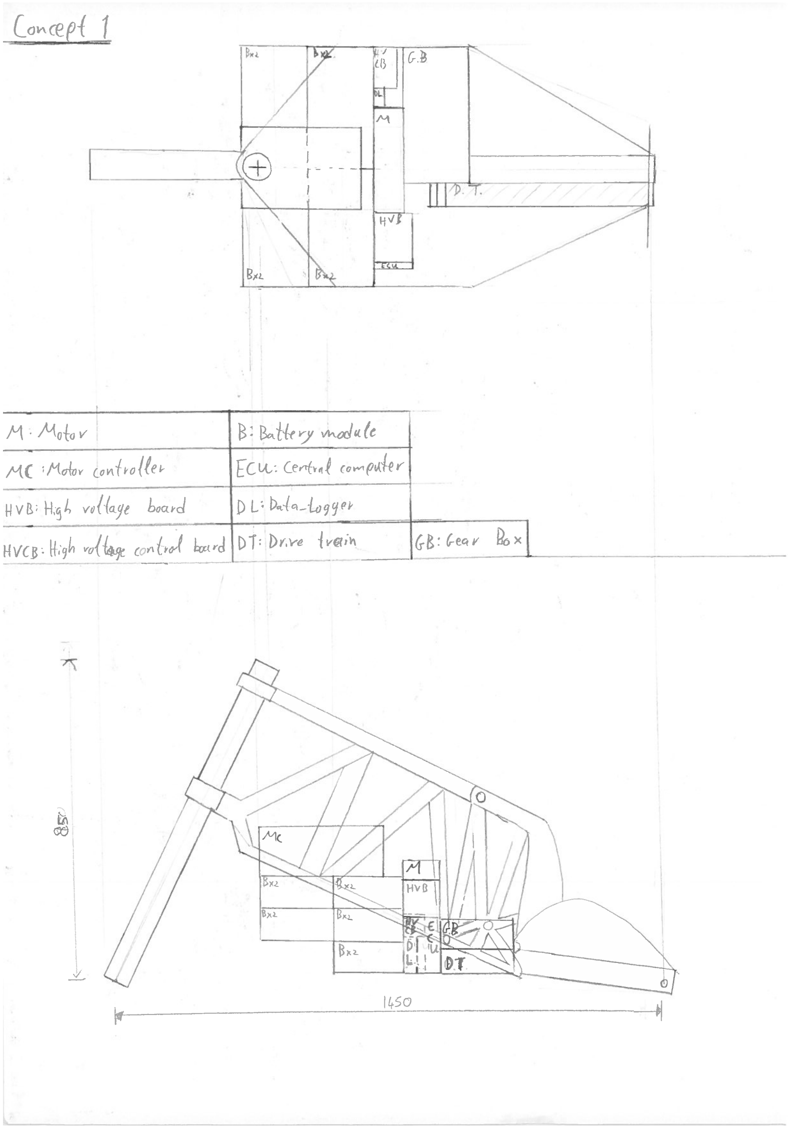
Concept 1
Bx2
Bx2
GB
DL
G.B
M
HVB
ECU
D.T.
Bx2
Bx2
880
MC
Bx2
Bx2
Bx2
Bx2
Bx2
M
HVB
E
C
U
GB
DL
DT
1450

M: Motor
B: Battery module
MC: Motor controller
ECU: Central computer
HVB: High voltage board
DL: Data-logger
HVCB: High voltage control board
DT: Drive train
GB: Gear Box

Figure A.1: Drawing of Concept 1

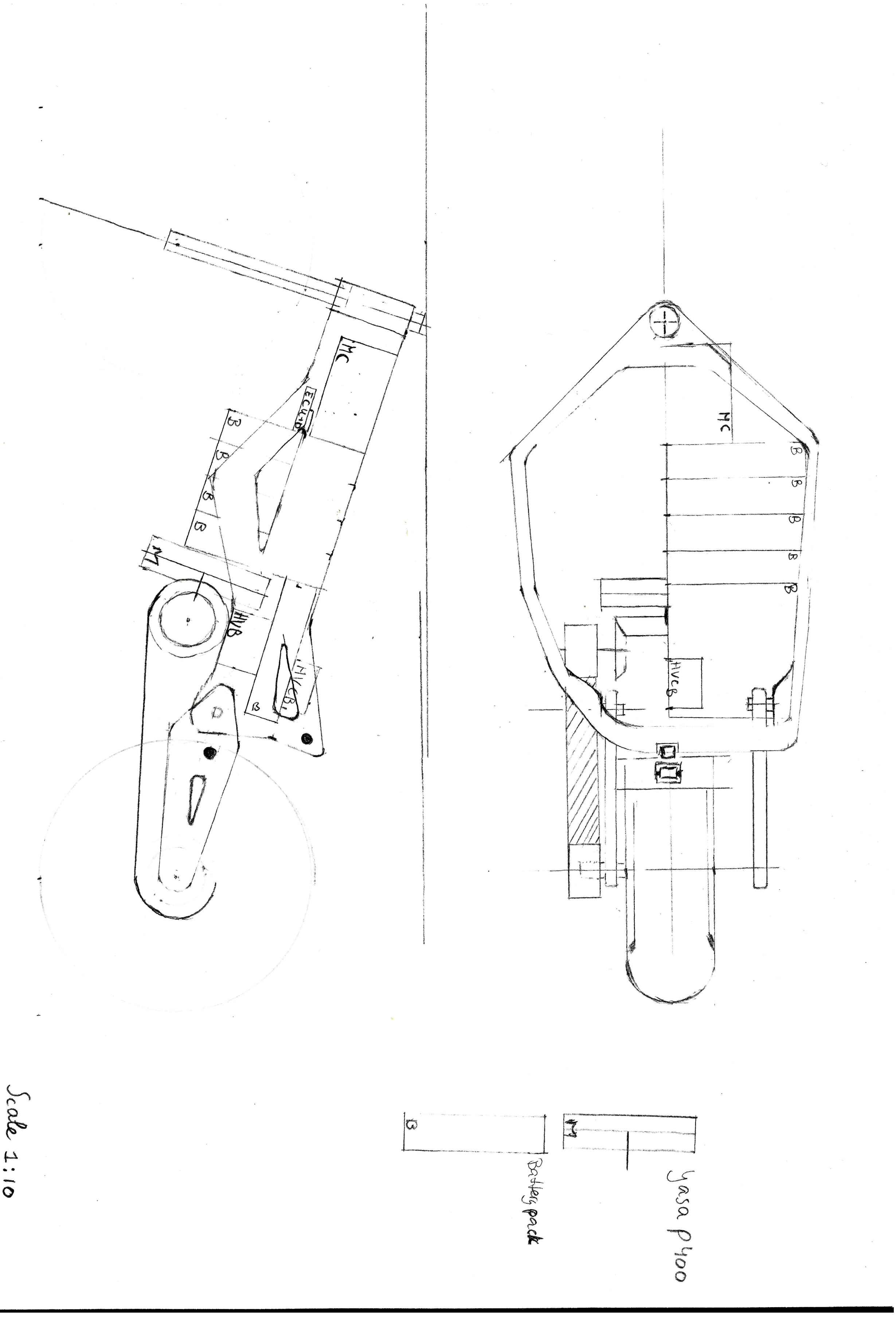
MC
ECU+D
B
B
B
B
B
M
HVB
HVCB
B
MC
B
B
B
B
B
HVCB
Scale 1:10
B
Battery pack
M
Yasa P400

Figure A.2: Drawing of Concept 2

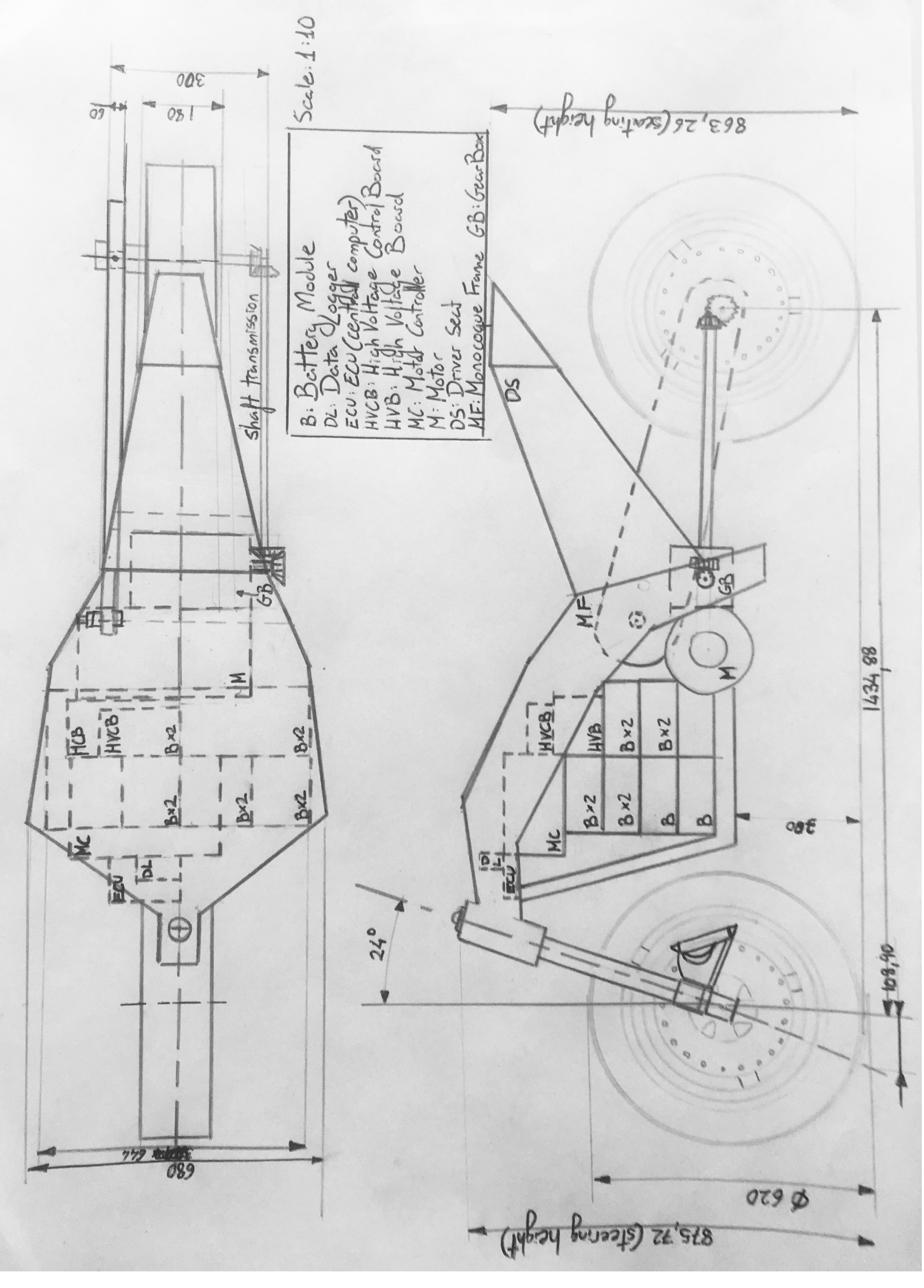
Scale: 1:10
B: Battery Module
DL: Data Logger
ECU: ECU (central computer)
HVCB: High Voltage Control Board
HVB: High Voltage Board
MC: Motor Controller
M: Motor
DS: Driver Seat
MF: Monocoque Frame
GB: GearBox
300
180
60
Shaft transmission
GB
M
HCB
HVCB
B×2
MC
ECU
DL
680
644
863,26 (seating height)
DS
MF
HVB
B
1434,88
380
24°
109,40
Ø 620
875,72 (steering height)

Figure A.3: Drawing of Concept 3

Appendix B

Dimensions of the superbike

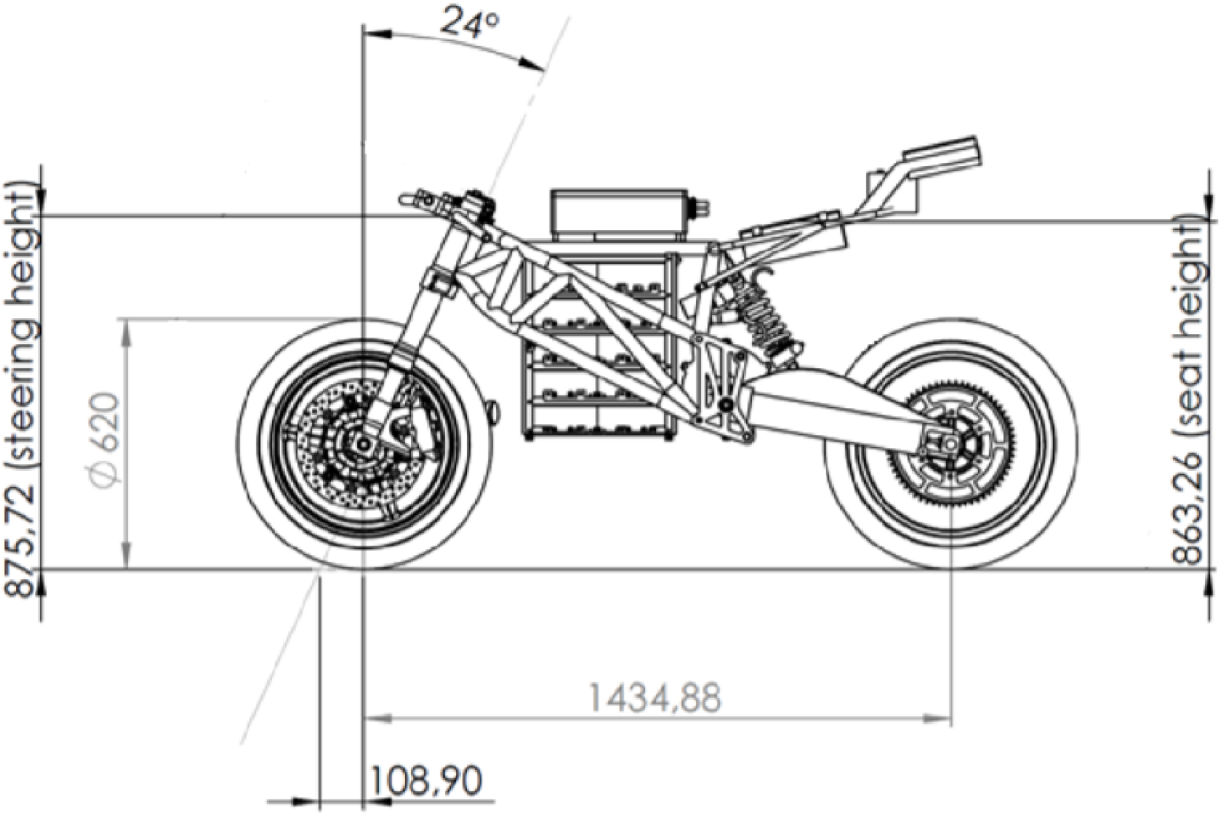
24°
875,72 (steering height)
∅ 620
863,26 (seat height)
1434,88
108,90

Figure B.1: Dimensions given on project description [1]

Appendix C

Product Sheet Yasa P400

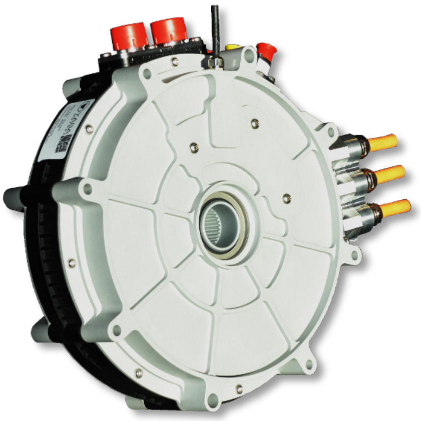

YASA

P400 Series E-Motors

YASA motors and generators are the smallest and lightest in their class. Based on YASA's unique Yokeless and Segmented Armature topology, the motors use less materials more efficiently to provide higher torque and power densities than any comparable motor or generator.

The **YASA P400 Series** of motor / generators are manufactured using advanced materials and proprietary construction techniques to enable high-volume production with significant customer cost benefits.

YASA P400 SERIES. Models from 20kW to 100kW continuous[1]:

Peak torque @450 A_{RMS} [2]	370 Nm
Continuous Torque [1]	Up to 300 Nm
Peak Power @700 V_{DC} [2]	160 kW
Continuous Power [1]	20 kW to 100 kW
Speed	0 – 8000 rpm
Peak Efficiency [3]	96%
Dry Mass [4]	from 24 kg

- Best-in-class torque and power density. Peak power density[2,4] > 6.7 kW/kg
- Dimensions from just 305mm (D) x 80.4mm (L)
- Through-shaft mounting and stacking capability
- Manufactured in volume

Applications where the YASA P400 Series excel include:

- Traction motors for on, off-road, rail and marine transport. Hybrid and full electric.
- Generators. Especially where size and weight are important in mobile and variable speed generation.
- P2 Hybrid. Generate, power boost and start from a small axial length. Ideal for transverse layout.
- Hydraulic replacement. Compact and efficient alternatives for hydraulic motors and starters.

AUTOMOTIVE OFF ROAD MARINE INDUSTRIAL AEROSPACE MOTORSPORT

The flexible, modular design of the P400 Series offers a range of torque and power combinations that can be tailored to optimise performance in specific applications.

Please call +44 (0) 1865 952 100 or email sales@yasa.com to discuss your requirements.

---

1. Maximum continuous ratings are based on extrapolated test data for a YASA P400 HC motor with integrated rotor cooling, 30°C Ambient temp, 20 ltrs/min coolant flow and coolant inlet temp <65°C.
2. Peak torque & power ratings are given at 60°C rotor and 60°C coolant inlet temperature and 450 A_{RMS}.
3. Peak efficiency measured at the optimal operating area of the YASA P400 and does not include controller efficiency.
4. Mass for flange mounted cartridge version with a single cover incorporating a standard rotary position sensor. Mass is 28kg for the P400 HC model with integrated rotor fan cooling. Mass does not include coolant fluid or phase cables (due to various possible lengths and fixing strategies).

All data subject to change without notice.

© 2018 YASA Limited. 11-14 Oxford Industrial Park, Kidlington OX5 1QU. UK. Registered in England & Wales No. 06975790

www.yasa.com +44 (0) 1865 952 100 sales@yasa.com

YASA

P400 S - Standard Version

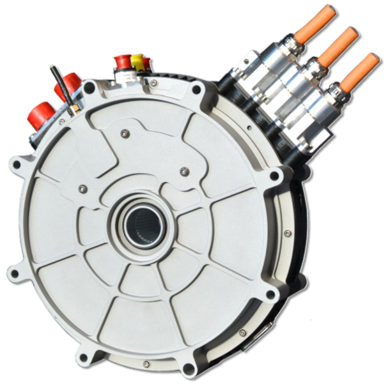

The P400 S is the versatile backbone of the P400 Series and offers exceptional peak performance in a lightweight sealed package. The S model is the first choice for simplified integration into automotive, marine and aerospace traction applications.

Mechanical

Casing Diameter	305mm
Mounting 8x Ø8.3	294mm PCD
Axial length	106.7mm
Dry Mass	27kg
Stator Cooling	Oil

Electrical

Peak Torque @450 A	up to 370 Nm
Continuous Torque	up to 300 Nm
Peak Power @700V	160 kW
Continuous Power	up to 60 kW
Maximum Speed	8000 rpm

Example Electrical Performance with 800V controller @450A$_{\mathrm{RMS}}$ **P400 S**

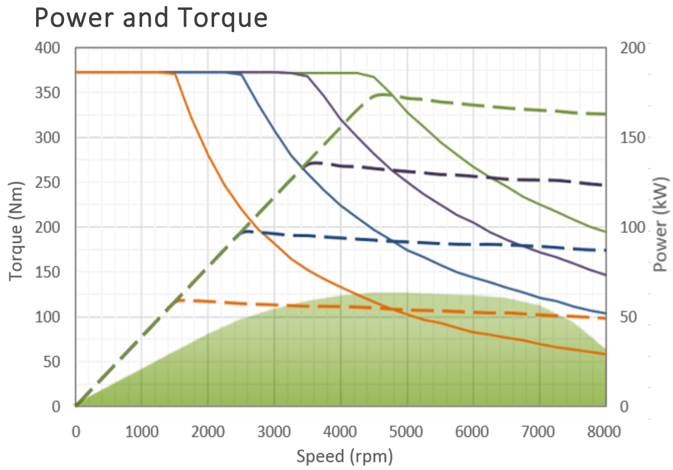

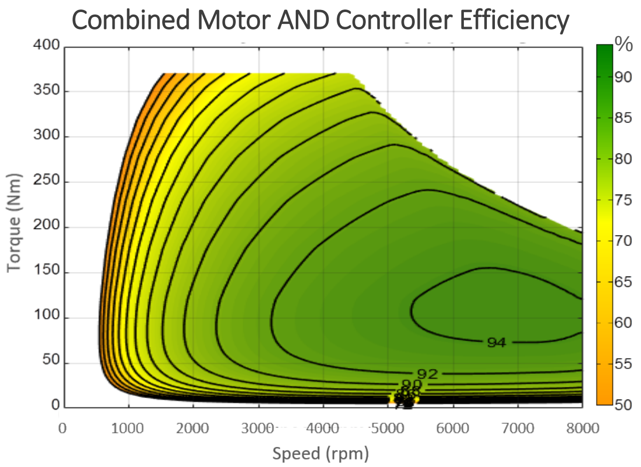

Peak (30 sec)

Torque		Power
▬	700V	▪▪▪▪
▬	550V	▪▪▪▪
▬	400V	▪▪▪▪
▬	250V	▪▪▪▪

Continuous Power
P400 S
🟩 24/7 Continuous
(Preliminary data)

The specified P400 S performance is based on dynamometer test data. The performance available in your application may be different and will depend on drive cycle and installation details. Please contact us for detailed information.

Peak data at 60°C rotor, 60°C coolant inlet @20 ltrs/min and 60°C ambient

Continuous ratings at coolant inlet <50°C @20 ltrs/min, <30°C ambient.

P400 HC and P400 C

P400 HC High Continuous Output

- Up to **100kW continuous** 24/7
- Integrated rotor air cooling via air duct.
- Traction and power generation solution for enclosed engine bay environments.

P400 C Cartridge

- **Axial length 80.4 mm**
- Cartridge model for project integration
- Flexible package for the optimum performance in your application.

Performance in your application

The YASA P400 Series motors are available in a range of torque and speed combinations and with a variety of mechanical and cooling options.

Please **contact us** to discuss your application requirements. We can then supply detailed information on the YASA products and options that may be suitable for you.

© 2018 YASA Limited.

Appendix D

FBD Calculations

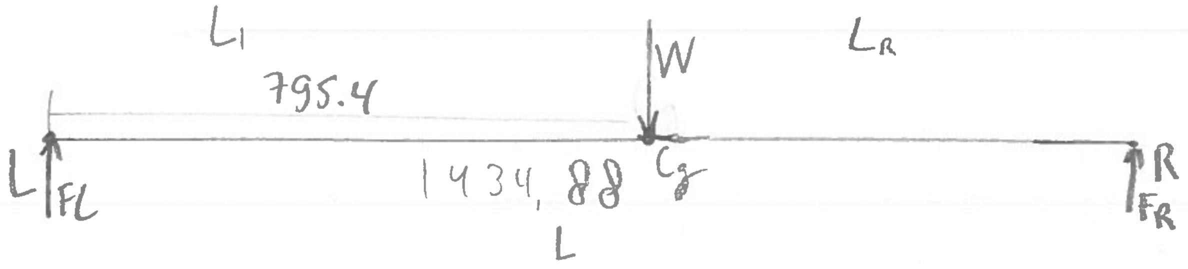

L_1
795.4
W
L_R
L
F_L
1434, 88
C_g
R
F_R
L

$W = M \cdot g$

M is assumed to be 400kg => $W = 3924\ N$

$(\circlearrowleft +)\ \sum M_L = 0 : -(L - L_R)W + L(F_L) \Rightarrow F_L = \frac{L - L_w}{L} W$

$= 1748.8\ N$

$\sum F_y = 0 : F_L + F_R - W \Rightarrow F_R = W - F_L$

$= 2175.2\ N$

(not exactly to scale)

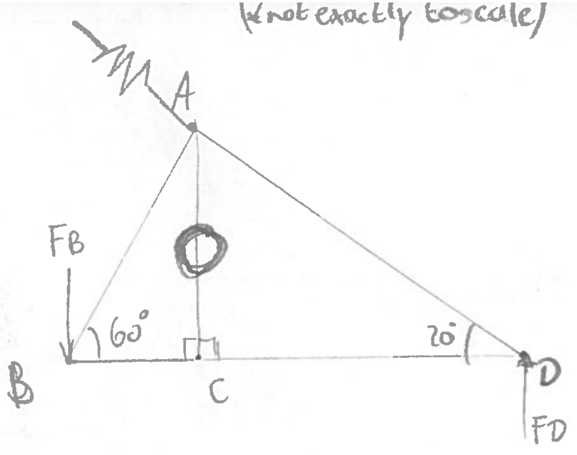

A is the connection between the spring and swivel arm.

B is the connection between the swivel arm and the frame.

D is the connection of the rear wheel to the frame

$F_D = 2175.2$ N

Joint D

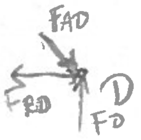

$\Sigma F_y = 0: \; F_D - \sin(20) \cdot F_{AD}$

$\Rightarrow F_{AD} = \frac{F_D}{\sin(20)} = 6359.9$ N

$\Sigma F_x = 0: \; \cos(20) F_{AD} - F_{BD} \Rightarrow \quad F_{BD} = \cos(20) F_{AD}$

$F_{BD} = 5976.3$ N

Joint B

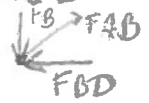

$\Sigma F_x = 0: \; \cos(60) \cdot F_{AB} - F_{BD} \quad \Rightarrow F_{AB} = \frac{F_{BD}}{\cos(60)} = \quad F_{AB} = 11952.6$

$\Sigma F_y = 0: \; \sin(60) \; F_{AB} \; - F_B$

$F_B = \sin(60) F_{AB} = \overset{(F_B)}{10351.3}$ N ! reaction

Joint A

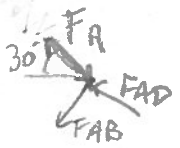

$\Sigma F_x = 0: \; -\cos(20) \; 6359.9 \; - \cos(60) \; 11952.6 \; + \cos(30) F_R$

$= F_R = 13801.7$ N ! reaction

$F_{Rx} = 11952.6$ N

$F_{yx}: 6900$ N

Appendix E

Frequently used axle and gear materials

Tabel 1-1 Vervolg

staalsoort		A % min.	R_{mN} min.	R_{eN} $R_{p0,2N}$ min.	$\sigma_{zd\,WN}$ ($\sigma_{zd\,SchN}$)	σ_{bWN} (σ_{bSchN})	τ_{tWN} (τ_{tSchN})	relatieve materiaalkosten[3]	eigenschappen en toepassingsvoorbeelden	
afkorting	materiaalnummer									
c) Veredelstaal, ongelegeerd volgens NEN EN 10083-2 en gelegeerd volgens NEN EN 10083-3, 1 in veredelde toestand (+QT).[4] Geschikt voor vlam- en inductieharden. genormaliseerde afmeting $d_N = 16$ mm									ongelegeerde of gelegeerde machinebouwstaalsoorten die vanwege hun chemische samenstelling geschikt zijn om te harden en die in veredelde toestand hoge sterkte combineren met goede taaiheid; voor het lassen is voorverwarmen vereist	
C22E	1.1151	20	500	340	200 (340)	250 (405)	150 (235)	1,6	licht belaste delen met gelijkmatige structuur en goede oppervlaktekwaliteit; hefbomen, flenzen, schijven, aandrijfassen, drijfstangen; oppervlakteharding	gering belaste constructiedelen met kleine veredelingsdiameters (< 100 mm)
C35E	1.1181	17	630	430	250 (430)	315 (515)	190 (300)			
C40E	1.1186	16	650	460	260 (460)	325 (550)	195 (320)	1,7	drijfwerkdelen met bijzonder gelijkmatige en zuivere structuur; op slijtage belaste onderdelen; oppervlakteharding; drijfwerkassen, tandwielen, wielbanden, krukassen, kruktappen	
C45E	1.1191	14	700	490	280 (490)	350 (590)	210 (340)			
C50E	1.1206	13	750	520	300 (515)	375 (625)	225 (360)			
C55E	1.1203	12	800	550	320 (540)	400 (660)	240 (380)			
C60E	1.1221	11	850	580	340 (570)	425 (695)	255 (400)			
28Mn6	1.1170	13	800	590	320 (540)	400 (680)	240 (410)			
38Cr2	1.7003	14	800	550	320 (540)	400 (660)	240 (380)	1,7	hefbomen, aandrijfassen, pennen, tandwielen, bouten, wormen, smeedstukken	zwaarder belaste constructie-elementen met grotere veredelingsdiameters
46Cr2	1.7006	12	900	650	360 (590)	450 (740)	270 (450)			
34Cr4	1.7033	12	900	700	360 (590)	450 (740)	270 (480)			
37Cr4	1.7034	11	950	750	380 (615)	475 (770)	285 (500)			
41Cr4	1.7035	11	1000	800	400 (640)	500 (800)	300 (525)			
25CrMo4	1.7218	12	900	700	360 (590)	450 (740)	270 (480)		inlaatkleppen, aandrijfassen, freesdoorns, spieassen, krukassen, krukpennen,grote drijfwerkassen	
34CrMo4	1.7220	11	1000	800	400 (640)	500 (800)	300 (525)			
42CrMo4	1.7225	10	1100	900	440 (685)	550 (855)	330 (565)			
50CrMo4	1.7228	9	1100	900	440 (685)	550 (855)	330 (565)			
36CrNiMo4	1.6511	10	1100	900	440 (685)	550 (855)	330 (565)	2,4	zwaarst belaste constructiedelen in de voertuig- en machinebouw; grote drijfwerkassen, turbinerotors, tandwielen	constructie-elementen die zeer zwaar belast worden; grote veredelingsdiameters
34CrNiMo6	1.6582	9	1200	1000	480 (725)	600 (910)	360 (605)			
30CrNiMo8	1.6580	9	1250	1050	500 (750)	625 (935)	375 (625)	2,7		
36NiCrMo16	1.6773	9	1250	1050	500 (750)	625 (935)	375 (625)			
51CrV4	1.8159	9	1100	900	440 (685)	550 (855)	330 (565)			
d) Carboneerstaal volgens NEN EN 10084 in blindgeharde toestand[5] genormaliseerde afmeting $d_N = 16$ mm									ongelegeerd en gelegeerd machinebouwstaal met laag C-gehalte dat aan de oppervlakte gecarboneerd of gecarbonitreerd en dan gehard wordt: voor vermoeiingssterke onderdelen met slijtvaste, harde oppervlakken; geschikt voor afbrandstuiklassen en smeltlassen	
C10E	1.1121	16	500	310	200 (310)	250 (370)	150 (215)	1,1	direct hardbare kleine onderdelen met minder sterk kernmateriaal; pennen, bussen, tappen, hefbomen, scharnieren, spindels	
C15E	1.1141	14	800	545	320 (540)	400 (655)	240 (380)			
17Cr3	1.7016	11	800	545	320 (540)	400 (655)	240 (380)	1,7	zwaar belaste onderdelen; kleinere tandwielen en aandrijfassen, pennen, nokkenassen, rollen, spindels, meetgereedschappen	
28Cr4	1.7030	10	900	620	360 (590)	450 (740)	270 (430)			
16MnCr5	1.7131	10	1000	695	400 (640)	500 (800)	300 (480)			
20MnCr5	1.7147	8	1200	850	480 (725)	600 (910)	360 (590)		direct hardbare onderdelen met sterk kernmateriaal; middelgrote tandwielen en assen in tandwielkasten en voertuigen	
20MoCr4	1.7321	10	900	620	360 (590)	450 (740)	270 (430)			
22CrMoS3-5	1.7333	8	1100	775	440 (685)	550 (855)	330 (535)		zwaar belaste aandrijfdelen met zeer hoge taaiheid; directe harding	
20NiCrMo2-2	1.6523	10	1100	775	440 (685)	550 (855)	330 (535)			
17CrNi6-6	1.5918	9	1200	850	480 (725)	600 (910)	360 (590)	2,1	zwaarst belaste onderdelen; rondsels, nokken, aandrijfassen, kegel-kroonwielen, kettingschakels	
18CrNiMo7-6	1.6587	8	1200	850	480 (725)	600 (910)	360 (590)			
e) Nitreerstaal volgens DIN EN 10085 in veredelde toestand (+QT) genormaliseerde afmeting $d_N = 100$ mm									gelegeerd veredelstaal, dat door nitridevormers (Cr, Al, Mo, V) voor het nitreren en nitrocarboneren bijzonder goed geschikt is; de zeer harde oppervlakteharding geeft deconstructiedelen een hoge slijtvastheid, hoge vermoeiingssterkte, roestbestendigheid, hittebestendigheid en geringe neiging tot ‘vreten’; weinig vervorming	
31CrMo12	1.8515	10	1030	835	410 (650)	515 (815)	310 (540)	2,6	op slijtage belaste, zuivere onderdelen tot 250 mm dik; zware krukassen, kalanderwalsen, matrijsgietwerk	
31CrMoV9	1.8519	9	1100	900	440 (685)	550 (855)	330 (565)		hittebestendige slijtdelen tot 100 mm dik; klepspindels, slijpmachinespindels	
33CrMoV12-9	1.8522	11	1150	950	460 (705)	575 (880)	345 (585)		op slijtage belaste onderdelen tot 250 mm dik; pennen, spindels	
34CrAlMo5-10	1.8507	14	800	600	320 (540)	400 (680)	240 (415)		kruipvaste slijtdelen tot boven 450 °C en 70 mm dikte; delen van stoomarmaturen	
34CrAlNi7-10	1.8550	10	900	680	360 (590)	450 (740)	270 (470)		voor grote op slijtage belaste constructie-elementen; zware plunjers, zuigerstangen	

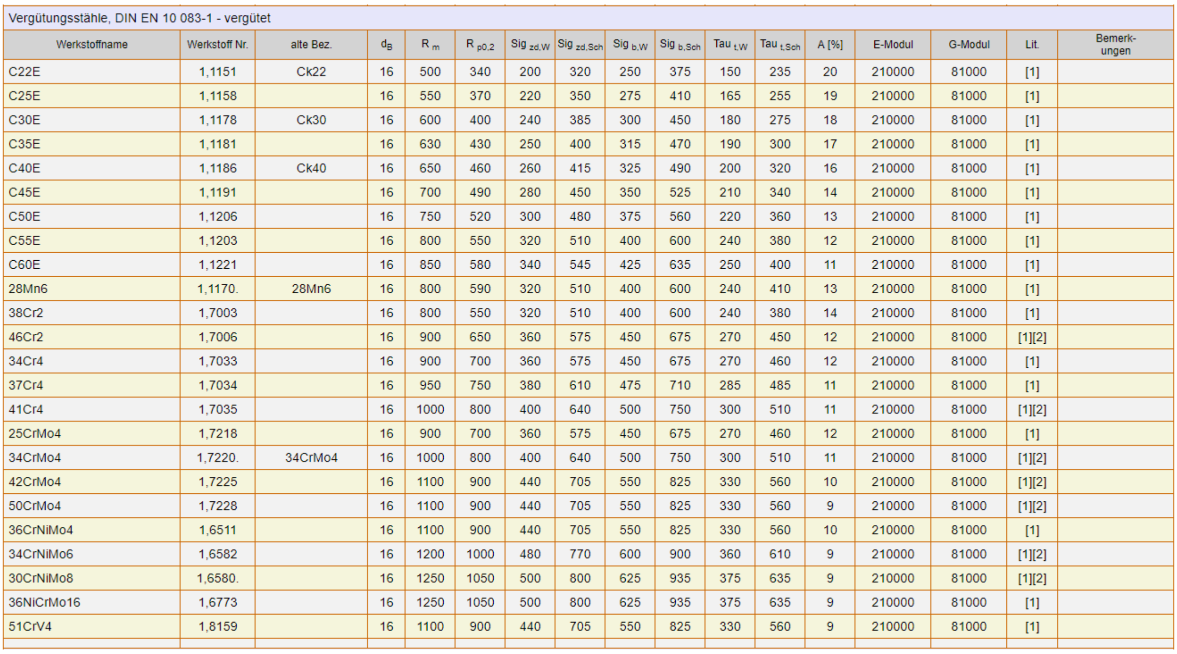

Vergütungsstähle, DIN EN 10 083-1 - vergütet

Werkstoffname	Werkstoff Nr.	alte Bez.	d_B	R_m	$R_{p0,2}$	Sig $_{zd,W}$	Sig $_{zd,Sch}$	Sig $_{b,W}$	Sig $_{b,Sch}$	Tau $_{t,W}$	Tau $_{t,Sch}$	A [%]	E-Modul	G-Modul	Lit.	Bemerkungen
C22E	1,1151	Ck22	16	500	340	200	320	250	375	150	235	20	210000	81000	[1]	
C25E	1,1158		16	550	370	220	350	275	410	165	255	19	210000	81000	[1]	
C30E	1,1178	Ck30	16	600	400	240	385	300	450	180	275	18	210000	81000	[1]	
C35E	1,1181		16	630	430	250	400	315	470	190	300	17	210000	81000	[1]	
C40E	1,1186	Ck40	16	650	460	260	415	325	490	200	320	16	210000	81000	[1]	
C45E	1,1191		16	700	490	280	450	350	525	210	340	14	210000	81000	[1]	
C50E	1,1206		16	750	520	300	480	375	560	220	360	13	210000	81000	[1]	
C55E	1,1203		16	800	550	320	510	400	600	240	380	12	210000	81000	[1]	
C60E	1,1221		16	850	580	340	545	425	635	250	400	11	210000	81000	[1]	
28Mn6	1,1170.	28Mn6	16	800	590	320	510	400	600	240	410	13	210000	81000	[1]	
38Cr2	1,7003		16	800	550	320	510	400	600	240	380	14	210000	81000	[1]	
46Cr2	1,7006		16	900	650	360	575	450	675	270	450	12	210000	81000	[1][2]	
34Cr4	1,7033		16	900	700	360	575	450	675	270	460	12	210000	81000	[1]	
37Cr4	1,7034		16	950	750	380	610	475	710	285	485	11	210000	81000	[1]	
41Cr4	1,7035		16	1000	800	400	640	500	750	300	510	11	210000	81000	[1][2]	
25CrMo4	1,7218		16	900	700	360	575	450	675	270	460	12	210000	81000	[1]	
34CrMo4	1,7220.	34CrMo4	16	1000	800	400	640	500	750	300	510	11	210000	81000	[1][2]	
42CrMo4	1,7225		16	1100	900	440	705	550	825	330	560	10	210000	81000	[1][2]	
50CrMo4	1,7228		16	1100	900	440	705	550	825	330	560	9	210000	81000	[1][2]	
36CrNiMo4	1,6511		16	1100	900	440	705	550	825	330	560	10	210000	81000	[1]	
34CrNiMo6	1,6582		16	1200	1000	480	770	600	900	360	610	9	210000	81000	[1][2]	
30CrNiMo8	1,6580.		16	1250	1050	500	800	625	935	375	635	9	210000	81000	[1][2]	
36NiCrMo16	1,6773		16	1250	1050	500	800	625	935	375	635	9	210000	81000	[1]	
51CrV4	1,8159		16	1100	900	440	705	550	825	330	560	9	210000	81000	[1]	

[26]

[25]

Appendix F

Gearbox assembly drawing

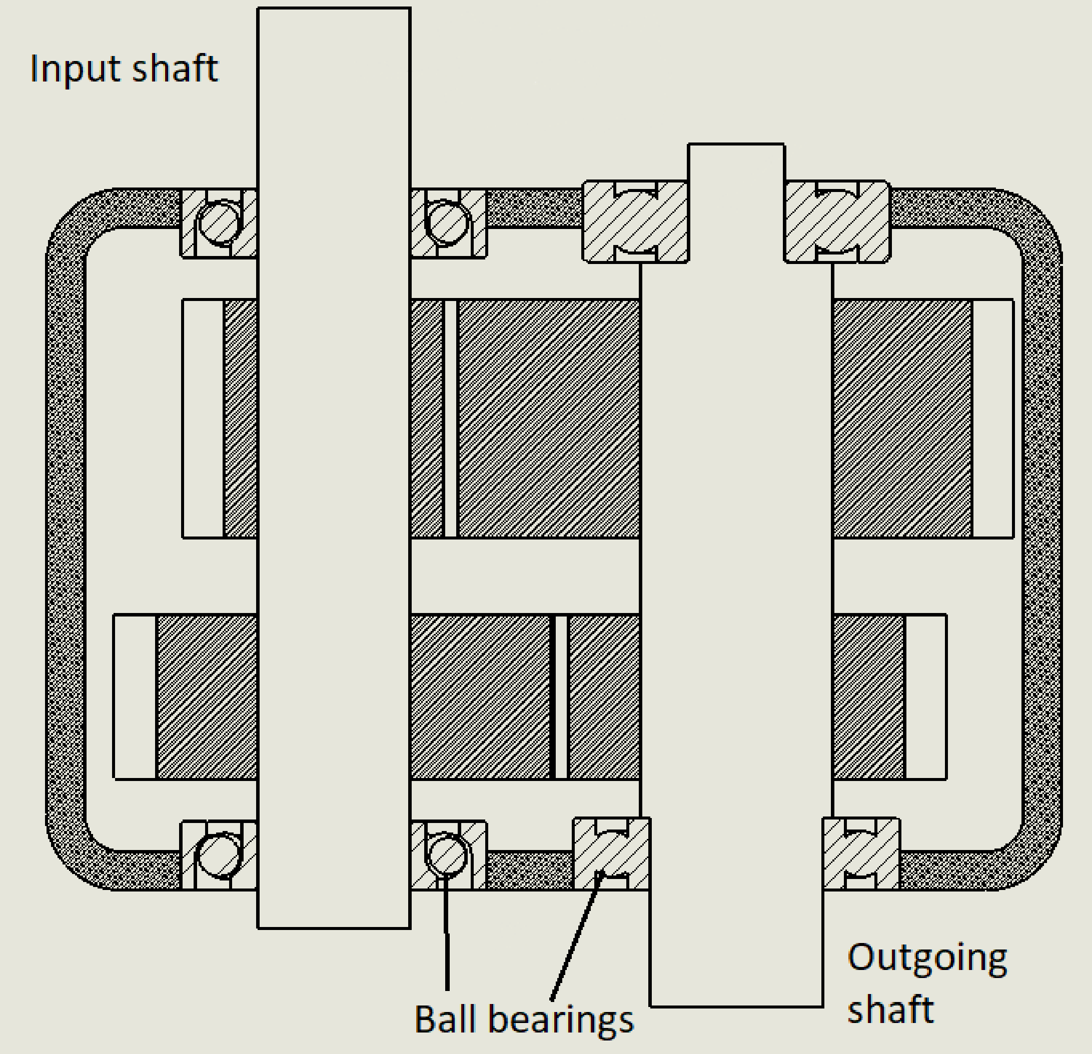
Input shaft
Ball bearings
Outgoing shaft

Figure F.1: Gearbox assembly drawing

Appendix G

V, M and T diagrams

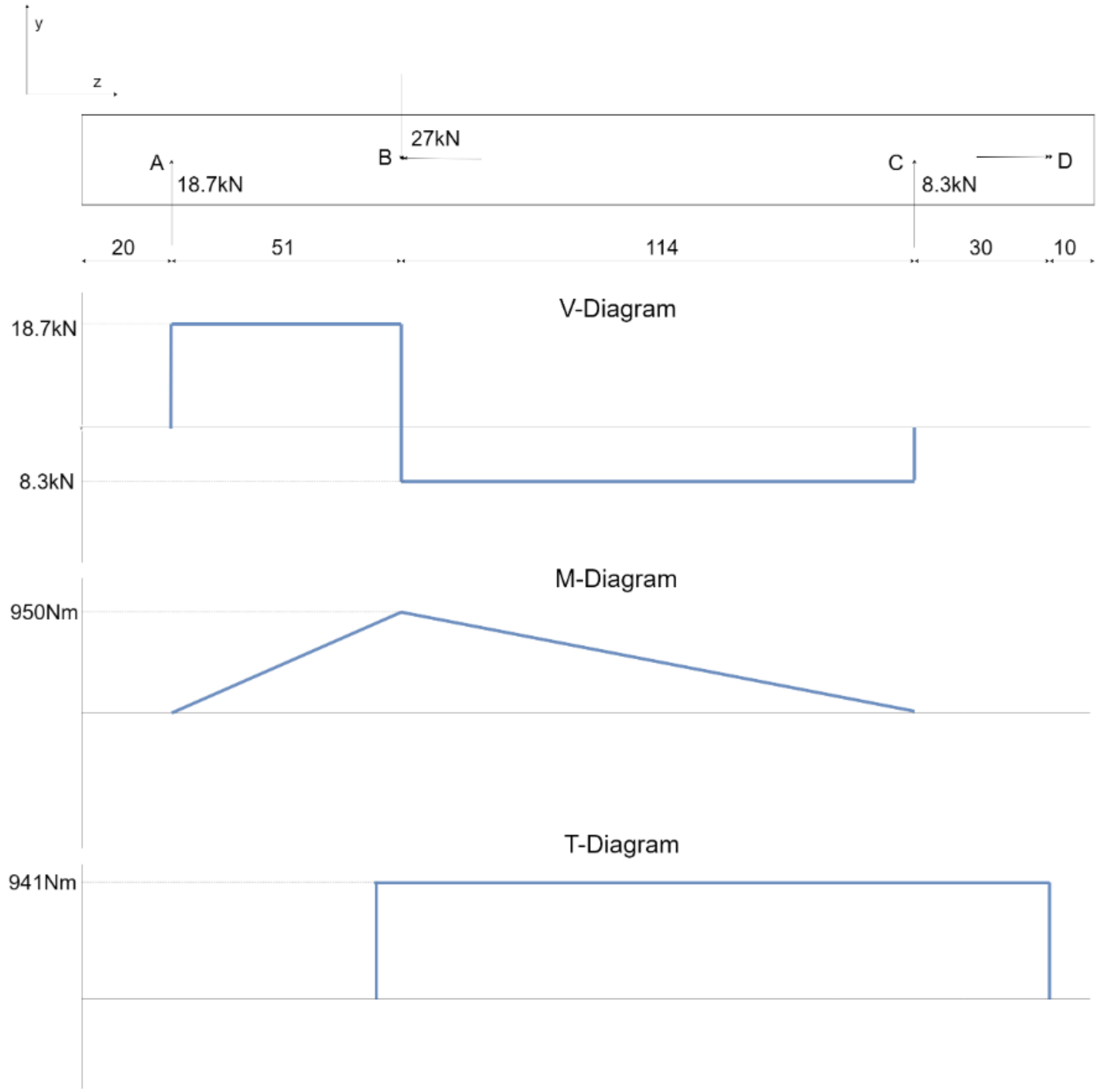
y
z
27kN
A
18.7kN
B
C
8.3kN
D
20
51
114
30
10
V-Diagram
18.7kN
8.3kN
M-Diagram
950Nm
T-Diagram
941Nm

Figure G.1: V, M and T diagrams of the front view

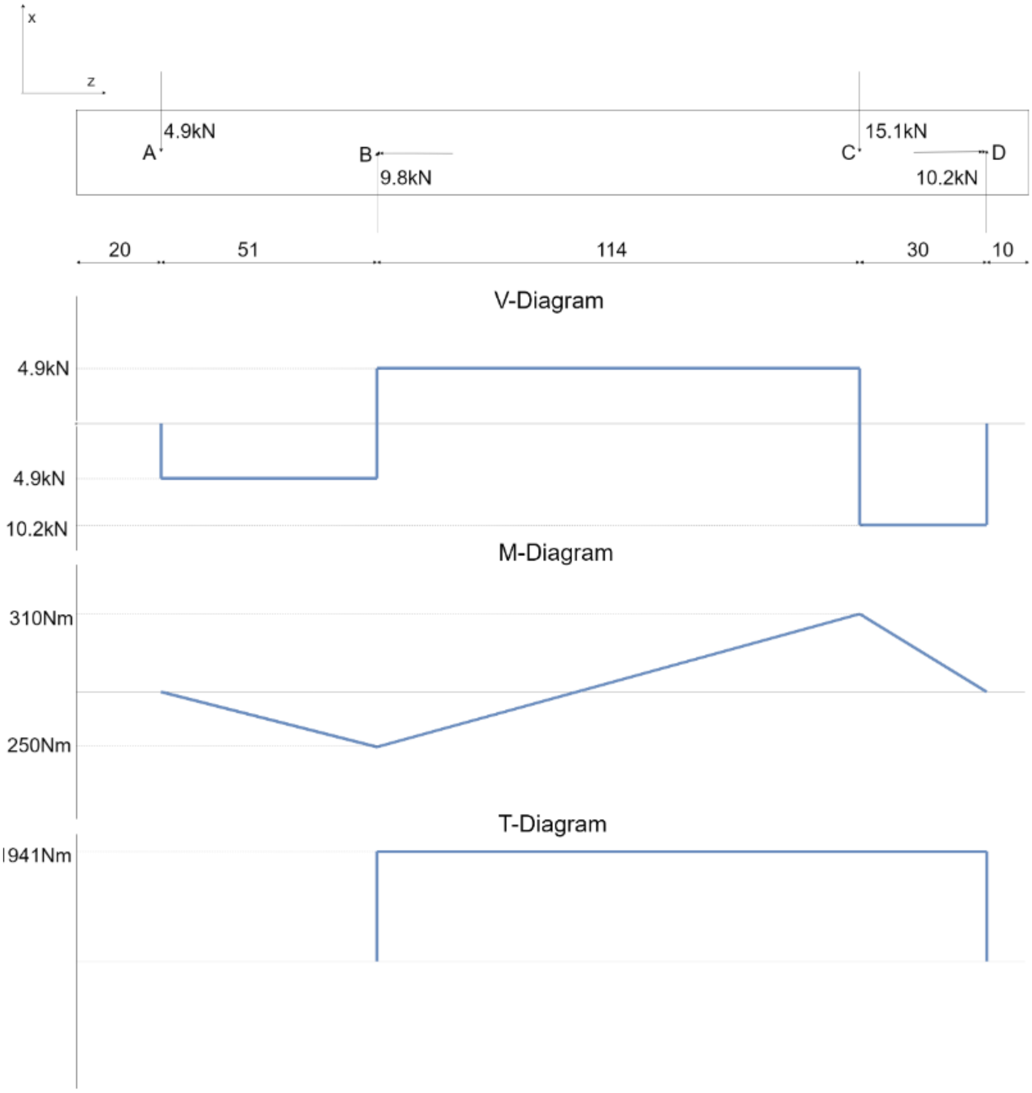
x
z
4.9kN
A
B
9.8kN
15.1kN
C
D
10.2kN
20
51
114
30
10
V-Diagram
4.9kN
4.9kN
10.2kN
M-Diagram
310Nm
250Nm
T-Diagram
1941Nm

Figure G.2: V, M and T diagrams of the top view

Appendix H

Bearing selection

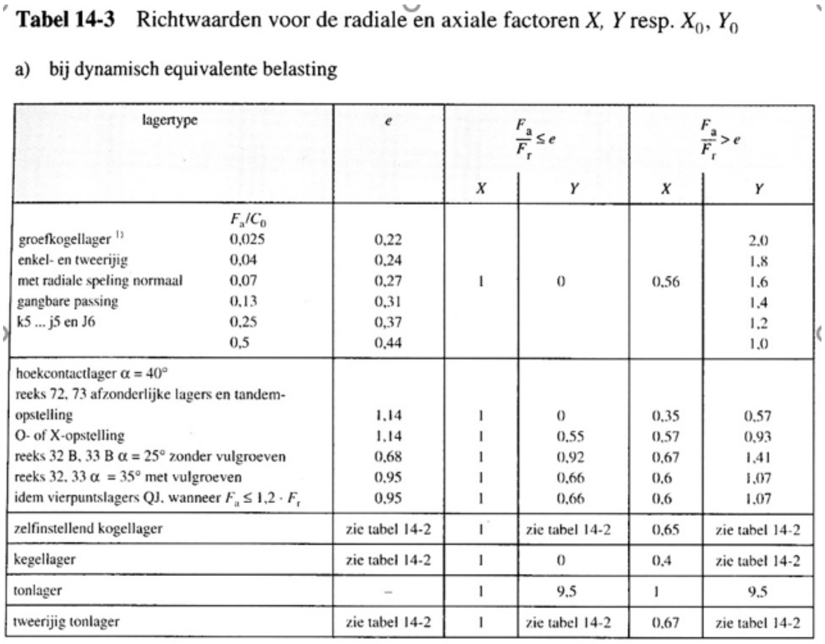

Tabel 14-3 Richtwaarden voor de radiale en axiale factoren X, Y resp. X_0, Y_0

a) bij dynamisch equivalente belasting

lagertype		e	$\frac{F_a}{F_r} \leq e$		$\frac{F_a}{F_r} > e$	
			X	Y	X	Y
	F_a/C_0					
groefkogellager [1]	0,025	0,22	1	0	0,56	2,0
enkel- en tweerijig	0,04	0,24				1,8
met radiale speling normaal	0,07	0,27				1,6
gangbare passing	0,13	0,31				1,4
k5 ... j5 en J6	0,25	0,37				1,2
	0,5	0,44				1,0
hoekcontactlager $\alpha = 40°$						
reeks 72, 73 afzonderlijke lagers en tandem-opstelling		1,14	1	0	0,35	0,57
O- of X-opstelling		1,14	1	0,55	0,57	0,93
reeks 32 B, 33 B $\alpha = 25°$ zonder vulgroeven		0,68	1	0,92	0,67	1,41
reeks 32, 33 $\alpha = 35°$ met vulgroeven		0,95	1	0,66	0,6	1,07
idem vierpuntslagers QJ, wanneer $F_a \leq 1{,}2 \cdot F_r$		0,95	1	0,66	0,6	1,07
zelfinstellend kogellager		zie tabel 14-2	1	zie tabel 14-2	0,65	zie tabel 14-2
kegellager		zie tabel 14-2	1	0	0,4	zie tabel 14-2
tonlager		–	1	9,5	1	9,5
tweerijig tonlager		zie tabel 14-2	1	zie tabel 14-2	0,67	zie tabel 14-2

Figure H.1: Axial and radial load factors for bearings

Appendix I

Tables of principle stress and elongation

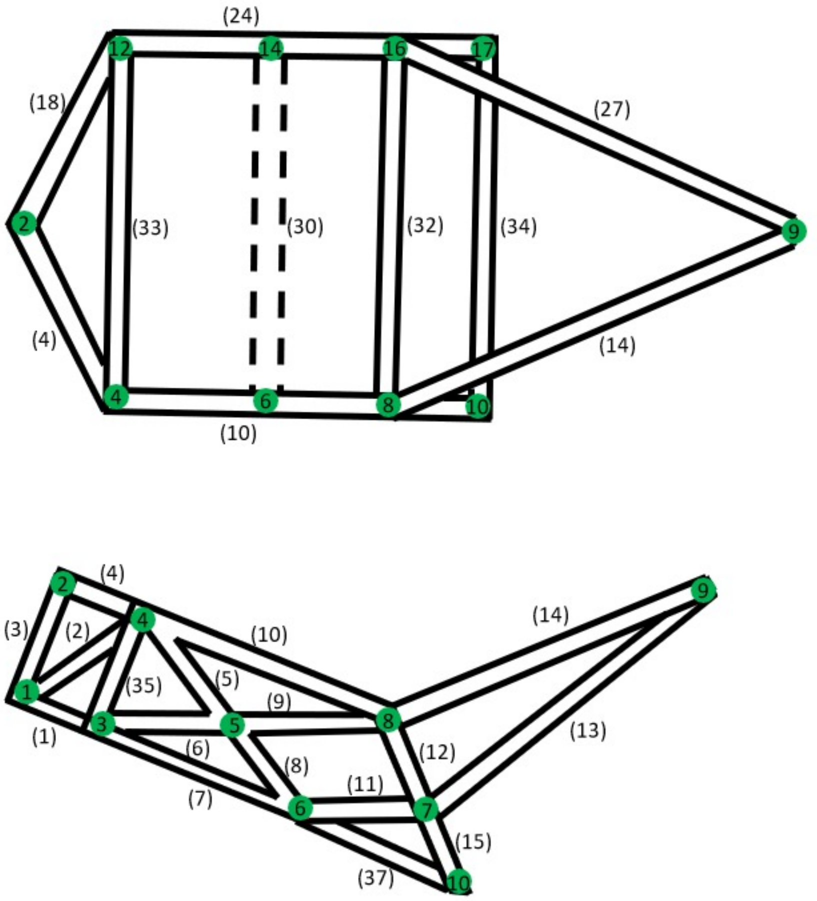
(24)
12
14
16
17
(18)
(27)
2
(33)
(30)
(32)
(34)
9
(4)
(14)
4
6
8
10
(10)
(4)
2
9
(3)
(2)
4
(10)
(14)
(35)
(5)
(9)
1
3
5
8
(1)
(6)
(12)
(13)
(8)
(11)
6
7
(7)
(15)
(37)
10

Figure I.1: Numbering of the nodes

Table I.1: Node numbering table

Node number	Opposite of
3	11
4	12
5	13
6	14
7	15
8	16
10	17

Table I.2: Displacement table

Element Nr.	Ux (m)	Uy (m)	Uz (m)	Rotx (rad)	Rot y (rad)	Rot z (rad)
1	-0.00013898	0	0	4.6027e-17	0.0010554	-1.661e-17
2	9.0385e-05	-6.3902e-18	-0.00010044	4.526e-17	0.0011395	2.0713e-1
3	-6.1438e-05	-3.4144e-05	-0.00014862	-0.00029718	2.223e-05	-8.1464e-0
4	-6.4878e-05	2.6161e-05	-0.00015032	-0.0001029	7.9197e-05	0.0002475
5	-5.3386e-05	-3.5337e-06	-0.00013467	-0.00021978	-0.00023032	0.0001675
6	-1.5096e-05	-2.1038e-06	-0.0001042	-9.666e-06	-0.00038	0.0001278
7	0	1.0856e-06	0	2.6078e-05	-0.00030872	-3.5348e-0
8	-4.5673e-05	9.1238e-07	-2.6458e-05	-2.582e-05	-0.00039845	-6.7704e-0
9	-0.00010549	-3.1954e-18	0.00014729	4.5184e-17	-0.00027392	-7.7979e-1
10	3.874e-05	1.7406e-07	1.6372e-05	-8.2266e-06	-0.00028379	-3.1064e-0
11	-6.1438e-05	3.4144e-05	-0.00014862	0.00029718	2.223e-05	8.1464e-0
12	-6.4878e-05	-2.6161e-05	-0.00015032	0.0001029	7.9197e-05	-0.000247
13	-5.3386e-05	3.5337e-06	-0.00013467	0.00021978	-0.00023032	-0.000167
14	-1.5096e-05	2.1038e-06	-0.0001042	9.666e-06	-0.00038	-0.000127
15	0	-1.0856e-06	0	-2.6078e-05	-0.00030872	3.5348e-0
16	-4.5673e-05	-9.1238e-07	-2.6458e-05	2.582e-05	-0.00039845	6.7704e-0
17	3.874e-05	-1.7406e-07	1.6372e-05	8.2266e-06	-0.00028379	3.1064e-0

Table I.3: Element numbering table

Element number	Opposite of
16	1
17	2
18	4
19	5
20	6
21	7
22	8
23	9
24	10
25	11
26	13
27	14
28	15
29	12
35	36
37	38

Table I.4: Stress table

Element number	Stress 1 (Pa)	Stress 2 (Pa)	Stress 3 (Pa)
1	7.064e+07	-1.4901e-08	-7.2963e+05
2	2.6803e+07	3.3528e-08	-2.8455e+05
3	3.2422e+07	2.6077e-08	-4.8712e+05
4	7.4436e+05	-8.9407e-08	-6.7869e+07
5	61132	7.4506e-09	-2.6474e+07
6	3.1268e+07	-4.0978e-08	-1.2955e+05
7	3.6796e+07	1.2293e-07	-56925
8	1.3906e+05	-3.3528e-08	-1.8869e+07
9	1.9832e+07	-1.1176e-08	-61686
10	25833	-2.0489e-08	-2.9845e+07
11	1.7827e+07	7.4506e-09	-12244
12	16439	-2.794e-09	-1.5856e+07
13	400.55	-5.099e-08	-1.6302e+06
14	2.7179e+06	3.1199e-07	-304.97
15	45955	0	-5.2862e+06
16	7.064e+07	1.3039e-07	-7.2963e+05
17	2.6803e+07	0	-2.8455e+05
18	7.4436e+05	-1.4901e-08	-6.7869e+07
19	61132	-1.0245e-07	-2.6474e+07
20	3.1268e+07	-6.333e-08	-1.2955e+05
21	3.6796e+07	-2.5332e-07	-56925
22	1.3906e+05	-6.6124e-08	-1.8869e+07
23	1.9832e+07	-8.8476e-08	-61686
24	25833	-2.9244e-07	-2.9845e+07
25	1.7827e+07	2.1327e-07	-12244
26	400.5	-5.1456e-08	-1.6302e+06
27	2.7179e+06	-2.8568e-07	-304.97
28	45955	-1.1409e-08	-5.2862e+06
29	16439	3.7253e-09	-1.5856e+07
30	2.5849e+07	5.5879e-09	-5.5879e-09
31	0	-1.6764e-08	-3.3052e+07
32	1.9365e+06	2.3283e-10	-5.8208e-10
33	2.3283e-10	-1.6298e-09	-3.8276e+06
34	6.6975e+05	0.0027162	-0.0027162
35	5.6663e+05	-4.6566e-09	-1.8e+07
36	5.6663e+05	-5.5879e-09	-1.8e+07
37	4.8206e+06	-2.0955e-09	-32543
38	4.8206e+06	-3.0268e-09	-32543